Deformation of Earth Materials

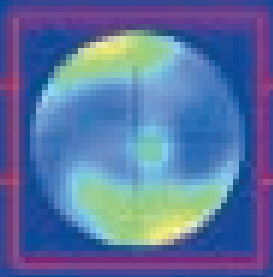

An Introduction to the Rheology of Solid Earth

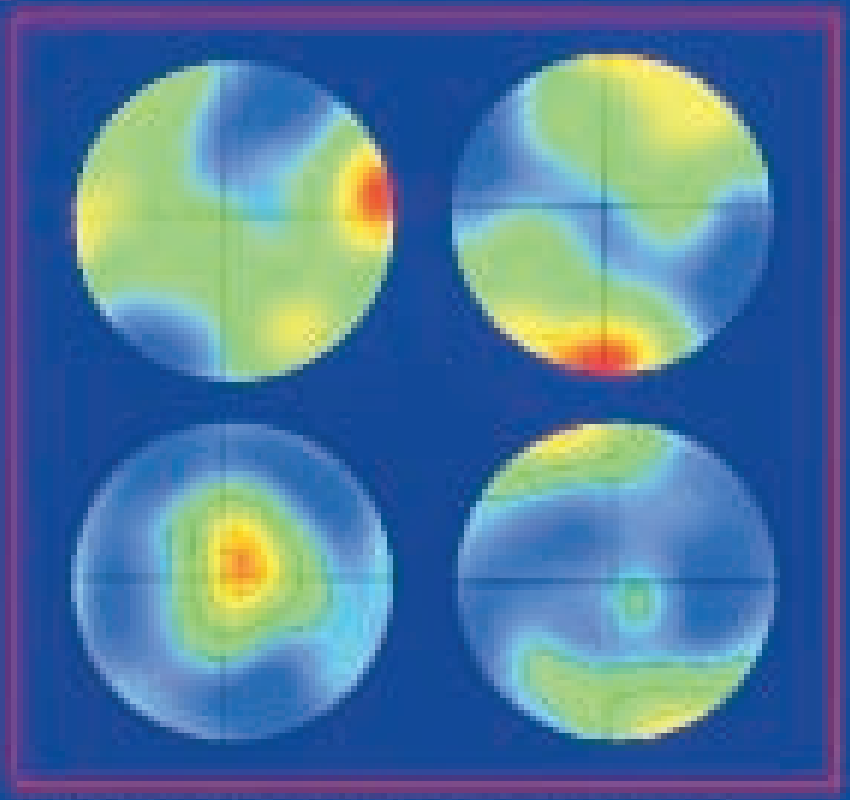

SHUN-ICHIRO KARATO

CAMBRIDGE

CAMBRIDGE www.cambridge.org/9780521844048

the volume fraction of melt is less than 0.1% (Spiegelman and Kenyon, 1992; Spiegelman and Elliott, 1993). Consequently, I conclude that there is little seismological observation to support the presence of a significant fraction of partial melting in most of the Earth's mantle. Melting must occur at least beneath volcanoes, but these observations suggest that the fraction of melt in a broad region beneath volcanoes (mid-ocean ridges) is small, presumably due to efficient melt transport. Also petrological studies have shown that the degree of melting in the deep upper mantle (>70 km) is controlled by the amount of water (and carbon dioxide) and is $\sim 0.1\%$ (Langmuir *et al.*, 1992). The ultra-low velocity zone near the bottom of the mantle might be a region of partial melting (Williams and Garnero, 1996; Lay *et al.*, 2004), but an alternative explanation in terms of high Fe content is also possible (Garnero and Jeanloz, 2000).

The above summary suggests that regions with a significant amount of melt are highly localized. Identifying these regions is important for Earth science. There are several ways by which the presence of melt can be inferred. For example, the presence of melt often leads to bulk attenuation (see Chapter 11). Bulk attenuation is expected to be very small for solid-state mechanisms of anelasticity. Consequently, the detection of bulk attenuation is a way to identify the presence of partial melt. Also, if a large lateral variation in seismic wave velocities is observed without a large variation in attenuation, the presence of partial melt is inferred when the influence of major element chemistry is small.

Grain size

Grain size should not have any effect on high-frequency seismic wave velocity, $V^{\infty}_{P(S,\phi)}$. However, grain size may affect anelasticity. Faul and Jackson (2005) proposed that in addition to temperature and pressure, grain size has some effects on seismic wave attenuation and hence indirectly seismic wave velocities in the upper mantle. Note, however, that the influence of grain size on seismic wave attenuation is probably not very large for a plausible range of grain size in Earth's upper mantle. The grain size for most of the upper mantle xenoliths is in the range of $\sim$3–10 mm (e.g., Mercier, 1980; Karato, 1984), and using the experimentally obtained grain-size sensitivity of attenuation, $Q \propto L^q$ with $q \sim 0.25$, one expects a change in Q of $\sim 30\%$, which results in a change in velocity of only 0.3% (0.1%) for $Q = 100$ ($Q = 300$). For thermoelasticity (see Chapter 11), grain-size sensitivity is stronger, $q \sim 0.5$ ($Q \propto (\omega\tau)^{\alpha}$, $\alpha \approx 0.25$, $\tau \propto L^2$). But the absolute value of attenuation due to thermoelasticity is small ($Q > 1000$, Chapter 11) and the influence of grain size on attenuation through this mechanism is not large. I conclude that the grain-size effect is modest compared to the effect of water (hydrogen) content and temperature.

20.3.2. Topography on discontinuities and its geodynamic significance

I have already discussed the lateral variation in seismic wave velocity due to the lateral variation in mineral phases. When the radial variation in mineral phases occurs as a seismic discontinuity, this lateral variation will appear as topography on the discontinuity. Fig. 20.6 shows some of the examples of topography on mantle discontinuities (for reviews on this topic see Gu *et al.* (1998), Shearer (2000) and Romanowicz (2003)). If we know what controls the depth of the discontinuity, then from the topography of the discontinuity we can learn the lateral variation of parameters that control the depth of the discontinuity. Seismic discontinuities may be caused by: (1) phase transformations, (2) changes in chemical composition and/or (3) changes in microstructures (such as the lattice-preferred orientation). Consequently, when the parameters (physical or chemical) that control the depth of discontinuities change laterally, then there will be lateral variation in the depth of the discontinuity. Generally, one can write

$$\delta z = \left(\frac{\partial z}{\partial T}\right)_{X_i,M} \delta T + \sum_i \left(\frac{\partial z}{\partial X_i}\right)_{T,M} \delta X_i + \left(\frac{\partial z}{\partial M}\right)_{T,X_i} \delta M \tag{20.18a}$$

or

$$\delta z = \frac{(\partial P/\partial T)_{X_i,M}\, \delta T + \sum_i (\partial P/\partial X_i)_{T,M} \delta X_i + (\partial P/\partial M)_{T,X_i} \delta M}{\rho g} \tag{20.18b}$$

where δz is the topography on a boundary and δT, δX_i and δM are anomalies in temperature, chemical composition and microstructure respectively. $(\partial P/\partial T)_{X_i,M}$, $(\partial P/\partial X_i)_{T,M}$ and $(\partial P/\partial M)_{T,X_i}$ are the parameters that are determined by material properties that can be investigated by laboratory studies (or by theoretical models).

The nature of these parameters depends on the physical origin of the discontinuity. Let us consider two examples. One is a discontinuity caused by a phase

transformation. In this case, the effects of microstructure are negligible. We need to consider only $(\partial P/\partial T)_{X_i,M}$ and $(\partial P/\partial X_i)_{T,M}$. $(\partial P/\partial T)_{X_i,M}$ is the Clapeyron slope that is known for most phase transformations (Table 2.3, Chapter 2). $(\partial P/\partial T)_{X_i,M}>0$ for olivine to wadsleyite transition (410 km) and $(\partial P/\partial T)_{X_i,M}<0$ for the ringwoodite to perovskite + magnesiowüstite transition (660 km). Consequently, the topography on the 410- and 660-km discontinuity would be anti-correlated if the topography were caused by the lateral variation in temperature.

The influence of the chemical composition on the phase boundary, $(\partial P/\partial X_i)_{T,M}$, is well known only for the variation in Fe/(Fe + Mg). For the olivine to wadsleyite transformation (the 410-km discontinuity), $(\partial P/\partial X_{\mathrm{Fe}})_{T,M}<0$, whereas for the ringwoodite to perovskite + magnesiowüstite transformation, $(\partial P/\partial X_{\mathrm{Fe}})_{T,M}\approx 0$. In addition to Fe/(Fe + Mg), water content may also modify the depth of discontinuity. Briefly, the presence of water (hydrogen) increases the stability fields of transition zone minerals relative to upper and lower mantle minerals, and consequently, the 410-km discontinuity will be shallower and the 660-km discontinuity will be deeper when a large amount of water is present (Wood, 1995; Higo *et al.*, 2001; Chen *et al.*, 2002a; Smyth and Frost, 2002; see also Karato, 2006b).

Another is the case of a discontinuity caused by microstructural variations. They include the Lehmann discontinuity at around 220 km (Karato, 1992; Gaherty and Jordan, 1995) and the discontinuity at the top of the D″ layer (at around 2700 km). The regional variation in the depths of these boundaries may reflect the regional variation in microstructures such as the lattice-preferred orientation. The nature of lattice-preferred orientation is sensitive to a number of parameters including stress, temperature and water content (Chapter 14), the details of which remain to be determined (e.g., Jung *et al.*, 2006). The above analysis shows that in order to infer δT, δX_i and δM from the topography of discontinuity, one needs to have more than one observation, a situation much the same as the situation in inferring thermal and chemical anomalies from tomographic images. Such studies include Gu *et al.* (2003) and Blum and Shen (2004), but separating various effects is not straightforward. An alternative way is to investigate the correlation of topography of various discontinuities. For example, if the topography of "410-" and "660-km" discontinuities in a certain region is caused by thermal anomalies associated with a vertical flow of materials, then temperature anomalies near these boundaries are likely to be similar (except for the effect due to latent heat). Consequently, $\delta z^{410}/\delta z^{660}=(dP/dT)^{410}\cdot\delta T^{410}/((dP/dT)^{660}\delta T^{660})\propto(dP/dT)^{410}/(dP/dT)^{660}$. The value of $(dP/dT)^{410}/(dP/dT)^{660}$ is known from laboratory studies (the Clapeyron slope, see Chapter 2), so that one can determine if the thermal origin of the topography of the boundaries is consistent with observations or not. We know $(dP/dT)^{410}/(dP/dT)^{660}<0$ from mineral physics, so if the anomaly is thermal, then $\delta z^{410}/\delta z^{660}<0$. Any deviation from this would imply that at least one of the assumptions is not met in this region.

As has been discussed above, several factors could cause the topography on the discontinuity. Therefore when the topography alone is investigated, its interpretation is non-unique. A combination with other observations could narrow the plausible causes for topography. For example, Blum and Shen (2004) combined the observations of topography of the 410-km discontinuity and velocity anomalies in the transition zone to infer the water content in the transition zone.

20.3.3. Summary of inversion scheme

A key issue in inverting tomographic images in terms of the physical and chemical state of the Earth's interior is to identify the cause for lateral variation (in velocities and in attenuation). If only one data value, say the anomaly in V_S, is available for a given point in the Earth, then the interpretation of anomalies in terms of physical or chemical conditions is non-unique. The same velocity anomaly could be due to an anomaly in temperature or in chemical composition or due to partial melting. For this reason it is critical to have multiple data sets for a given region. These multiple data sets must be for those quantities whose dependence on thermal or chemical anomalies are distinctly different. In this sense a joint inversion of velocity and attenuation anomalies is very useful because the sensitivity of velocity and attenuation to thermal and chemical anomalies are quite distinct as summarized above. Similarly, a joint inversion of V_P and V_S (or V_ϕ and V_S) is useful because the sensitivity of these two velocities, particularly V_ϕ and V_S, to thermal and chemical anomalies is different. In doing a joint inversion of multiple data sets, one must make sure that the data sets that one uses have a similar resolution. Technical issues for obtaining joint V_P and V_S (or V_ϕ and V_S) tomographic images are discussed by Masters *et al.*

(2000). In many cases, the quality of data from which anomalies of V_P and V_S are obtained is quite different and consequently, there can be systematic difference in errors for these anomalies. In addition, the wavelengths are different between the two waves for the same frequency, which could also cause a systematic difference in errors. Consequently, it is important to check the consistency of the data when tomographic images of two different velocities are compared. One way is to see if the relation (20.6) is satisfied by the data on V_P and V_S (or V_ϕ and V_S) (KARATO and KARKI, 2001). Deviation from the relation (20.6) means that the joint inversion contains some inconsistency. When tomographic images are analyzed in regions where seismic discontinuities occur (e.g., a transition zone), then the topography on the discontinuities can also be used to infer the origin of lateral heterogeneity.

Some issues in identifying the cause for heterogeneity have already been discussed using a ratio–ratio plot (Fig. 20.10). Here I will summarize some additional points using the velocity and attenuation tomography together. For simplicity, let us first treat a case in which the influence of partial melting and grain size is negligible. In this case, the influence of temperature, water content and major element chemistry can be summarized as follows.

(1) If the major cause for lateral variation of properties is the lateral variation in major element chemistry, then attenuation will be nearly constant whereas seismic wave velocities will have a large variation.
(2) If the major cause for lateral variation of properties is the lateral variation in water content, then attenuation will have a large lateral variation, whereas seismic wave velocities will have a relatively small lateral variation.
(3) If the major cause for lateral variation of properties is the lateral variation in temperature, then both seismic wave velocities and attenuation will have a large lateral variation.

Consequently, a plot such as that shown in Fig. 20.14 provides a guide for inferring the cause of lateral variation. If the variation in seismic wave velocities is large but the variation in attenuation is small, then we can infer that there is a large variation in major element chemistry. If, in contrast, there is a large variation in attenuation but a relatively small variation in seismic wave velocities, the most likely cause of lateral variation is the lateral variation in water content. More quantitatively, equation (20.2) can be solved to determine the lateral variation of temperature, major

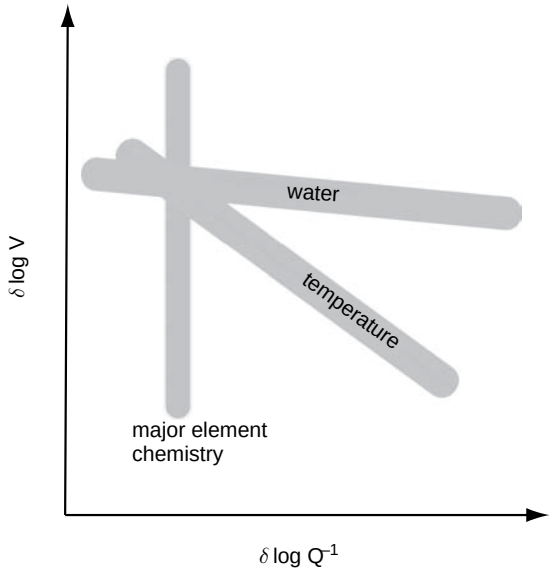

FIGURE 20.14 A schematic diagram of the attenuation anomaly–velocity anomaly relationship showing distinct trends for temperature-control, major element chemistry-control and water-control cases (after SHITO and SHIBUTANI, 2003b).

element composition and water content, if more than three observations are available and a simplified parameterization for the influence of major element chemistry is used. SHITO *et al.* (2006) performed such an inversion for a region where high-resolution velocity and attenuation tomography are available.

I note that although such an inversion is possible in certain regions, the ability to determine thermal and chemical anomalies is limited at this time. One of the main reasons for this is the resolution of seismic tomography. In order to separately determine these parameters, one needs to have high-resolution tomography of two seismic wave velocities (V_P and V_S (or V_ϕ and V_S)) and attenuation from the same region with a similar level of resolution. Another obvious limitation is the incomplete knowledge of mineral physics parameters, i.e., A_{ij}. Progress in these two areas is critical to make this approach useful. In the next section, I will review some of the results of such an inversion to infer thermal and chemical anomalies in Earth's interior.

20.3.4. Origin and geodynamic significance of lateral heterogeneity: Some examples

Upper mantle

A large lateral variation in seismic waves is observed in the upper mantle. Key mineral physics parameters, $A_{V_{P(S,\phi)}T}$, are reasonably well constrained for the upper

mantle. The application of these mineral physics results to tomographic images of the oceanic upper mantle yields plausible temperature and density anomalies if the effects of anelasticity are included.

One of the most significant conclusions on the oceanic upper mantle is that the low-velocity anomalies associated with mid-ocean ridges are shallow and sometimes asymmetric (e.g., Zhang and Tanimoto, 1992, 1993). These observations provide strong support for the notion that upwelling at mid-ocean ridges is in most cases passive: upwelling occurs because of the separation of the overlying plates but not by the buoyancy force of hot materials. In contrast, low velocity regions associated with ocean islands such as Hawaii and Island extends deeper to the transition zone or deeper (e.g., Montelli *et al.*, 2004). Using the model presented here, amplitude of temperature anomalies in plumes can be estimated. The results yield $\sim$200–300 K for plumes in most cases that is much less than the temperature anomalies expected from a classic model of plume originating from the bottom thermal boundary layer.

Continental roots are deep but the exact depth of continents is somewhat controversial. Influence of anisotropy has an important effect on the estimated depth (e.g., Anderson, 1979; Gung *et al.*, 2003). Velocity and density anomalies associated with continents cannot be solely attributed to thermal anomalies (e.g., Jordan, 1981; Forte *et al.*, 1994). Continental upper mantle has different major element chemical composition than that of oceanic upper mantle. However, mapping the anomalies in chemical compositions is challenging because the seismic wave velocities are less sensitive to major element chemistry than temperature (e.g., Matsukage *et al.*, 2005; Schutt and Lesher, 2006). The contrast between oceanic and continental upper mantle is mostly in density but the anomalies in seismic wave velocities are subtle.

In addition to the heterogeneity in major element chemistry, evidence for heterogeneity in water (hydrogen) content has been suggested. Based on the combination of high-resolution velocity and attenuation tomography, Shito *et al.* (2006) and Shito and Shibutani (2003b) found that in addition to the high lateral variation in major element chemistry in the shallow upper mantle ($<$150 km), there is a water-rich region in the deep upper mantle ($\sim$300–400 km) beneath the Philippine Sea (Fig. 20.15). Subduction of an old and cold lithosphere in this region is likely to have transported water deep into the upper mantle. However, inverting the velocity and attenuation anomalies is challenging both from seismological and mineral physics points of view. One needs reliable high-resolution velocity and attenuation tomography from the same region, and also the water content dependence of seismic wave velocities and attenuation must be characterized in detail.

Transition zone

One of the most prominent features of tomographic images on the transition zone is the presence of high-velocity anomalies in the broad regions of the transition zone particularly in the western Pacific. This implies that subducted slabs are deformed and stagnant in some of the transition zone (e.g., Fukao *et al.*, 1992, 2001; Romanowicz, 2003; Zhao, 2004). The transition zone or the 660-km discontinuity provides a strong resistance to subduction, presumably due to the negative Clapeyron slope at the 660-km discontinuity or high viscosity of the lower mantle. Also note that this means that subducted slabs are relatively soft (Karato *et al.*, 2001). However, there is a distinct ring of high-velocity anomalies in the bottom of the lower mantle corresponding to surface trenches, suggesting that stagnation of materials at the transition zone is only a temporal feature and these cold materials ultimately sink to the bottom of the mantle. This type of hybrid convection was demonstrated by numerical modeling incorporating the negative Clapeyron slope corresponding to the phase transformation at the 660-km discontinuity (e.g., Honda *et al.*, 1993; Tackley *et al.*, 1993).

Observations on the topography on discontinuities can be used to infer the presence of chemical heterogeneity. If the lateral variation in temperature is the cause for lateral variation in topography, the topography on the two discontinuities ("410-" and "660-km") would be anti-correlated because the Clapeyron slope has different signs for the phase transformation corresponding to these two discontinuities. In general, topography on the 410-km discontinuity is less pronounced than that on the 660-km discontinuity and the correlation (or anti-correlation) between the topography on the 410-km and the 660-km discontinuity is poor (e.g., Flanagan and Shearer, 1998; Gu *et al.*, 1998, 2003). These results suggest the presence of chemical heterogeneity in the transition zone, although the nature of chemical heterogeneity is not clearly understood.

An important subject about the transition zone is its water content. The mineral physics studies clearly show that the transition zone minerals can dissolve up to $\sim$3 wt% of water (see Chapter 17). If indeed

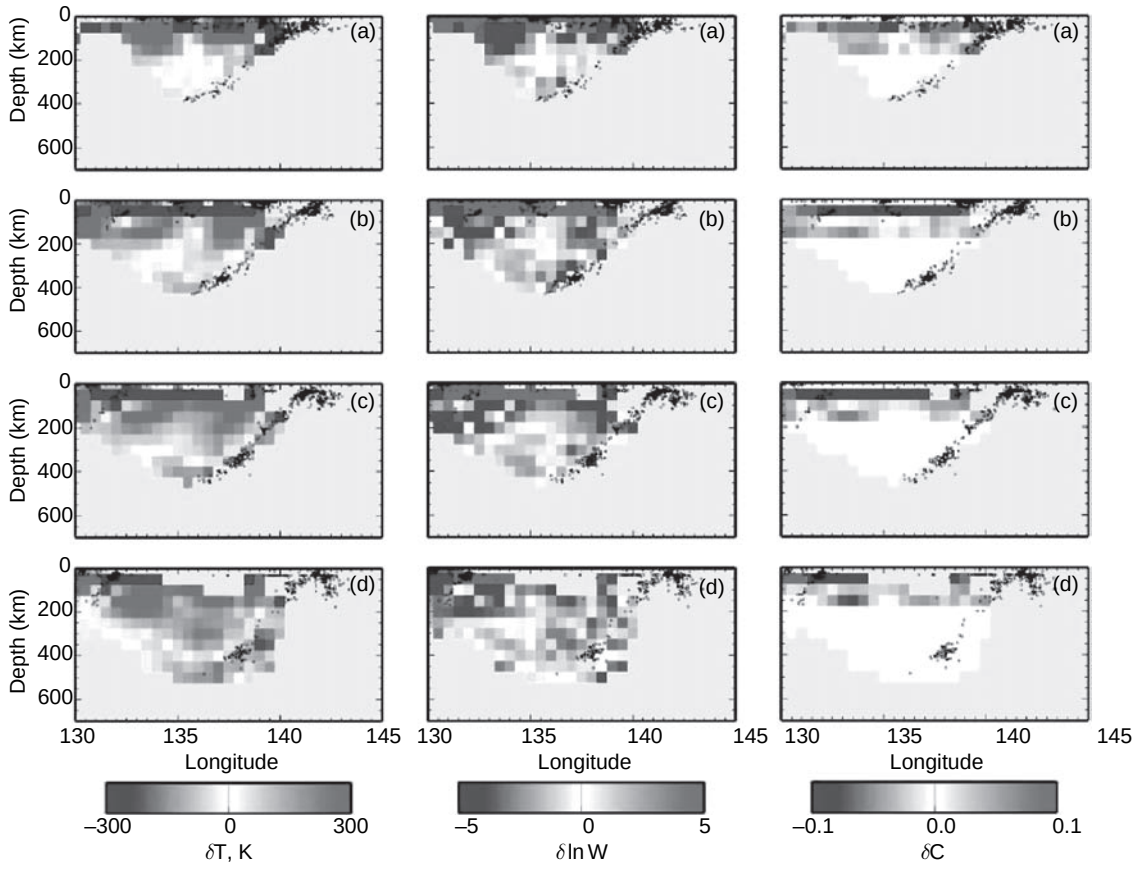

FIGURE 20.15 Inversion of velocity and attenuation tomography in terms of temperature (*T*), major element composition (*C*; Mg#) and water content (*W*) anomalies in the upper mantle beneath the Philippine Sea (Shito *et al.*, 2006). High-resolution tomography is available both for seismic wave velocities and attenuation from this region. A region of unusually high water content is identified in the deep upper mantle where attenuation is high but velocities are not so low. Plate 12.

the water content is this much, it will have an important influence on the dynamics and chemical evolution of Earth. There have been some attempts at inferring water content of the transition zone based on seismological observations (e.g., van der Meijde *et al.*, 2003; Blum and Shen, 2004; Suetsugu *et al.*, 2006). van der Meijde *et al.* (2003) used the sharpness of the 410-km discontinuity to infer the water content, and Blum and Shen (2004) and Suetsugu *et al.* (2006) used the topography of the 410-km discontinuity and the velocity anomalies in the transition zone to infer the water content. Again, inferring the water content remains a challenging subject.

Lower mantle

The most prominent feature of the lower mantle is the high-velocity ring corresponding roughly to the surface trenches, and the presence of two broad regions of low velocities (beneath south Pacific and Africa). Also the continuation of high-velocity anomalies associated with subducting slabs can be seen down to the deep lower mantle at least in the eastern Pacific and beneath Tibet to western Asia (e.g., Grand, 1994; van der Hilst *et al.*, 1997). These observations, together with the observations on the transition zone, suggest that mantle convection is, at least at present and in the recent past, whole mantle wide although evidence of significant resistance for convection currents is clear in the transition zone. The two broad low-velocity regions correspond to the broad swell in the Pacific (e.g., McNutt, 1998) as well as in Africa (Lithgow-Bertelloni and Silver, 1998). The location of these broad low-velocity regions corresponds roughly to the location of surface hotspots (e.g., Woodhouse and Dziewonski, 1989; Garnero, 2000). Consequently, it is considered that these low velocity regions represent upwelling. However, these low velocities are not all due to high temperatures. The anti-correlation of the S-wave

velocity anomaly and the bulk-sound velocity anomaly ($R_{S/\phi} < 0$), and the very large values of $R_{S/P}$ indicate that anomalies in this region cannot be due solely to thermal anomalies (KARATO and KARKI, 2001). A sharp boundary extending from the core–mantle boundary (CMB) to ~ 500 km above the CMB suggests that chemical heterogeneity is likely to be present in the deep lower mantle (WEN, 2001). However, the extent to which chemical heterogeneity is present in the lower mantle is not clear. KELLOGG *et al.* (1999) proposed, based largely on the interpretation of tomographic images of VAN DER HILST and KÁRASON (1999), that the bottom ~ 1000 km of the lower mantle is chemically distinct from the regions above. I should emphasize that the physical basis for such an argument is weak. Because $|A_{V_{P(S,\phi)T}}|$ decreases significantly with depth while $|A_{V_{P(S,\phi)X_i}}|$ does not, chemical effect becomes more visible than thermal effect with depth (Problem 20.2). Consequently, the observations suggesting a more important role for chemical effect with depth do not necessarily mean that the degree of chemical heterogeneity increases with depth. KARATO and KARKI (2001) discussed that chemical anomalies are required to explain available seismological data only in the bottom ~ 500 km (or less). FORTE and MITROVICA (2001) attempted to map the chemical heterogeneity in the deep lower mantle. Presence of partial melting was proposed by WILLIAMS and GARNERO (1996).

The recent discovery of the post-perovskite phase of $(Mg, Fe)SiO_3$ has introduced another complexity in interpreting seismological data on the bottom of the mantle (e.g., MURAKAMI *et al.*, 2004; OGANOV and ONO, 2004; TSUCHIYA *et al.*, 2004a). OGANOV and ONO (2004) argued that most of the seismological observations such as the large $R_{S/P}$ and negative $R_\phi/_S$ can be attributed to the phase transformation from perovskite to post-perovskite. However, the currently available data on seismic wave velocities such as $R_{S/P}$ and $R_\phi/_S$ are not enough to distinguish thermally-induced phase transformation from the influence of this phase transformation. The sharpness of velocity contrast (e.g., WEN, 2001) and/or some data on density distribution (e.g., ISHII and TROMP, 1999; GARNERO and JEANLOZ, 2000; TRAMPERT *et al.*, 2004) suggest the presence of chemical heterogeneity in the D″ layer. Detecting density anomalies from geophysical observations remains challenging, however (e.g., MASTERS and GUBBINS, 2003).

21 Seismic anisotropy and its geodynamic implications

Earth materials are anisotropic to some extent and the nature of anisotropic structures can be inferred from a range of seismological observations. Anisotropic structures carry valuable information as to the anisotropic fields that reflect the dynamic processes in Earth's interior including the geometry of flow. Therefore seismic anisotropy provides an important insight into the dynamics of Earth's interior. However, both observations and the interpretation of seismic anisotropy are not straightforward. Following the description of some of the fundamentals of seismic wave propagation in an anisotropic material, I will review the basic seismological observations on anisotropy. This is followed by a brief summary of the essence of the processes that may cause anisotropic structure formation. They include lattice-preferred orientation of anisotropic crystals and shape-preferred orientation of (isotropic or anisotropic) materials with distinct elastic moduli (or other types of layered structure). In most cases, seismic anisotropy is caused by lattice-preferred orientation of elastically anisotropic minerals. The relation between seismic anisotropy and deformation in such a case is mineral specific, and also depends on the physical and chemical conditions that change the elastic and plastic anisotropy of minerals. Following detailed discussions on the mechanisms of lattice-preferred orientation and other microscopic processes of anisotropic structure formation, some geodynamic implications of seismic anisotropy are discussed in the final section.

Key words azimuthal anisotropy, polarization anisotropy, shear wave splitting, Christoffel equation, lattice-preferred orientation, shape-preferred orientation.

21.1. Introduction

In the previous chapter, we learned how to investigate the dynamics of Earth's interior through the study of small deviations of real Earth structure from an ideal model assuming that Earth materials are isotropic. However, most rocks in Earth's interior show some degree of anisotropy and the magnitude of velocity variation with direction is in many cases comparable to that of heterogeneity. Therefore the results of seismic tomography summarized in the previous chapter are valid only when they represent anomalies of velocities averaged over the directions.

However, by taking the average over the directions, one will lose some important information on Earth's structure. In this chapter, we will focus on the directional dependence of seismic wave velocities, i.e., *seismic anisotropy*. The anisotropic structure of a rock reflects the *anisotropic field* in which the rock was formed or deformed. Anisotropic field includes stress or strain field as well as a temperature gradient or a magnetic field, all of which have an important influence on the way in which Earth works. Therefore studies of anisotropic structure can provide valuable information for understanding the dynamics of Earth's interior.

Although its potential importance is obvious, there are two important complications in investigating the dynamics of Earth's interior from seismic anisotropy. First, the measurement of anisotropy from seismology is not straightforward. In most cases, complete characterization of anisotropic structure is impossible and consequently, some simplifying schemes are used in the seismological measurements of anisotropy. Furthermore, depending on the technique used, the spatial resolution for the determination of anisotropic structure can be quite different. In order to interpret seismological observations on anisotropic structures, it is important to understand the merits and limitations of each technique. Second, geodynamic interpretation of seismic anisotropy requires the understanding of processes of anisotropic structure formation. There has been major progress in both the experimental and the theoretical sides of this issue, but there remain some major issues particularly concerning the physical processes of anisotropic structure development for materials in Earth's deep interior.

In this chapter I will first provide a brief summary of the essence of seismic wave propagation in an anisotropic material (section 21.2). Key concepts such as azimuthal and polarization anisotropy will be defined in section 21.3 and the nature of seismological observations on anisotropy is reviewed. Then some important observations are summarized in section 21.4 including anisotropy in the crust, the upper mantle, the transition zone, the lower mantle and the inner core. In section 21.5, some key mineral physics models are summarized that provide the bases for the geodynamic interpretation of seismic anisotropy. A brief summary of the processes of lattice-preferred orientation and the formation of a layer structure will be presented. Finally, in section 21.6, some geodynamic interpretations of seismic anisotropy are discussed.

21.2. Some fundamentals of elastic wave propagation in anisotropic media

Wave propagation in an anisotropic media is complicated. Recall that in the most general case, there are 21 independent elastic constants (Chapter 4) and consequently, in order to fully characterize anisotropic structures, one would need an impractically large number of data. Consequently, in almost all seismological studies on anisotropy, only some aspects of anisotropy are studied. In interpreting these results, it is important to understand the nature of the approximations or assumptions behind these studies. This section provides a brief summary of the fundamentals of seismic wave propagation in anisotropic media to help the geodynamical interpretation of seismological data. A more detailed account of elastic wave propagation in an anisotropic material is given in SMITH and DAHLEN (1973), CRAMPIN (1981) and MONTAGNER and NATAF (1986).

When the body-force such as gravity can be ignored (this is the case for short wavelength waves), the equation of motion of an anisotropic elastic material is given by (e.g., LANDAU and LIFSHITZ, 1959),

$$\rho \frac{\partial^2 u_i}{\partial t^2} = \sum_{j,k,l} C_{ijkl} \frac{\partial^2 u_k}{\partial x_j \partial x_l} \tag{21.1}$$

where ρ is density, u_i is displacement, t is time, x is the spatial coordinate and C_{ijkl} is the elastic constant tensor.

Let us consider a plane wave,

$$u_i = a_i \exp\left[i\omega \left(t - \sum_k q_k x_k \right) \right] \tag{21.2}$$

where a_i is the polarization vector that defines the direction of displacement, q_k is the slowness vector. Substituting equation (21.2) into (21.1), one has,

$$\rho a_i = \sum_{j,k,l} C_{ijkl} q_j q_l a_k. \tag{21.3}$$

Now let us define

$$q_j = \frac{1}{V} n_j \tag{21.4}$$

where V is the (phase) velocity[1] of seismic wave, and $\boldsymbol{n}$ is the unit vector parallel to the direction of propagation of waves. Then

$$\sum_k (T_{ik} - \rho V^2 \delta_{ik}) a_k = 0 \tag{21.5}$$

where

$$T_{ik} = \sum_{j,l} C_{ijkl} n_j n_l. \tag{21.6}$$

[1] The velocity defined here is called "phase velocity" because it is a velocity with which the phase of a plane wave, $-\omega\left(t - \sum_k q_k x_k\right)$, propagates. There is another definition of velocity of elastic waves, called "group velocity" that is the velocity at which the energy propagates with a wave. The distinction between them is important when a seismic wave contains various frequency components.

Problem 21.1

Derive equation (21.5).

Solution

Inserting (21.4) into (21.3), one has $\rho V^2 a_i = \sum_{j,k,l} C_{ijkl} q_j q_l a_k$. Therefore $\sum_{j,k,l} C_{ijkl} n_j n_l a_k - \rho V^2 a_i = \sum_k \left(\sum_{j,l} C_{ijkl} n_j n_l - \rho V^2 \delta_{ik} \right) a_k = \sum_k (T_{ik} - \rho V^2 \delta_{ik}) a_k = 0.$

Equation (21.5) is called the *Christoffel equation*. T_{ik} is a 3×3 symmetric matrix and therefore, for a given propagation direction n_i, (21.5) has three solutions. For an isotropic material, it can be shown from (21.6) that T_{ik} has a form (we choose $i = 1$ as a direction of propagation) (note that $K = (C_{11} + 2C_{12})/3$ and $\mu = C_{44} = (C_{11} - C_{12})/2$),[2]

$$T = \begin{bmatrix} K + \frac{4}{3}\mu & 0 & 0 \\ 0 & \mu & 0 \\ 0 & 0 & \mu \end{bmatrix}. \tag{21.7}$$

Problem 21.2

Derive equation (21.7).

Solution

By definition $\boldsymbol{n} = (1,0,0)$. So $T_{11} = \sum_{j,l} C_{1j1l} n_j n_l = C_{1111} = C_{11}$, $T_{22} = \sum_{j,l} C_{2j2l} n_j n_l = C_{2121} = C_{44} = T_{33}$ and all other $T_{ij} = 0$. Now for an isotropic material, $K = (C_{11} + 2C_{12})/3$ and $\mu = C_{44} = (C_{11} - C_{12})/2$, so $C_{11} = K + \frac{4}{3}\mu$, hence $T = \begin{bmatrix} K + \frac{4}{3}\mu & 0 & 0 \\ 0 & \mu & 0 \\ 0 & 0 & \mu \end{bmatrix}$.

For an isotropic material, the Christoffel equation becomes

$$\begin{bmatrix} (K + \frac{4}{3}\mu) - \rho V^2 & 0 & 0 \\ 0 & \mu - \rho V^2 & 0 \\ 0 & 0 & \mu - \rho V^2 \end{bmatrix} \cdot \begin{bmatrix} a_1 \\ a_2 \\ a_3 \end{bmatrix} = 0. \tag{21.8}$$

[2] For the relationship between the Voigt notation of elastic constants, C_{ij}, and the full tensor notation of elastic constants, C_{ijkl}, see Chapter 4. Typical values of elastic constants are given in Table 21.1 (for olivine).

This equation has three eigenvalues ($\rho V^2 = K + \frac{4}{3}\mu$, and two degenerated solutions $\rho V^2 = \mu$) and corresponding eigenvectors, $\boldsymbol{a} = (100)$, (010) and (001). Thus the first solution corresponds to the P-wave for which the polarization direction is parallel to the direction of propagation, whereas the other two solutions correspond to S-waves for which the polarization directions are perpendicular to the propagation direction (transverse waves). Such a clear distinction between P- and S-waves is no longer present in a general anisotropic material. However, in a weakly anisotropic material, such a relation holds approximately and terms quasi-P (qP) wave and quasi-S (qS) waves are sometimes used to refer to these waves. Note that the directions of polarization of transverse waves are controlled by the symmetry of the anisotropic structure of the material (this is how an optical polarizer works). In the above case, two orthogonal directions of polarization are (010) and (001) directions.

From the above analysis, one should note that there are two different ways of observing anisotropy in an elastic medium. First is the variation of elastic wave velocity with the orientation of wave *propagation*. This is often referred to as *azimuthal anisotropy*. Second is the difference in two shear wave velocities (of the same propagation direction) with different *polarization* directions. This is referred to as *polarization anisotropy*. Obviously, polarization anisotropy occurs only for shear waves, and the nature of polarization anisotropy, in general, changes with the direction of wave propagation. These two concepts are schematically shown in Fig. 21.1.

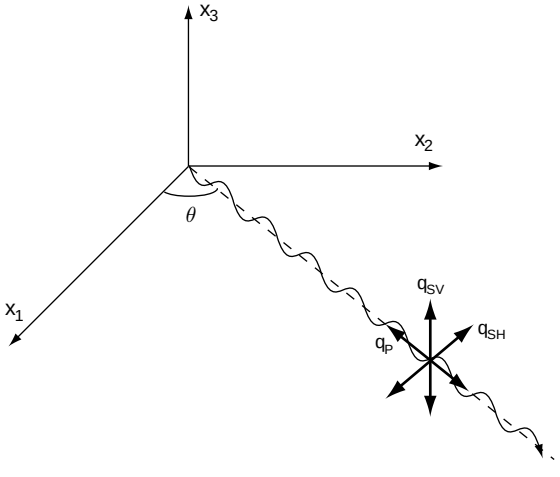

FIGURE 21.1 A schematic diagram showing the wave propagation in an anisotropic medium. Velocity can be dependent on the direction of wave propagation (azimuthal anisotropy). For shear waves (transverse wave), velocities of two waves with different polarization can be different (polarization anisotropy).

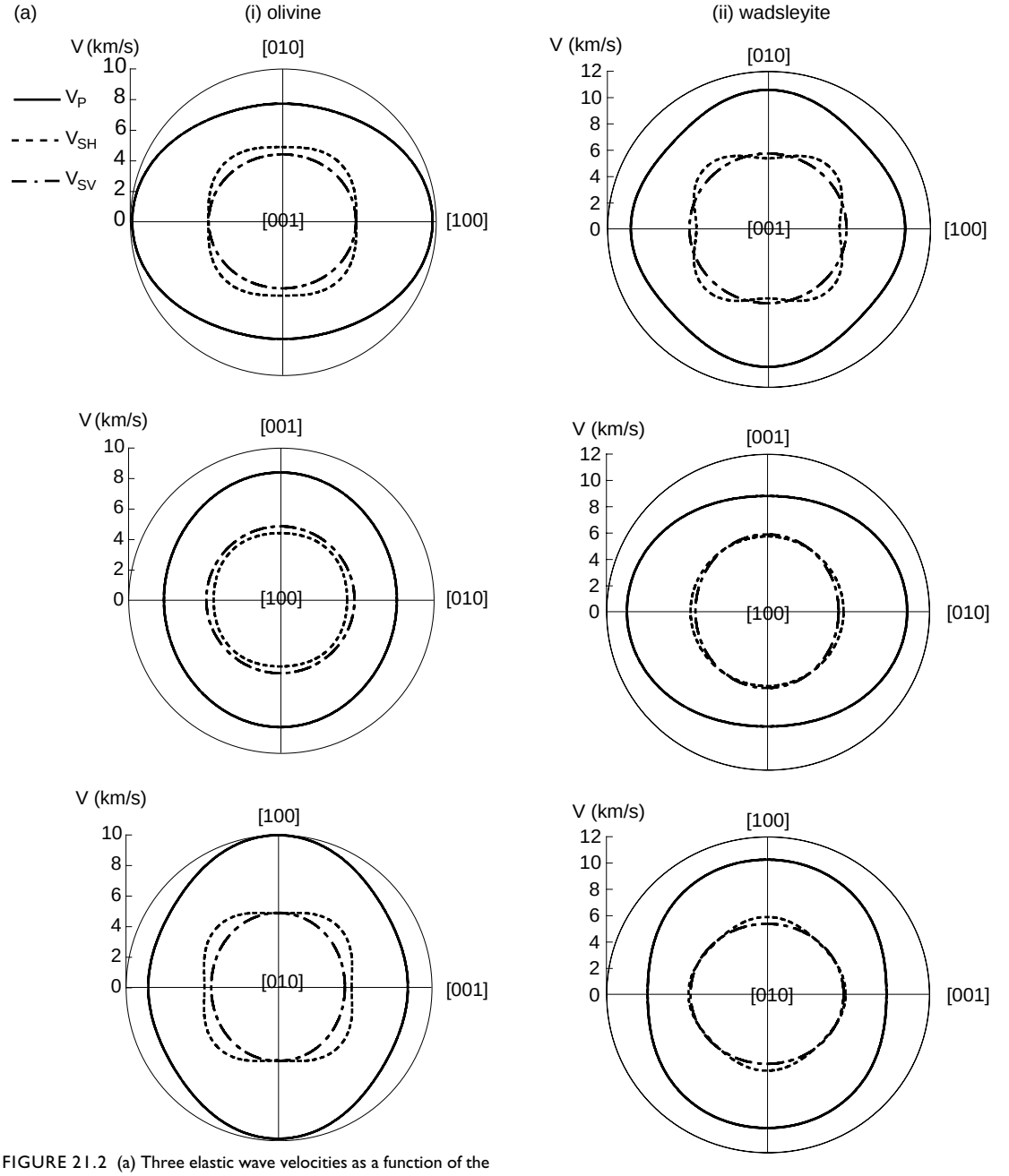

FIGURE 21.2 (a) Three elastic wave velocities as a function of the propagation direction in typical mantle minerals, (b) directions (shown by bars) of polarization of the faster S-wave as a function of the direction of the wave propagation. Both results are under ambient conditions (note that anisotropy can change with pressure, see Fig. 21.14). In (a), V_{SH} indicates the phase velocity of shear waves whose polarization direction is on the plane of wave propagation and V_{SV} is the phase velocity of shear waves whose polarization direction is normal to the plane of wave propagation. For pyrope these two velocities are nearly identical.

Velocity anisotropy can be illustrated by several diagrams. Because seismic wave velocities are the function of direction of propagation and (in the case of shear waves) also the function of polarization, one can represent the values of three velocities as a function of direction of propagation using the coordinate fixed to a crystal. Figure 21.2a is an example in which two-dimensional cross sections of such velocity surfaces are

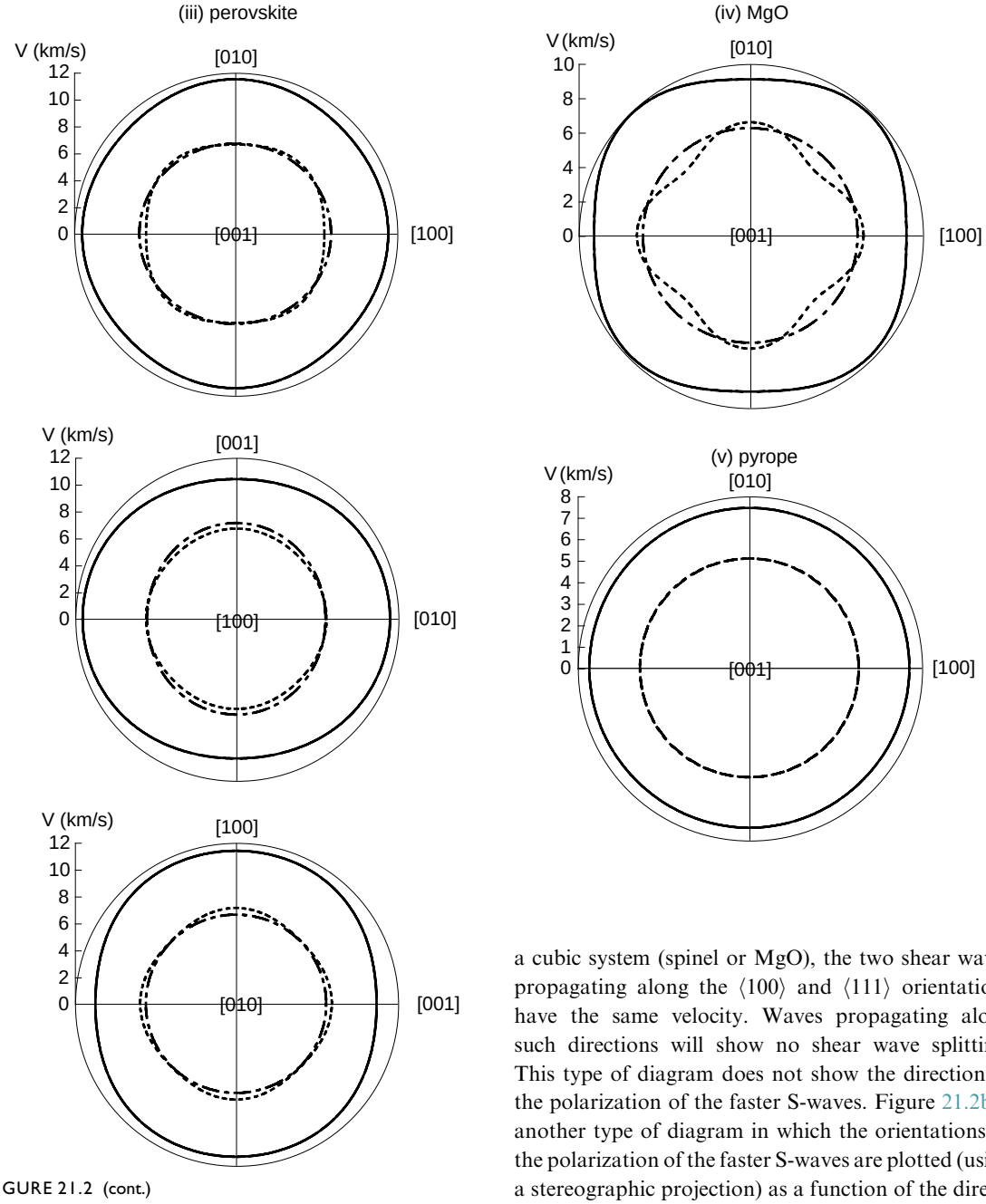

FIGURE 21.2 (cont.)

shown for three different waves as a function of direction of propagation. For a given direction of wave propagation, there are three velocities. Polarization of each wave can be determined by solving the Christoffel equation (21.5). For a certain symmetry orientation, two shear wave velocities are the same. For example, in a cubic system (spinel or MgO), the two shear waves propagating along the ⟨100⟩ and ⟨111⟩ orientations have the same velocity. Waves propagating along such directions will show no shear wave splitting. This type of diagram does not show the direction of the polarization of the faster S-waves. Figure 21.2b is another type of diagram in which the orientations of the polarization of the faster S-waves are plotted (using a stereographic projection) as a function of the direction of wave propagation.

The nature of azimuthal anisotropy can be shown from the extension of the above discussions. In the following we shall make an assumption of weak anisotropy. In this case we shall investigate a small deviation from isotropic case, so that the directions of quasi-P and quasi-S waves' polarization are the same as those in an isotropic material. We define the coordinate system as follows: x_1 is the direction of propagation

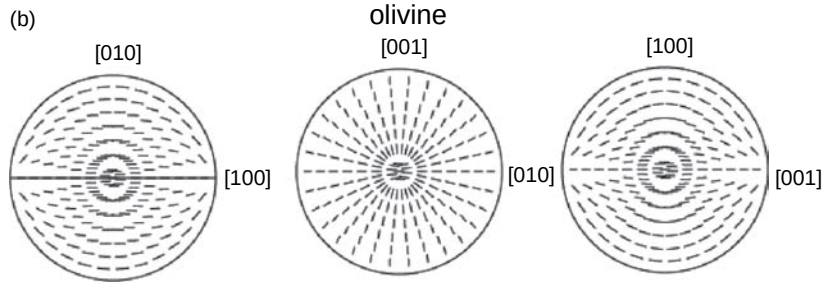

FIGURE 21.2 (cont.)

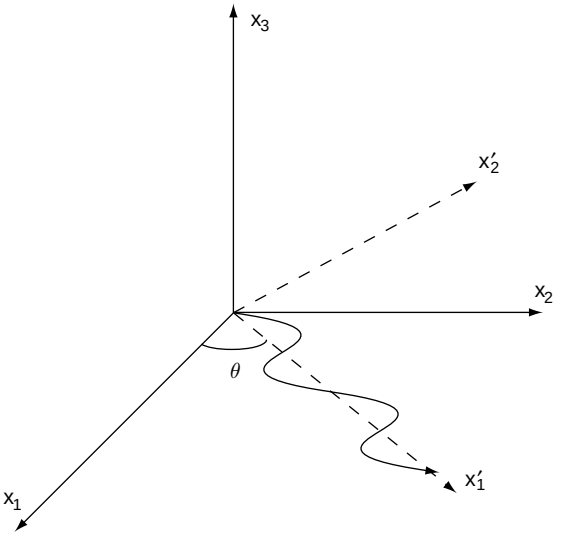

FIGURE 21.3 Rotation of the coordinate system.

of waves, x_3 is the vertical plane normal and x_2 is the direction normal to both x_1 and x_3. Azimuthal anisotropy can be investigated either by changing the orientation of n_i in the $x_3 = 0$ plane or by rotating the elastic constant matrix but fixing the propagation direction of waves.

Let us use the second approach (which is equivalent to the first approach). In this case, the nature of azimuthal anisotropy is determined by the nature of change in elastic constant matrix, C_{ijkl}, upon rotation. The change in matrix due to rotation across an axis can be determined by the operation of a 3×3 matrix, a_{ij}, (see Fig. 21.3)

$$a_{ij} = \begin{bmatrix} \cos\theta & \sin\theta & 0 \\ -\sin\theta & \cos\theta & 0 \\ 0 & 0 & 1 \end{bmatrix}. \tag{21.9}$$

The elastic constant matrix is transformed into a new form by this rotation,

$$C'_{ijkl} = \sum_{r,s,t,u=1}^{3} a_{ir} a_{js} a_{kt} a_{lu} C_{rstu}. \tag{21.10}$$

The seismic wave velocities have azimuthal dependence only up to 4θ terms ($\cos 4\theta$, $\sin 4\theta$). This is not a result of truncation but the exact result. The reason for this is the fact that the azimuthal anisotropy comes from the rotation of C_{ijkl} matrix (a fourth rank tensor), so that the rotation involves multiplying four matrices containing $\sin\theta$ and $\cos\theta$ (see (21.10)).

The matrix T_{ik} in this case is given by,

$$T_{ik} = \begin{bmatrix} C_{11} & C_{16} & C_{15} \\ C_{16} & C_{66} & C_{56} \\ C_{15} & C_{56} & C_{55} \end{bmatrix}. \tag{21.11}$$

If the $x_3 = 0$ plane is a symmetry plane, then all the elastic constants which contain an odd number of suffices equal to 3 will vanish so that C_{15} ($= C_{1113}$) $= C_{56}$ ($= C_{1312}$) $= 0$, then,

$$T_{ik} = \begin{bmatrix} C_{11} & C_{16} & 0 \\ C_{16} & C_{66} & 0 \\ 0 & 0 & C_{55} \end{bmatrix} \tag{21.12}$$

with $C_{11}, C_{66}, C_{55} \gg C_{16}$. Solving the Christoffel equation one obtains,

$$\begin{aligned} \rho V_{\mathrm{P}}^2 &= C_{11} - \frac{C_{16}^2}{C_{11} - C_{66}} \\ \rho V_{\mathrm{SH}}^2 &= C_{66} + \frac{C_{16}^2}{C_{11} - C_{66}} \\ \rho V_{\mathrm{SV}}^2 &= C_{55}. \end{aligned} \tag{21.13}$$

Here V_{SH} is the velocity of quasi-shear wave with the polarization direction in the x_2 direction (i.e., the horizontal polarization), and V_{SV} is the velocity of quasi-shear waves with the polarization direction in the x_3 (the vertical polarization) (for the definition of SH and SV waves see Box 21.1).

Box 21.1 Seismological nomenclatures

Seismology is a science that is more than a century old, and consequently some technical jargon has been introduced in seismology. In order to read and understand the seismological literature, an understanding of the basic terminology is necessary. For an introduction to seismology, LAY and WALLACE (1995) is a good start, and for a higher level presentation, see DAHLEN and TROMP (1998) and AKI and RICHARDS (2002).

The displacement of materials associated with elastic waves is called *polarization*. The polarization vector for the P-wave is always parallel to the propagation direction. For S-waves, the polarization vectors are on a plane that is perpendicular to the propagation direction (for simplicity, we consider only weak anisotropy). A combination of the polarization direction and the direction of wave propagation defines the plane on which material displacement occurs. Seismologists often classify S-waves into SH and SV waves based on the orientation of these planes. As discussed in the text, the directions of polarization of S-waves are controlled by the symmetry of anisotropy. When one of the symmetry axes of the elastic constants lies on the horizontal plane, then one of the polarization directions of the S-waves will be in the horizontal plane. When one considers a wave that propagates nearly horizontally (i.e., surface waves), then the other direction of polarization will be the vertical direction. In these cases, one can classify S-waves into SH (S-waves in which material motion is in the horizontal plane) and SV waves (material motion in the vertical plane). Similarly, PH (PV) wave is a P-wave in which material motion (and propagation direction) is horizontal (vertical). Other technical terms include:

Love wave	a type of surface wave in which displacement is in the horizontal plane;
Rayleigh wave	a type of surface wave in which displacement is mostly in the vertical plane (both A. E. H. Love (1863–1940) and Lord Rayleigh (J. W. Strutt; 1842–1919) were physicists who did their major work in late nineteenth century);
S (*P*)	an S- (P-) wave directly coming from a source to a receiver;
ScS	a body wave that originates as an S-wave and is reflected at the core–mantle boundary and comes back as an S-wave;
SKS	a body wave that originates as an S-wave and is converted to a P-wave in the outer core and converted back to the mantle as an S-wave. An advantage of using this wave is that any information on the polarization in the initial S-wave phase is eliminated as the wave goes into the liquid outer core, so any information on anisotropy must be from the place after the last P- to S-wave conversion. This helps to locate the region of anisotropy below the receiver.

Problem 21.3

Derive equation (21.13).

Solution

Inserting equation (21.12) into equation (21.5), one obtains, $\begin{bmatrix} C_{11}-\rho V^2 & C_{16} & 0 \\ C_{16} & C_{66}-\rho V^2 & 0 \\ 0 & 0 & C_{55}-\rho V^2 \end{bmatrix} \cdot \begin{bmatrix} a_1 \\ a_2 \\ a_3 \end{bmatrix} = \begin{bmatrix} 0 \\ 0 \\ 0 \end{bmatrix}$. For this equation to have non-trivial solution, one needs to have $\begin{vmatrix} C_{11}-\rho V^2 & C_{16} & 0 \\ C_{16} & C_{66}-\rho V^2 & 0 \\ 0 & 0 & C_{55}-\rho V^2 \end{vmatrix} = 0$. Therefore $(C_{55}-\rho V^2)\{(C_{11}-\rho V^2)(C_{66}-\rho V^2)-C_{16}^2\} = 0$, and the solutions (the eigen-values) are: $\rho V_1^2 = C_{55}$, $\rho V_2^2 \approx C_{11} - C_{16}^2/(C_{11}-C_{66})$ and $\rho V_3^2 \approx C_{66} + C_{16}^2/(C_{11}-C_{66})$ where I used an approximation $C_{16} \ll C_{11}, C_{66}$. The corresponding eigenvectors can be calculated from (21.5) to obtain the relation (21.13).

Now in order to investigate the azimuthal anisotropy, we will rotate the crystal around the x_3 axis. Using equations (21.9) and (21.10), one gets a new elastic constant matrix. Then using this new elastic constant matrix, one calculates T_{ik} and solves equation (21.5) to obtain velocities and the polarizations of three elastic waves. In the case where $x_3 = 0$ is a symmetry plane, the velocities of seismic waves propagating on the $x_3 = 0$ plane are given by (CRAMPIN, 1981),

$$\rho V_{\mathrm{P}}^2 = A + B_c \cos 2\theta + B_s \sin 2\theta + C_c \cos 4\theta + C_s \sin 4\theta \tag{21.14a}$$

$$\rho V_{\mathrm{SH}}^2 = D + E_c \cos 4\theta + E_s \sin 4\theta \tag{21.14b}$$

$$\rho V_{SV}^2 = F + G_c \cos 2\theta + G_s \sin 2\theta \tag{21.14c}$$

with

$$\begin{aligned}
A &= \frac{3(C_{11}+C_{22})+2(C_{12}+2C_{66})}{8}\\
B_c &= \frac{(C_{11}-C_{22})}{2}\\
B_s &= C_{16}+C_{26}\\
C_c &= \frac{C_{11}+C_{22}-2(C_{12}+2C_{66})}{8}\\
C_s &= \frac{C_{16}-C_{26}}{2}\\
D &= \frac{C_{11}+C_{22}-2(C_{12}-2C_{66})}{8}\\
E_c &= -C_c\\
E_s &= -C_s\\
F &= \frac{C_{44}+C_{55}}{2}\\
G_c &= \frac{C_{55}-C_{44}}{2}\\
G_s &= C_{45}
\end{aligned} \tag{21.15}$$

where the elastic constants are defined with respect to a coordinate system in which x_3 is the vertical axis, and the seismic wave propagates in the horizontal plane and the angle θ is measured from the x_1 axis.

If in addition, the $x_2 = 0$ plane is the symmetry plane then out of C_{ijkl}, those containing an odd number of suffices equal to 2 vanish (e.g., C_{16} $(= C_{1112}) = C_{26}$ $(= C_{2212}) = 0$). Then equation (21.14) is reduced to

$$\rho V_P^2 = A + B_c \cos 2\theta + C_c \cos 4\theta \tag{21.16a}$$

$$\rho V_{SH}^2 = D + E_c \cos 4\theta \tag{21.16b}$$

$$\rho V_{SV}^2 = F + G_c \cos 2\theta. \tag{21.16c}$$

Note that in both cases an SH-wave has only 4θ terms but an SV-wave has only 2θ terms.

Problem 21.4*

Explain why an SH-wave has the four-fold symmetry (only 4θ terms) whereas an SV-wave has the two-fold symmetry (only 2θ terms) in the plane of wave propagation if the plane is a symmetry plane.

Solution

Without the loss of generality, we can choose a coordinate system in which x_3 is the vertical axis, and the seismic wave propagates in the horizontal plane normal to x_3 (the angle θ is measured from the x_1 axis). Then remembering that the particle motion occurs on the x_1–x_2 plane for an SH-wave, we note that the velocity of an SH-wave is determined to the first order by an elastic constant corresponding to the shear strain ε_{12} associated with the shear stress σ_{12}, i.e., $C_{1212}(= C_{66})$. If one rotates the coordinate (around the x_3 axis) by $\pi/4$, then by exchanging $x_1 \leftrightarrow x_2$ one finds $C_{1212}(= C_{66}) \leftrightarrow C_{2121}(= C_{66})$. Therefore the velocity of an SH-wave is invariant for the rotation of $\pi/4$ so that it has four-fold symmetry. The velocity of an SV-wave propagating along the x_1 axis is controlled by the shear strain of ε_{13} associated with the shear stress σ_{13}, i.e., C_{1313} $(= C_{55})$. Upon exchanging $x_1 \leftrightarrow x_2$, it will change to $C_{2323}(= C_{44} \neq C_{55})$. Consequently, it has the two-fold symmetry but not the four-fold symmetry (obviously by exchanging $x_1 \leftrightarrow -x_1$, the elastic constant does not change).

21.3. Seismological methods for detecting anisotropic structures

21.3.1. Azimuthal anisotropy

The case for azimuthal anisotropy is straightforward from the above analysis. The azimuthal anisotropy of P-waves propagating in the horizontal plane can be analyzed using equation (21.14a) (or (21.16a)). In many cases, the cos 2θ term dominates and

$$\frac{\Delta V_P}{V_P} \approx \frac{B_c}{A} = \frac{4}{3}\frac{C_{11}-C_{22}}{(C_{11}+C_{22})+2(C_{12}+2C_{66})} \quad (\cos 2\theta \text{ term}). \tag{21.17}$$

The azimuthal anisotropy was first proposed by Hess (1964) and found in the uppermost mantle by Raitt *et al.* (1969) in the eastern Pacific by an explosion seismological experiment (they only determined P-wave anisotropy, i.e., A and B_c). Similar azimuthal anisotropy was also found in some portions of continents (Bamford, 1977) and in the inner core (Song, 1997; Tromp, 2001).

Azimuthal anisotropy can also be observed for shear waves. For an SH-wave,

$$\frac{\Delta V_{SH}}{V_{SH}} \approx \frac{E_c}{D} = -\frac{(C_{11}+C_{22})-2(C_{12}+2C_{66})}{(C_{11}+C_{22})-2(C_{12}-2C_{66})} \quad (\cos 4\theta \text{ term}) \tag{21.18}$$

and for an SV-wave,

$$\frac{\Delta V_{SV}}{V_{SV}} \approx \frac{C_{55} - C_{44}}{C_{55} + C_{44}} \qquad (\cos 2\theta \text{ term}). \tag{21.19}$$

Note that the anisotropy of a Rayleigh wave is controlled by that of P- and SV-waves, so that the $\cos 2\theta$ term usually dominates. Azimuthal anisotropy of surface waves has been studied by FORSYTH (1975), TANIMOTO and ANDERSON (1984, 1985), MONTAGNER and TANIMOTO (1990, 1991) and MONTAGNER (2002). Most of these studies are on the upper mantle because surface waves are sensitive to the structures of shallow portions. However, by using the overtones (higher modes), one can infer anisotropy in the deeper portions. TRAMPERT and VAN HEIJST (2002) reported azimuthal anisotropy of the mantle transition zone using the overtones of surface waves (signals contained in the overtones are weak and the robustness of the results of this paper is not yet well established).

Azimuthal anisotropy is determined by measuring the wave velocities in a place in Earth as a function of the direction of wave propagation. To do this one needs a large number of source–station combinations. One of the important limitations of this method is that different waves passing through a place with different directions must pass different regions outside the study region. Consequently, the influence of lateral heterogeneity needs to be corrected (Fig. 21.4). This is not trivial because the amplitude of lateral heterogeneity is similar to that of anisotropy in most cases.

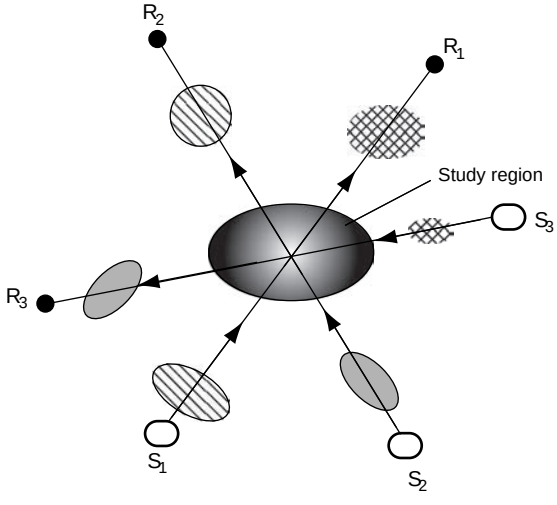

FIGURE 21.4 A schematic diagram showing a way in which azimuthal anisotropy is measured. S_i indicates the source and R_i denotes the receiver. Note that waves used to determine azimuthal anisotropy in a study region must pass through different regions between a source and a receiver.

Problem 21.5

Derive equation (21.19).

Solution

Following (21.14c), we obtain $\rho(V_{S_1}^2 - V_{S_1}^2) = 2c_{7c}$ where V_{S_1}, V_{S_2} are the fast and slow velocities of SV waves. Therefore

$$\frac{V_{S1}^2 - V_{S2}^2}{V_{S1}^2 + V_{S2}^2} = \frac{C_{55} - C_{44}}{C_{55} + C_{44}} \approx \frac{\Delta V_S}{V_S}.$$

21.3.2. Polarization anisotropy

The difficulty of correcting the influence of lateral heterogeneity can be eliminated if one focuses on the difference in seismic wave velocities between two shear waves with different polarizations. In this case, the polarization anisotropy can be determined from one seismic record and consequently there is no influence of lateral heterogeneity. In practice, this polarization anisotropy is analyzed in two different ways. First, when a seismic wave propagates through an anisotropic medium, then two shear waves with different polarization vectors will have different velocities and therefore they arrive at different times. This phenomenon is called *shear wave splitting*. By looking at seismic records one can determine the travel time difference of two shear waves, and if one has records of shear waves with two different directions of displacement, then one can also determine the directions of polarization (Fig. 21.5). In the case where one looks at a vertically traveling wave (e.g., SKS wave), then one can use the analysis from (21.11) through (21.13) to find the velocities and the polarization vectors of two shear waves. The directions of the two polarization vectors are controlled by the symmetry of the elastic constants, and the magnitude of splitting is given by

$$\frac{\Delta V_S}{V_S} \approx \frac{C_{55} - C_{44}}{C_{55} + C_{44}} \tag{21.20}$$

where I use the coordinate system such that x_3 is the vertical axis. Note that this result is identical to (21.19) because we are looking at the same type of waves (SV-waves). The relation between the body- and the surface-wave anisotropy was investigated by MONTAGNER *et al.* (2000).

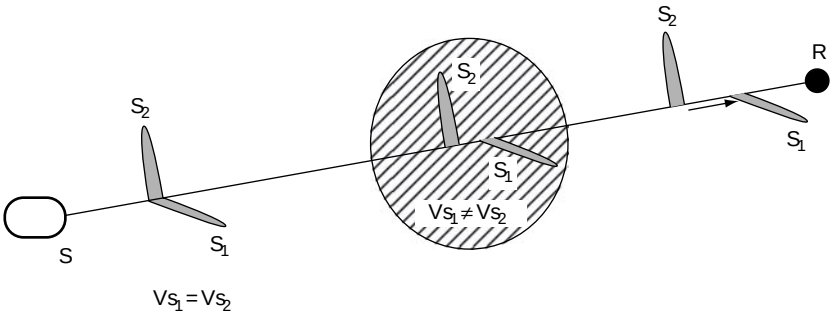

FIGURE 21.5 A schematic diagram showing how shear wave splitting occurs.

Shear wave splitting is a powerful tool to investigate anisotropic structure. One advantage of this method is that because anisotropic structure can be inferred from a single record, the result is free from the influence of lateral heterogeneity. However, a major limitation is that it is hard to identify where shear wave splitting occurs. For example, when one uses an SKS wave (shear wave that goes to the outer core and comes back from the core–mantle boundary, see Box 21.1), any place from the core–mantle boundary to the station can cause shear wave splitting. There is some progress to determine three-dimensional anisotropic structures from shear wave splitting measurements. When one uses a wave converted from P- to S- at a discontinuity, then shear wave splitting must occur in the materials above the discontinuity (e.g., PARK and LEVIN, 2002). Also using the back-azimuth and/or frequency dependence of splitting one can obtain some constraints on the depth variation of anisotropy (e.g., CHEVROT, 2000; SALTZER *et al.*, 2000; CHEVROT and VAN DER HILST, 2003), but the uncertainties in locating the anisotropic structures are still large.

Second, and another commonly used approach, is to analyze seismological data assuming *transverse isotropy* and determine the ratio of V_{SH}/V_{SV}. Transverse isotropy is a particular type of anisotropic structure in which the elastic properties do not depend on the orientation in the horizontal plane, but they are different between properties in the horizontal and vertical directions. One example is a horizontally layered structure. In such a case, the P-wave has anisotropy with respect to the direction of propagation (PH, PV), and the horizontally propagating S-wave has anisotropy with respect to the direction of polarization (SH, SV). Since polarization anisotropy is better constrained, the ratio of velocities of SH and SV waves, V_{SH}/V_{SV}, is investigated in most of the literature. The amplitude of SH–SV anisotropy can be calculated from the previously given relation, (21.14), as

$$\left(\frac{V_{SH}}{V_{SV}}\right)^2 = \frac{D}{F} = \frac{C_{11} + C_{22} - 2(C_{12} - 2C_{66})}{4(C_{44} + C_{55})} \qquad (21.21)$$

where as before the elastic constants are defined using a coordinate system in which x_3 is the vertical axis.

In contrast to the azimuthal anisotropy, the measurements of the polarization anisotropy of S-waves can be made with less problems of heterogeneity. In a measurement of polarization anisotropy, one investigates a seismogram at a single station and determines the difference in velocities of two shear waves that have different polarizations. One may compare the phase velocities of Love and Rayleigh waves that depend on SH- and SV-wave velocities respectively. Indeed, this SH–SV *polarization anisotropy* was recognized in the early 1960s in one of the first reports on the evidence of seismic anisotropy (AKI and KAMINUMA, 1963). By using the fact that surface waves with different frequencies sample different ranges of depth, one can determine the depth variation of anisotropic structures. Such studies include FORSYTH (1975), NATAF *et al.* (1986), MONTAGNER and TANIMOTO (1990, 1991) and BEGHEIN and TRAMPERT (2003a).

Similarly, the analysis of free oscillation provides information as to the anisotropic structure of Earth. The principle is similar to the surface waves, because both surface waves and free oscillation belong to the same class of elastic vibration in which the displacement of materials is constrained by the boundary conditions. Anisotropic structures can be determined by investigating the *splitting* of peaks of free oscillation. Free oscillation of Earth has many peaks corresponding to various "modes." If Earth were a perfectly homogeneous sphere, then these peaks would be sharp and well defined. Anisotropy (as well as rotation and heterogeneity) will cause the splitting of these peaks. Consequently, by investigating the nature of splitting of free oscillation peaks with various frequencies, one

can investigate the depth variation of anisotropic structures (e.g., Woodhouse *et al.*, 1986; Montagner and Kennett, 1996).

21.4. Major seismological observations

Important seismological observations on anisotropy can be summarized as follows.

(i) Significant anisotropy is observed in the crust, particularly in the areas with intense deformation (e.g., Crampin, 1984).

(ii) Significant azimuthal anisotropy of P-waves (Fig. 21.6, Raitt *et al.*, 1969; Shimamura *et al.*, 1983) and Rayleigh waves (Fig. 21.7, Tanimoto and Anderson, 1984, 1985; Montagner and Tanimoto, 1990, 1991; Debayle *et al.*, 2005) is observed in the shallow oceanic upper mantle and in some of the continental upper mantle (Bamford, 1977; Fuchs, 1983; Savage, 1999).

(iii) In most of the shallow upper mantle $V_{SH} > V_{SV}$ (Aki and Kaminuma, 1963; Nataf *et al.*, 1984, 1986; Gaherty and Jordan, 1995; Beghein and Trampert, 2003a). However, in the old oceanic upper mantle and also beneath mid-ocean ridges $V_{SV} > V_{SH}$ (Nataf *et al.*, 1986; Montagner and Guillot, 2000, 2002).

(iv) Seismic anisotropy beneath hotspots is somewhat different. In the upper mantle beneath Hawaii, $V_{SH} > V_{SV}$ anisotropy is stronger than other regions (Montagner and Guillot, 2000) (Fig. 21.8). Gaherty (2001) reported that beneath Iceland, $V_{SH} > V_{SV}$ is observed in the deep upper mantle (> 100 km) whereas $V_{SV} > V_{SH}$ anisotropy is observed in the shallow upper mantle (< 100 km). The modifications to the azimuthal anisotropy (shear wave splitting pattern) are found around hotspots (e.g., Walker *et al.*, 2001).

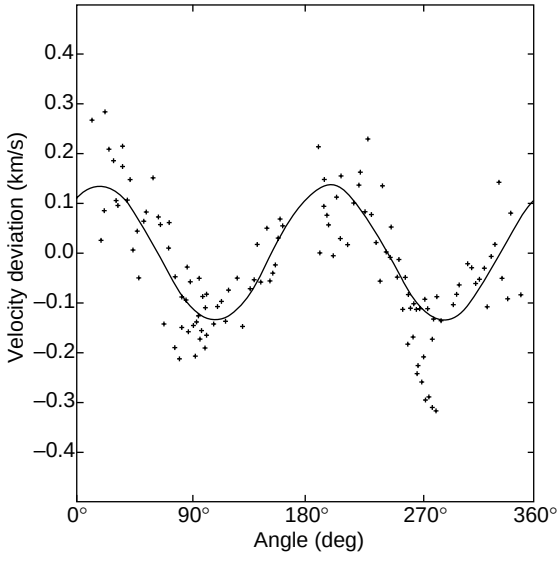

FIGURE 21.6 Azimuthal anisotropy in the uppermost mantle in the Pacific (after Raitt *et al.*, 1969). The measured P-wave velocities are plotted as a function of the azimuth.

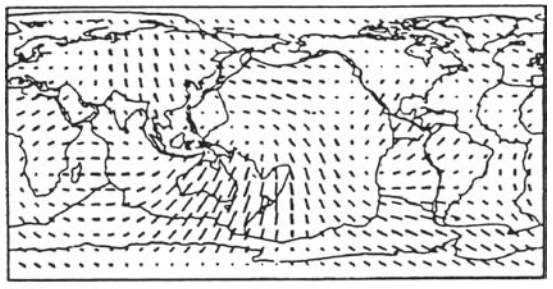

FIGURE 21.7 Azimuthal anisotropy of Rayleigh waves of 200 s period. Bars indicate the propagation direction of fast Rayleigh waves. The results represent the anisotropic structure of the asthenosphere, ~100–200 km depth (after Tanimoto and Anderson, 1984).

(v) In most regions, strong shear wave splitting, up to ~2 s (typically ~1 s) is observed. Usually such a splitting result shows good correlation with surface geology and is interpreted to be due to the anisotropic structure in the shallow upper mantle. The polarization of the fast shear wave is nearly parallel to the direction of geological structure (e.g., Fig. 21.9, Silver, 1996; see also Savage, 1999). Similarly, the direction of polarization of the faster S-wave in a convergent boundary is nearly parallel to the strike of a trench near the trench whereas it becomes orthogonal to the trench away from the trench (e.g., Smith *et al.*, 2001; Nakajima and Hasegawa, 2004; Long and van der Hilst, 2005; Fig. 21.10).

(vi) The amplitude of anisotropy in the upper mantle decreases with depth (Montagner and Tanimoto, 1990, 1991) (there are some exceptions, see Debayle *et al.*, 2005).

(vii) However, there are some hints as to the presence of anisotropy in the *transition zone* around 400–800 km depth (Montagner and Kennett, 1996; Vinnik and Montagner, 1996; Wookey *et al.*, 2002; Beghein and Trampert, 2003a). Trampert and van Heijst (2002) reported azimuthal anisotropy in the transition zone using the higher mode data of surface waves (Fig. 21.11).

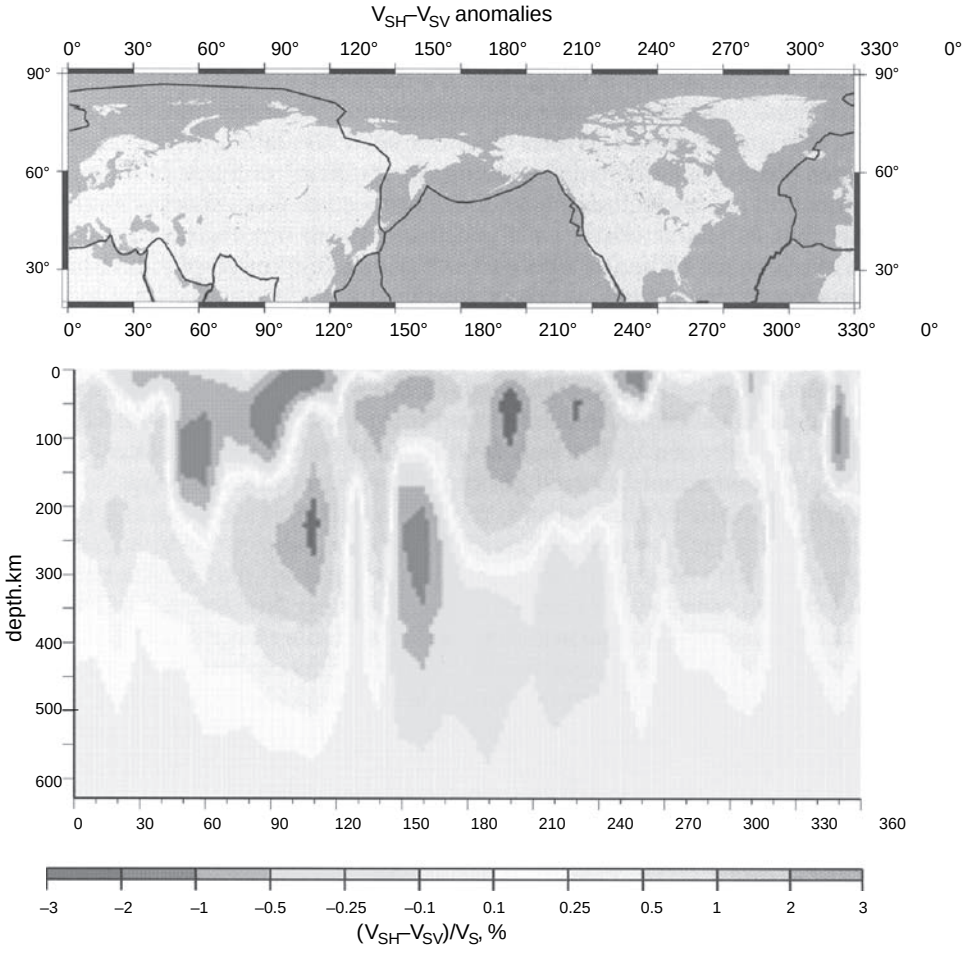

FIGURE 21.8 The V_{SH}/V_{SV} polarization anisotropy of the upper mantle (after Montagner and Guillot, 2000).
The deviation of V_{SH}/V_{SV} polarization anisotropy in the upper mantle from the PREM model is shown along a cross section shown in the top map (the unit is %). Plate 13.

(viii) Most of the *lower mantle* is devoid of any significant anisotropy (Meade *et al.*, 1995; Montagner and Kennett, 1996). However, significant shear wave anisotropy is documented in some portions of the D″ layer (the bottom of the mantle) (Kendall and Silver, 1996; Vinnik *et al.*, 1998; Garnero *et al.*, 2004; Panning and Romanowicz, 2004). Usually $V_{SH} > V_{SV}$ in the D″ layer, but the magnitude of anisotropy changes from one place to another. Anisotropy is strong in regions where average velocity is higher than normal. Evidence for azimuthal anisotropy in the D″ layer is controversial.

(ix) There is a strong anisotropy in the *inner core*. The anisotropy has nearly axial symmetry and the fast P-waves are along the rotation axis (Fig. 21.12; Morelli *et al.*, 1986; Woodhouse *et al.*, 1986; Durek and Romanowicz, 1999; Tromp, 2001). However, anisotropy is depth-dependent (e.g., Song, 1997) and there is some suggestion for hemispheric asymmetry (e.g., Tanaka and Hamaguchi, 1997).

21.5. Mineral physics bases of geodynamic interpretation of seismic anisotropy

In order to translate observed seismic anisotropy in the geodynamic context, one needs to understand the physical mechanisms by which anisotropic structures are formed. There are two distinct structures that can cause seismic anisotropy. One is a layered structure including the shape-preferred orientation (SPO) of isotropic or anisotropic materials and another is lattice-preferred orientation (LPO) of anisotropic minerals.

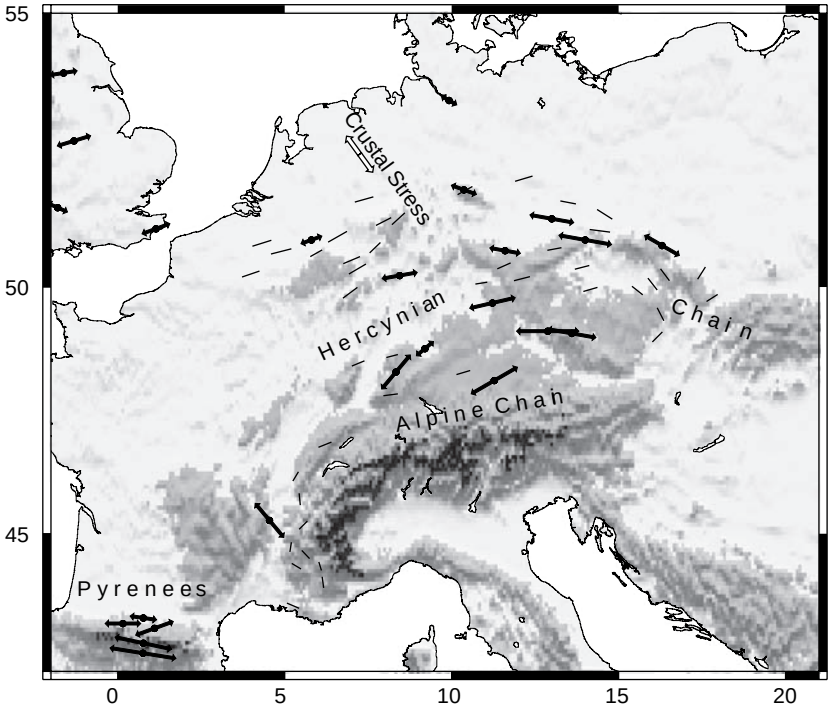

FIGURE 21.9 The direction of polarization of faster shear waves (SKS) in the continent (after SILVER, 1996). The direction of polarization of a faster S-wave is nearly parallel to the trend of the orogenic belt.

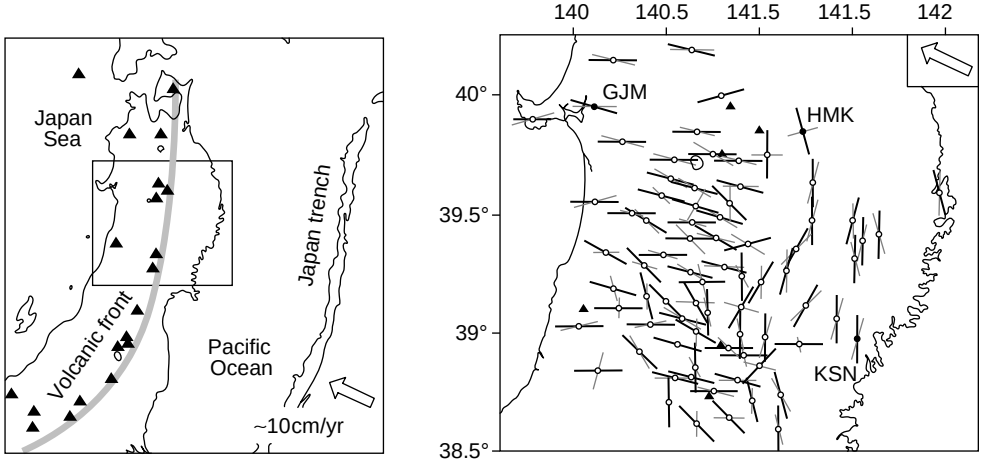

FIGURE 21.10 Shear wave splitting in the Tohoku, Japan (after NAKAJIMA and HASEGAWA, 2004). In regions near the trench, the direction of polarization of the faster S-wave is nearly parallel to the trench, whereas in regions far from the trench its direction becomes normal to the trench. Such a trend is common to many subduction zones.

21.5.1. Anisotropy due to a layered structure

When a material contains two components with different properties (chemical composition, density or viscosity), upon deformation the two regions will change their shape. After large deformation, one could obtain a highly layered structure (e.g., CHRISTENSEN and HOFMANN, 1994). The scale of layering, i.e., the mean thickness of layers depends on the mechanisms of deformation (stirring), but in many cases it can reach a small size compared to the wavelength of seismic waves ($\sim$10–100 km for body waves, $\sim$100–1000 km for surface waves). If the layer thickness is much smaller than the wavelength of seismic waves, then

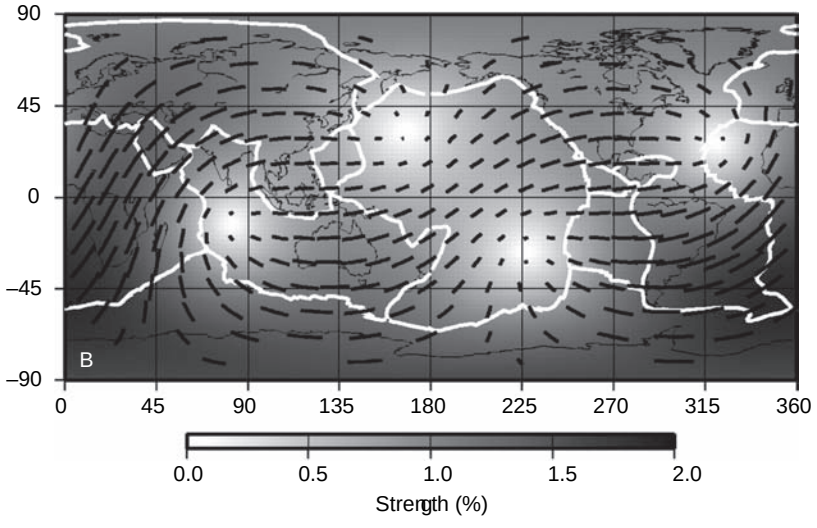

FIGURE 21.11 Azimuthal anisotropy of the transition zone as determined by the overtones of surface waves (after TRAMPERT and VAN HEIJST, 2002).

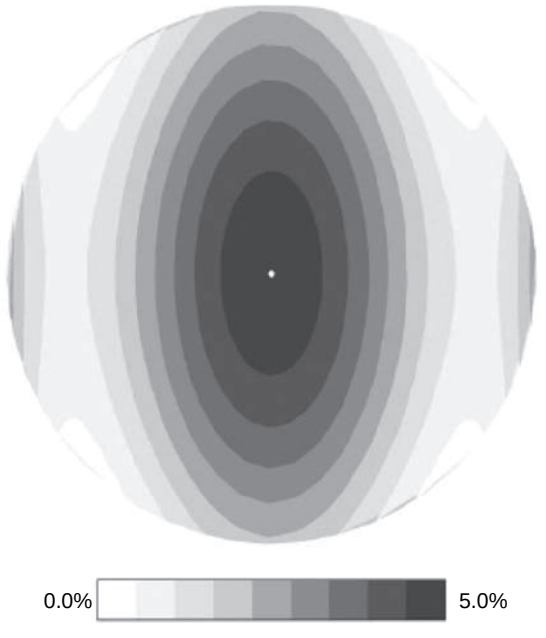

FIGURE 21.12 Anisotropy in the inner core (after DUREK and ROMANOWICZ, 1999; TROMP, 2001). The velocities of P-waves propagating nearly parallel to the rotation axis are significantly faster than those propagating normal to the rotation axis. The details of the anisotropic structure such as the depth variation of anisotropy are not well constrained.

such a layered structure will appear to be a homogeneous but anisotropic structure.

Consider a layered structure made of two isotropic materials (Fig. 21.13). By definition, there is a symmetry axis normal to the plane. The elastic constants corresponding to such a structure have the same symmetry as the elastic constants for a hexagonal structure and have

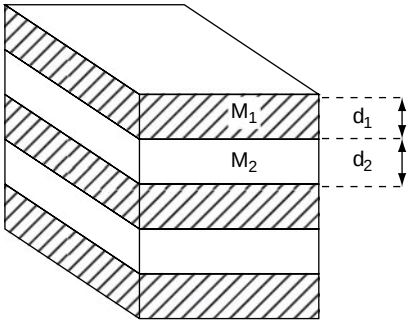

FIGURE 21.13 A finely layered structure. The elastic constants for deformation in the layering plane and normal to the layering plane are different, and are characterized by five independent elastic constants.

five independent components (see Chapter 4).[3] This type of anisotropy is referred to as *transverse isotropy* or *radial anisotropy*. In order to fully characterize the nature of a layered structure, one would need to determine five independent seismic wave velocities (for a more complete analysis, see BACKUS, 1962).

Consider the deformation of a layered material. For compression normal to the layer (corresponding to deformation associated with a PV-wave), stress in each layer must be identical, whereas for compression within the plane of a layer (deformation associated with a PH-wave), strain must be the same for each layer (because of the assumption that the wavelength of the wave is much larger than that of the thickness of each layer). A similar argument applies to the

[3] Using the elastic constants of a material with a hexagonal symmetry (see Chapter 4), it can easily be shown that all the coefficients of azimuthal anisotropy in equation (21.14) vanish ($B_c = B_s = C_c = C_s = E_c = G_c = G_s = 0$).

deformation associated with SH- and SV-motion. For SH-wave propagation, the particle motion is in the layering plane. By assumption the wavelength of the seismic wave is much larger than that of the thickness of each layer, and therefore the strain in each layer must be the same for SH-motion. For SV-motion, materials move vertically in each layer. Strain in each layer can be different, but stress must be the same. Therefore the elastic moduli for the two types of deformation correspond to homogeneous stress for the horizontal motion and homogeneous stress for vertical motion and hence,

$$M_{\mathrm{H}} = M_1 d_1 + M_2 d_2 \tag{21.22}$$

and

$$M_{\mathrm{V}} = \frac{1}{d_1/M_1 + d_2/M_2} \tag{21.23}$$

where $M_{1(2)}$ is the elastic modulus of phase 1 (2) and $d_1 + d_2 = 1$. It follows that for a horizontally layered structure with any elastic constants, we *always* have

$$V_{\mathrm{SH}}(V_{\mathrm{PH}}) > V_{\mathrm{SV}}(V_{\mathrm{PV}}) \tag{21.24}$$

where $V_{\mathrm{SH(SV,\,PH,\,PV)}}$ are the velocities of SH(SV, PH, PV)-waves.[4]

The contrast in elastic modulus is given by

$$\frac{M_{\mathrm{H}} - M_{\mathrm{V}}}{\langle M \rangle} \approx \phi \left(\frac{\Delta M}{\langle M \rangle} \right)^2 \tag{21.25}$$

and hence

$$\frac{V_{\mathrm{PH(SH)}} - V_{\mathrm{PV(SV)}}}{\langle V_{\mathrm{P(S)}} \rangle} \approx \frac{\phi}{2} \left(\frac{\Delta M}{\langle M \rangle} \right)^2 \tag{21.26}$$

where ϕ is the fraction of a secondary phase, $\Delta M \equiv M_1 - M_2$ and $\langle M \rangle \equiv \sqrt{M_1 M_2}$. Note that the elastic modulus ratio is proportional to the square of elastic modulus contrast. This makes sense because the elastic constant ratio does not depend on which material is softer (always $M_{\mathrm{H}} > M_{\mathrm{V}}$). But this also means that in order for this mechanism to cause significant seismic anisotropy, one needs a large contrast in elastic moduli. For example, for $\phi \sim 1\%$, $\Delta M/M$ must be on the order of 1. The only plausible mechanism for this to happen is partial melting. If $\Delta M/M \sim 10\%$, then the only way to obtain substantial anisotropy is when the fraction of secondary material is large, $\phi \sim 50\%$. The latter combination works only for special cases. A plausible case is a layering due to the stirring in a two-phase mixture such as the deformed mixture of a mixture of peridotite and eclogite (e.g., Allègre and Turcotte, 1986). Similar layering may occur in the transition zone (a mixture of garnetite and peridotite (with wadsleyite or ringwoodite)) and in the D″ layer (a mixture of paleo-oceanic crust and peridotitic components (made of perovskite and magnesiowüstite)).

When a two-phase mixture is deformed to large strains, a layered structure will be formed. However, the plane of layering is parallel to the shear plane only at infinite strain. At a finite strain there will be a finite tilt (Gay (1968) investigated the geometry of an inclusion in an infinite matrix and concluded that the tilt depends on the viscosity contrast between the inclusion and the matrix). In this case, a layered structure will result in azimuthal anisotropy with azimuthal dependence through a 2θ term (Karato, 1998e). In such a case, the sense of shear can be inferred if the sign of 2θ is determined from seismology.

21.5.2. Lattice-preferred orientation (see Chapter 14)

Most rock-forming minerals are elastically anisotropic. Therefore when the crystallographic orientations are non-random, an aggregate of minerals will show macroscopic anisotropy (when viewed at a scale significantly larger than grain size).[5] The plastic deformation of a polycrystalline material often leads to a non-random distribution of crystallographic axes called *lattice-preferred orientation* (*LPO*). LPO can also be made by anisotropic nucleation and/or growth of crystals during crystallization from melt, phase transformations and recrystallization.

Elastic anisotropy caused by LPO depends on the elastic anisotropy of constituent minerals and the orientations of each mineral (i.e., LPO). Elastic constants of most minerals are anisotropic (Chapter 4), except for garnet (see Fig. 21.2). Consequently, any non-random distribution of crystallographic axes will cause elastic anisotropy of an aggregate. A typical case is summarized in Table 21.1 where the elastic constants of deformed olivine aggregates under typical upper mantle conditions are shown based on the experimental

[4] The second subscript indicates the direction of the particle motion. Therefore PH (PV) is a P-wave that *propagates* along the horizontal (vertical) direction.

[5] The assumption that the grain size is significantly smaller than the wavelength of seismic waves is valid, except perhaps for the inner core where grain size is probably not much smaller than the wavelength of body waves (this causes significant scattering of body waves, see Chapter 17).

TABLE 21.1 Elastic constants, C_{ij} (GPa), of deformed olivine aggregates evaluated at pressure of 5 GPa and temperature of 1573 K (these are typical values and the actual values can vary from these values dependent on the strength of lattice-preferred orientation).

$i \backslash j$	1	2	3	4	5	6
A-type fabric						
1	236.3	84.5	81.5	0.4	3.4	0.3
2		218.5	82.9	− 1.8	1.2	0.3
3			208.0	− 1.3	6.1	0.2
4				64.9	− 0.1	− 1.9
5					68.7	0.3
6						66.6
B-type fabric						
1	221.3	84.3	83.3	− 0.3	0.8	1.6
2		223.5	81.7	− 1.4	1.0	1.6
3			215.5	− 1.3	1.1	− 0.4
4				68.9	0.7	− 0.4
5					67.4	− 0.4
6						69.4
C-type fabric						
1	223.2	83.6	83.3	0.3	− 3.7	0.3
2		209.8	81.9	0.8	1.5	0.3
3			228.5	0.4	− 5.9	0.2
4				67.9	0.2	− 1.9
5					71.1	0.3
6						66.6
E-type fabric						
1	236.8	82.3	84.1	− 0.6	0.4	0.1
2		207.7	82.7	− 2.6	− 0.3	− 1.0
3			217.4	− 2.1	− 1.9	− 0.7
4				65.0	0.1	0.4
5					71.1	1.4
6						68.5

Reference axes are defined as 1: shear direction, 3: shear plane normal and 2: perpendicular to both 1 and 3 directions.

data. Also note that the nature of elastic anisotropy for a given mineral can change with pressure (and temperature) (Fig. 21.14). A particularly notable case is MgO for which even the qualitative feature of anisotropy (faster or slower direction) changes with pressure (see Chapter 4). This unique feature is common to many minerals with cubic structure (e.g., ringwoodite (silicate spinel)) that have an intrinsic instability caused by the softening of C_{44} upon compression (see Chapter 4).

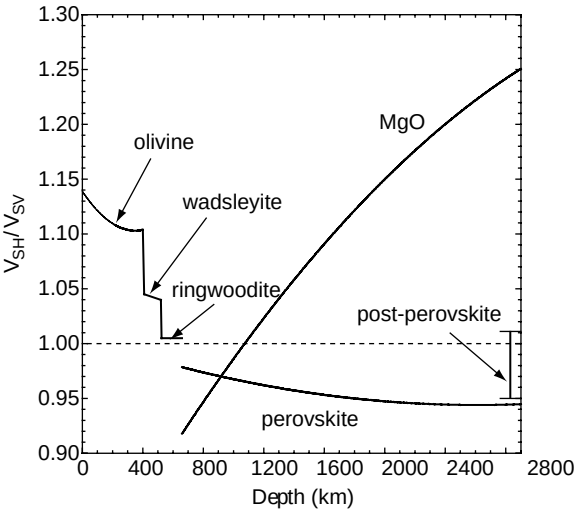

FIGURE 21.14 The depth variation of V_{SH}/V_{SV} due to the perfect alignment of major constituent minerals. The horizontal plane is assumed to be (010) for all minerals. Note the large effects of pressure on elastic anisotropy. The seismic anisotropy may change with depth due to the depth variation in LPO (the horizontal plane may change from (010) to another plane or to a more complicated LPO).

The elastic constants of an aggregate can be calculated from the elastic constants of its constituent minerals and their orientations (see Chapter 12).

Two points need to be emphasized concerning the nature of LPO. First, LPO will be developed by plastic deformation only when deformation occurs by some specific mechanisms (dislocation creep and/or twinning). Among them, deformation by dislocation creep is the most important mechanism to cause LPO in Earth's interior. Deformation by diffusional creep (or grain-boundary sliding) does not usually produce LPO. Deformation by dislocation creep (or twinning) occurs at relatively high stress and/or large grain size. Consequently, anisotropic structures tend to develop in certain regions in Earth where stress is high (i.e., boundary layers, see KARATO, 1998d; MONTAGNER, 1998).

Second, when deformation is due to dislocation creep, the resultant LPO depends on (i) the physical and chemical conditions of deformation and (ii) the geometry of deformation (and in some cases the geometry of stress and other fields such as the magnetic field). The physical conditions of deformation control the relative ease of deformation by different slip systems. The relative contributions from different slip systems determine the nature of LPO for a given deformation geometry. Consequently, in order to infer the geometry of deformation from seismic anisotropy, one needs to know the dominant slip system(s) under a given physical and chemical condition.

One obvious, but important conclusion is that the relation between seismic anisotropy and the geometry of flow is mineral specific and also depends on the physical and chemical conditions. The $V_{SH}/V_{SV} > 1$ corresponds to the horizontal flow for a case where anisotropy is caused by LPO of olivine under limited conditions (A-, B-, E-type, but not for C-type; for olivine LPO see Chapter 14, also see Problem 12.6), but is not necessarily true for other conditions and for other minerals. Similarly, the notion that the direction of polarization of the faster S-wave is parallel to the flow direction is true only for the olivine-dominated case under limited physical and chemical conditions (A-, C- and E-type, but not for B-type). It is also important to recall that the nature of elastic anisotropy can change with pressure (and temperature). In short, both elastic and plastic anisotropies are different among different minerals, and both of them can change with physical and chemical conditions, and therefore the relation between seismic anisotropy and the nature of flow (e.g., flow geometry) can change from one region of Earth to another. *In order to interpret seismic anisotropy in terms of geodynamics in one region (say the lower mantle), one needs to know the relation between seismic anisotropy and the nature of flow appropriate for materials in that region. A relation appropriate for a certain region of Earth (e.g., the lithosphere) cannot be applied to other regions in general.*

Important progress in recent years includes: (i) experimental studies on the variation of LPO (in olivine) under various physical and chemical conditions that have revealed a rich variety of LPO (e.g., Jung and Karato, 2001b; Katayama *et al.*, 2004; Jung *et al.*, 2006; Katayama and Karato, 2006), and (ii) the new development of a high-pressure large-strain deformation technique (e.g., Xu *et al.*, 2005) that allows us to investigate LPOs in deep Earth materials. (iii) Also there has been much progress in the numerical modeling of LPO (e.g., Kaminski and Ribe, 2001; Kaminski, 2002; Wenk, 2002). One advantage of this approach is the ability to simulate complicated deformation history. However, a major limitation of this approach is the fact that most of the conclusions from this approach, such as the geometry of LPO and the rate at which LPO changes with deformation, hinge on the material properties that are not always well constrained.

Problem 21.6

Using the results given in Table 21.1, calculate V_{SH}/V_{SV} for A-, B-, C- and E-type olivine fabric corresponding to the horizontal shear. Also calculate the direction of the polarization of the faster shear waves.

Solution

Simply use the numbers from Table 21.1 into equation (21.21) to obtain: $V_{SH}/V_{SV} = 1.02$ (A-type), 1.01 (B-type), 0.98 (C-type) and 1.01 (E-type). The direction of polarization can be inferred from the comparison of C_{44} and C_{55}. For A-, C- and E-type fabrics, $C_{55} > C_{44}$ and therefore the polarization of the fast S-wave is along the x_1 direction (flow direction), whereas for B-type fabric $C_{55} < C_{44}$, so the flow direction is normal to the polarization direction of the fast S-wave.

21.6. Geodynamic interpretation of seismic anisotropy

21.6.1. Generalities

The first issue in the geodynamic interpretation of anisotropy is to identify the type of anisotropic structure that causes seismic anisotropy, namely either it is due to a layered structure or to lattice-preferred orientation (LPO). This can be made through several methods. For example, anisotropy due to horizontal layering would result in transverse isotropy, namely a type of anisotropy in which wave propagation is isotropic in the horizontal plane. Therefore if azimuthal anisotropy is significant, one can conclude that horizontal layering is unlikely to be the cause of anisotropy. One caveat in this inference, however, is that even in strictly horizontal shear flow, the resulting layered structure may have some tilt (Karato, 1998e). In this case, the structure will have azimuthal anisotropy where the seismic wave velocities depend on 2θ. If anisotropy is found to be due to LPO, then one needs to find out the relation between LPO and flow field for the materials in the relevant region of Earth.

21.6.2. Seismic anisotropy and its geodynamic implications

Gross distribution of anisotropy in Earth's interior

Figure 21.15 shows a gross depth distribution of anisotropy in Earth's interior. Distribution of anisotropy is three dimensional and this diagram is certainly an oversimplification of the actual distribution, but does show some essential features. The average amplitude of

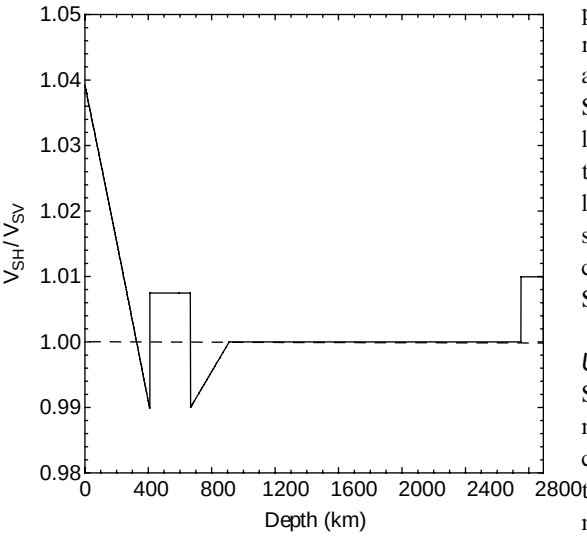

FIGURE 21.15 The depth variation of the polarization anisotropy, V_{SH}/V_{SV}, in the Earth's mantle (after MONTAGNER and KENNETT, 1996).

seismic anisotropy is large in the shallow Earth (upper mantle) and at the very bottom (D″ layer). The amplitude of anisotropy in the inner core (not shown) is again large. The depth variation of seismic anisotropy partly reflects the depth variation of elastic anisotropy of constituent materials, but it also reflects the depth variation of dynamic processes that cause LPO. For example, the elastic anisotropy of minerals in the upper mantle does not change with depth so much whereas the amplitude of anisotropy decreases significantly with depth. Similarly, the elastic anisotropy of lower mantle minerals is comparable to that of the upper mantle, yet the amplitude of anisotropy of the bulk of the lower mantle is much less than that of the upper mantle. These observations suggest that the depth variation of the amplitude of seismic anisotropy mainly reflects the depth variation in the dynamic processes of Earth's interior.

Crust

The deformation of the crust occurs mostly by brittle fracture in its shallow part (e.g., continental upper crust) but by ductile deformation in the deeper part (e.g., continental lower crust). Consequently, the most important anisotropic structure in the shallow crust is aligned cracks (i.e., SPO). In this case, the pattern of anisotropy reflects the stress field as opposed to the strain field[6] (e.g., CRAMPIN, 1978; KANESHIMA, 1990). In the lower crust, however, deformation occurs by plastic flow. Most of the plastically deformed crustal rocks show significant lattice-preferred orientation and have some degree of elastic anisotropy (e.g., SIEGESMUND *et al.*, 1989). However, the anisotropic layer in the crust is thin (compared to the mantle) and the anisotropic structure is not always persistent at a large scale, and consequently, there is a relatively small signal from the crustal anisotropy in the seismic record compared to those from the upper mantle (e.g., SILVER, 1996).

Upper mantle

Seismic anisotropy in the upper mantle is well documented both by body- and surface-wave studies. The classic work by RAITT *et al.* (1969) demonstrated the azimuthal anisotropy in the uppermost oceanic mantle. They found significant azimuthal anisotropy of P-waves ($\sim \pm 3\%$), the fast direction nearly parallel to the (paleo) spreading direction. Global studies include TANIMOTO and ANDERSON (1984, 1985), MONTAGNER and TANIMOTO (1990, 1991), MONTAGNER and RITSEMA (2001), BEGHEIN and TRAMPERT (2003a). Seismic anisotropy in the upper mantle is in most cases attributed to the lattice-preferred orientation of minerals particularly that of olivine (e.g., NICOLAS and CHRISTENSEN, 1987). The role of layering such as layering of partial melt was also suggested (e.g., AKI, 1968; BLACKMAN and KENDALL, 1997), but evidence for melt-induced anisotropy has not been convincingly demonstrated yet. In fact, one of the most striking observations on the oceanic upper mantle is the failure to observe evidence for partial melting from shear wave splitting measurements near a mid-ocean ridge (e.g., WOLFE and SOLOMON, 1998). Melt appears to be concentrated in very narrow regions beneath a mid-ocean ridge.

When anisotropy is attributed to LPO, then the relation between LPO and the tectonic field must be understood to interpret seismic anisotropy in terms of tectonic field. The classic work by Nicolas (reviewed in NICOLAS and CHRISTENSEN, 1987; BEN ISMAIL and MAINPRICE, 1998) is used in most geodynamic interpretations of upper mantle seismic anisotropy (e.g., VAUCHEZ and NICOLAS, 1991; NICOLAS, 1993; SILVER, 1996; SAVAGE, 1999; MONTAGNER and GUILLOT, 2000; TOMMASI *et al.*, 2000). In this model, anisotropy is due mainly to the A-type olivine fabric. Consequently, the direction of polarization of the fast shear wave is parallel to the flow direction, the direction of the fast Rayleigh wave is parallel to the flow direction and $V_{SH}/V_{SV} > 1$ (< 1) corresponds to the

[6] The distinction between stress and strain is critical for finite strain (see Chapter 1).

horizontal (vertical) flow. Such a relation was used to infer the convection pattern in the upper mantle (e.g., Tanimoto and Anderson, 1984; Nataf *et al.*, 1986). The observed convergent boundary-parallel shear wave splitting is interpreted, in this model, by the shear motion *along* the convergent boundary called *transpression* (e.g., Nicolas, 1993). When this model is applied to interpret subduction zone anisotropy, then one needs to invoke a complicated flow pattern where flow near the trench is dominated by trench parallel flow as opposed to trench normal flow (e.g., Russo and Silver, 1994; Smith *et al.*, 2001). A major challenge to this paradigm came from the experimental finding that olivine LPO changes with physical and chemical conditions particularly with water content as reviewed in Chapter 14 (Jung and Karato, 2001b). When deformation in olivine occurs (with some water) at relatively low temperatures (above a certain stress), then the direction of polarization of the faster shear wave will be perpendicular to the flow direction (B-type fabric). Similarly, when olivine is deformed at high temperature with a large amount of water, then the horizontal flow will result in $V_{SH}/V_{SV} < 1$ (C-type fabric). Karato (2003b) proposed an alternative model to explain trench-parallel (or convergent boundary-parallel) anisotropy by the B-type olivine fabric. Kneller *et al.* (2005) made a detailed numerical modeling to investigate the spatial variation of olivine LPO in the subduction zones. However, in most of the lithosphere or in the asthenosphere, olivine fabric is either A-, E- or C-type, and consequently, the correlation between the fast shear waves (Rayleigh waves) and flow pattern is similar to what has been assumed based on the A-type olivine fabric (see Problem 12.6). There is evidence of convergent boundary-parallel flow in the structures of deformed rocks from the shallow upper mantle (e.g., Nicolas, 1993; Mehl *et al.*, 2003). However, the degree to which transpression occurs at a greater depth is not known. To distinguish these models, it is critical to map out the depth variation of anisotropy in the subduction zone.

In addition to olivine, another volumetrically important mineral that may affect seismic anisotropy is orthopyroxene. However, the LPO of orthopyroxene is less extensively studied than that of olivine (e.g., Christensen and Lundquist, 1982).

Transition zone

The transition zone is the key to a number of geodynamic problems. In Chapter 20, we learned that there is evidence for a significant modification to the convection pattern in the transition zone. Therefore one expects a signature in the seismic anisotropy of a change in flow pattern in the transition zone. However, very little is known about the nature of anisotropy in the transition zone at the present time. Earlier works using shear wave splitting suggested only weak anisotropy in the transition zone (e.g., Fischer and Wiens, 1996), but the resolution of these studies is not high. Some later studies using overtones of surface waves or free oscillations have revealed some degree of anisotropy in the transition zone. Montagner and Kennett (1996) and Beghein and Trampert (2003a) showed evidence for SH–SV polarization anisotropy in the transition zone. Trampert and van Heijst (2002) showed the presence of azimuthal anisotropy (see also Vinnik and Montagner, 1996). The pattern of transition zone azimuthal anisotropy, from their study, is quite distinct from that of the upper mantle. However, the geodynamic significance of this observation is unknown because we do not know the nature of LPO of minerals in the transition zone (at the time of writing, 2007). In the transition zone, a volumetrically important mineral that has a large elastic anisotropy is wadsleyite (in the upper transition zone). However the LPO of wadsleyite is not well known. Tommasi *et al.* (2004) presented the results of numerical modeling of LPO in wadsleyite and discussed the geodynamic implications of transition zone anisotropy. However, the results of such a model depend entirely on the assumed plastic anisotropy of wadsleyite that is unconstrained at the present time. In the lower transition zone, volumetrically important minerals, i.e., ringwoodite and majorite, are all nearly elastically isotropic and they cannot contribute to seismic anisotropy. If there is any seismic anisotropy present it must be due to a layered structure or LPO of a volumetrically small but highly anisotropic mineral such as akimotoite (silicate ilmenite).

Lower mantle

The majority of the lower mantle is devoid of anisotropy. This was first noted by the study of shear wave splitting by Meade *et al.* (1995), who showed that the magnitude of shear wave splitting from most of the lower mantle is less than ~ 0.2 s. This is surprising because the lower mantle minerals are elastically as anisotropic as upper mantle minerals (Figs. 21.2 and 21.15). Karato *et al.* (1995b) compared this value with the expected shear wave splitting resulting from LPO in perovskite (and magnesiowüstite) (~ 10 to

$\sim$20 s) and concluded that the most likely cause for the lack of anisotropy is that lower mantle minerals deform by diffusional creep (or superplasticity). The absence of anisotropy is also suggested by the analysis of free oscillation (Montagner and Kennett, 1996). However, anisotropy does exist in some regions of the lowermost mantle (e.g., Vinnik *et al.*, 1995; Kendall and Silver, 1996, 1998; Garnero *et al.*, 2004).

The absence of strong anisotropy in the bulk of the lower mantle, and the presence of significant anisotropy in the D″ layer can be naturally explained by the dynamics of mantle convection and the general nature of deformation mechanisms in polycrystalline aggregates. The D″ layer is likely to be a boundary layer of convecting mantle and therefore deformation there probably occurs at higher stress and strain than deformation elsewhere. If this view is combined with another well-established mineral physics concept that LPO develops only at high stress, then the localized distribution of anisotropy can be attributed to the stress–strain distribution and the change in deformation mechanisms in minerals (Karato, 1998d). In particular, Karato (1998e) emphasized the role of highly anisotropic (Mg, Fe)O (see also Yamazaki and Karato, 2002). This hypothesis has been explored by numerical modeling (McNamara *et al.*, 2001, 2002, 2003) who showed that anisotropy in the lower mantle is confined to regions where subducted slabs collide at the core–mantle boundary in which deformation occurs at high stress to large strains. A serious limitation to current knowledge is the lack of definitive experimental data on the LPO of silicate perovskite. Karato *et al.* (1995b) determined the LPO of $CaTiO_3$ perovskite (an orthorhombic perovskite) under the high-temperature, power-law dislocation creep regime, and inferred that the [100](010) slip system dominates. But a similar study on (Mg, Fe)SiO_3 perovskite is missing at this time (2007).

Panning and Romanowicz (2004) reported highly variable anisotropy in the D″ layer beneath the central Pacific and suggested that variable anisotropy might reflect a complicated flow pattern in that region from which plumes are considered to rise. However, the mineral physics basis for such an inference is missing because the relation between the anisotropic structure of minerals in the D″ layer and the flow pattern is not yet well known. Similarly, a detailed study on anisotropy was conducted in the D″ layer beneath Cocos plate (Rokosky *et al.*, 2004). A major complication to the interpretation of D″ layer anisotropy is the discovery of a post-perovskite phase. According to theoretical calculations, this phase is likely to have modest elastic anisotropy (Oganov and Ono, 2004; Tsuchiya *et al.*, 2004a), and therefore its role in seismic anisotropy needs to be included in the analysis, but the nature of LPO of this mineral is not known. Oganov *et al.* (2005) estimated the slip system of a post-perovskite phase based on the first-principle calculation in which the concept of crystal dislocation is not included. They predicted slip planes of (110). However, the recent experimental results on an analog material of post-perovskite ($CaIrO_3$) by Yamazaki *et al.* (2006) show a slip plane of (010) (with a slip direction of [100]). I note that the validity of the use of analog materials to infer the dominant slip system is unknown. For materials with a B-1 structure (NaCl-type crystals), NaCl and MgO show quite different LPOs. The slip systems and LPO of perovskite and post-perovskite phases of (Mg, Fe)SiO_3 are poorly constrained at this time.

In addition to the anisotropy in the D″ layer, there are reports on anisotropy in the top lower mantle (Wookey *et al.*, 2002; Wookey and Kendall, 2004). These authors reported evidence for anisotropy by shear wave splitting and the nature of anisotropy there is $V_{SH} > V_{SV}$. Anisotropy caused by (Mg, Fe)O will be very small there because the elastic properties of (Mg, Fe)O at this depth are nearly isotropic. Consequently, anisotropy in the shallow lower mantle is likely to be caused by LPO of perovskite, but the nature of LPO in perovskite is poorly known at this time.

Inner core

The inner core, the central part of Earth, has strong anisotropy (e.g., Song, 1997; Tromp, 2001). To a good approximation, anisotropy has an axial symmetry and P-waves propagate faster along the rotation axis than perpendicular to it (by $\sim$3%). The presence of strong anisotropy in the inner core is remarkable. The inner core is very likely to be in a calm environment because the lateral variation in temperature should be low because of the efficient heat transfer both in the outer and the inner core. Melt-induced anisotropy (aligned melt pocket) was suggested by Singh *et al.* (2000), but the presence of a significant melt fraction is unlikely because of efficient compaction due to gravity (Sumita *et al.*, 1996). Therefore anisotropy due to LPO is the most likely cause. Indeed, the material composing the inner core of Earth is most likely to be hcp iron, which has a highly anisotropic crystal structure and hence anisotropic elastic constants. This anisotropy also implies that either plastic deformation in the inner

core occurs by dislocation creep or the crystallization of hcp iron occurs anisotropically or both. If the latter is the dominant mechanism, then the influence of deformation must be small.

Since the stress levels in the inner core are likely to be low, it is not obvious if dislocation creep operates or not. Consequently, KARATO (1993b) and BERGMAN (1997) proposed that LPO in the inner core may develop by anisotropic crystallization. Similarly, YOSHIDA *et al.* (1996) proposed that LPO in the inner core may develop by stress-induced grain-boundary migration. However, as I discussed in Chapter 17, the grain size of the inner core is likely to be large, of the order of 100–1000 m. In such a case, dislocation creep can operate if stress is modest (e.g., above $\sim 10^2$ Pa). After the evaluation of various sources of stress in the inner core (KARATO, 1999, 2000) concluded that the stress caused by the magnetic field is the most important stress in the inner core. In this case, there is a connection between the magnetic field and the anisotropy of the inner core, and seismological observations of anisotropy may provide a clue as to the generation of a geomagnetic field. However, the details of flow due to the magnetic force are unknown (also see BUFFETT and BLOXHAM, 2000).

References

Aaronson H. I. (1990) Atomic mechanisms of diffusional nucleation and growth and comparisons with their counterparts in shear transformations. *Metallurgical Transactions A* **24**, 241–276.

Abe Y. (1997) Thermal and chemical evolution of terrestrial magma ocean. *Physics of Earth and Planetary Interiors* **100**, 27–39.

Adams B. L., Wright S. I., and Kunze K. (1993) Orientation imaging: the emergence of a new microscopy. *Metallurgical Transactions A* **24**, 819–831.

Agee C. B. (1993) Petrology of the mantle transition zone. *Annual Review of Earth and Planetary Sciences* **21**, 19–42.

Aines R. D. and Rossman G. R. (1984) The hydrous component in garnets: pyralsites. *American Mineralogist* **69**, 1116–1126.

Aizawa Y., Yoneda A., Katsura T., Ito E., Saito T., and Suzuki I. (2004) Temperature derivatives of elastic moduli of $MgSiO_3$ perovskite. *Geophysical Research Letters* **31**, 10.1029/2003GL018762.

Akaogi M., Ito E., and Navrotsky A. (1989) Olivine-modified spinel–spinel transitions in the system Mg_2SiO_4–Fe_2SiO_4: calorimetric measurements, thermochemical calculation, and geophysical application. *Journal of Geophysical Research* **94**, 15 671–15 685.

Aki K. (1968) Seismological evidence for the existence of soft thin layers in the upper mantle under Japan. *Journal of Geophysical Research* **73**, 585–594.

Aki K., Christoffersson A., and Husebye F. S. (1977) Determination of three-dimensional seismic structure of the lithosphere. *Journal of Geophysical Research* **82**, 277–296.

Aki K. and Kaminuma K. (1963) Phase velocity of Love waves in Japan (part 1): Love waves from the Aleutian shock of March 1957. *Bulletin of Earthquake Research Institute* **41**, 243–259.

Aki K. and Richards P. G. (2002) *Quantitative Seismology*. University Science Books.

Akimoto S., Akaogi M., Kawada K., and Nishizawa O. (1976) Mineralogic distribution of iron in the upper half of the transition zone in the Earth's mantle. In *The Geophysics of the Pacific Ocean Basin and Its Margin*, pp. 399–405. American Geophysical Union.

Akulov N. S. (1964) On dislocation kinetics. *Acta Metallurgica* **12**, 1195–1196.

Alfé D., Gillan M. J., and Price G. D. (2002a) Composition and temperature of Earth's core constrained by combining *ab-initio* calculations and seismic data. *Earth and Planetary Science Letters* **95**, 91–98.

Alfé D., Price G. D., and Gillan M. J. (2000) Constraints on the composition of the Earth's core from *ab-initio* calculations. *Nature* **405**, 172–175.

Alfé D., Price G. D., and Gillan M. J. (2002b) *Ab initio* chemical potentials of solid and liquid alloys and the chemistry of the Earth's core. *Journal of Chemical Physics* **116**, 7127–7136.

Allègre C. J. and Turcotte D. L. (1986) Implications of a two-component marble-cake mantle. *Nature* **323**, 123–127.

Allen F. M., Smith B. K., and Buseck P. R. (1987) Direct observation of dissociated dislocations in garnet. *Science* **238**, 1695–1697.

Amadeo R. J. and Ghoniem N. M. (1988) A review of experimental observations and theoretical models of dislocation cells and subgrains. *Res Mechanica* **23**, 137–160.

Amin K. E., Mukherjee A. K., and Dorn J. E. (1970) A universal law for high-temperature diffusion controlled transient creep. *Journal of Mechanics and Physics of Solids* **18**, 413–426.

Anand L., Kim K. H., and Shawki T. G. (1987) Onset of shear localization in viscoplastic solids. *Journal of Mechanics and Physics of Solids* **35**, 407–429.

Anderson D. L. (1979) The deep structure of continents. *Journal of Geophysical Research* **84**, 7555–7560.

Anderson D. L. (1987a) A seismic equation of state II. Shear properties and thermodynamics of the lower mantle. *Physics of Earth and Planetary Interiors* **45**, 307–323.

Anderson D. L. (1987b) Thermally induced phase changes, lateral heterogeneity of the mantle, continental roots, and deep slab anomalies. *Journal of Geophysical Research* **92**, 13 968–13 980.

Anderson D. L. and Bass J. D. (1986) Transition region of the Earth's upper mantle. *Nature* **320**, 321–328.

Anderson D. L. and Given J. W. (1982) Absorption band Q model for the Earth. *Journal of Geophysical Research* **87**, 3893–3904.

Anderson D. L. and Minster J. B. (1979) The frequency dependence of Q in the Earth and implications for mantle rheology and Chandler wobble. *Geophysical Journal of Royal Astronomical Society* **58**, 431–440.

Anderson D. L., Sammis C. G., and Phinney R. A. (1969) Brillouin scattering – A new geophysical tool. In *The Application of Modern Physics to the Earth and Planetary Interiors* (ed. S. K. Runcorn), pp. 465–477. Wiley-Interscience.

Anderson D. L., Tanimoto T., and Zhang Y. (1992) Plate tectonics and hotspots – the third dimension. *Science* **256**, 1645–1651.

Anderson O. L. (1968) Comments on the negative pressure dependence of the shear modulus found in some oxides. *Journal of Geophysical Research* **73**, 7707–7712.

Anderson O. L. (1996) *Equation of State of Solids for Geophysics and Ceramic Sciences*. Oxford University Press.

Anderson O. L. (2002) The three-dimensional phase diagram of iron. In *Earth's Core: Dynamics, Structure, Rotation* (ed. V. Dehant, K. C. Creager, S. Karato, and S. Zatman), pp. 83–103. American Geophysical Union.

Anderson O. L. and Isaak D. G. (1995) Elastic constants of mantle minerals at high temperature. In *Mineral Physics & Crystallography* (ed. T. J. Ahrens), pp. 64–97. American Geophysical Union.

Anderson O. L. and Liebermann R. C. (1970) Equations for elastic constants and their pressure derivatives for three cubic lattices and some geophysical applications. *Physics of Earth and Planetary Interiors* **3**, 61–85.

Ando J., Shibata Y., Okajima Y., Kanagawa K., and Furusho M. (2001) Striped iron zoning of olivine induced by dislocation creep in deformed olivine. *Nature* **414**, 893–895.

Ando K. (1989) Self-diffusion in oxides. In *Rheology of Solids and of the Earth* (ed. S. Karato and M. Toriumi), pp. 57–82. Oxford University Press.

Andrade E. N. d. C. (1910) On the viscous flow in metals and allies phenomena. *Proceedings of the Royal Society of London A* **84**, 1–12.

Andrault D., Fiquet G., Guyot F., and Hanfland M. (1998) Pressure-induced Landau-type transition in stishovite. *Science* **282**, 720–724.

Ardell A. J. (1997) Harper–Dorn creep – Prediction of the dislocation network theory of high temperature deformation. *Acta Materialia* **45**, 2971–2981.

Argon A. S. (1973) Stability of plastic deformation. In *The Inhomogeneity of Plastic Deformation* (ed. R. E. Reed-Hill), pp. 161–189. American Society of Metals.

Artemieva I. M. (2006) Global $1^{\circ} \times 1^{\circ}$ thermal model TC1 for the continental lithosphere: implications for lithosphere secular evolution. *Tectonophysics* **416**, 245–277.

Arzi A. A. (1978) Critical phenomena in the rheology of partially melted rocks. *Tectonophysics* **44**, 173–184.

Arzt E., Ashby M. F., and Verrall R. A. (1983) Interface controlled diffusional creep. *Acta Metallurgica* **31**, 1977–1989.

Ashby M. F. (1969) On interface reaction-control of Nabarro–Herring creep and sintering. *Scripta Metallurgica* **3**, 837–842.

Ashby M. F. (1970) The deformation of plastically non-homogeneous crystals. *Philosophical Magazine* **21**, 399–424.

Ashby M. F. (1972) A first report on deformation-mechanism maps. *Acta Metallurgica* **20**, 887–897.

Ashby M. F. and Brown A. M. (1982) Flow in polycrystals and the scaling of mechanical properties. In *Deformation of Polycrystals: Mechanisms and Microstructures* (ed. N. Hansen, A. Horsewell, T. Leffers, and H. Lilholt), pp. 1–13. RISØ National Laboratory.

Ashby M. F., Edward G. H., Davenport J., and Verrall R. A. (1978) Application of bound theorems for creeping solids and their application to large strain diffusional flow. *Acta Metallurgica* **26**, 1379–1388.

Ashby M. F. and Verrall R. A. (1973) Diffusion accommodated flow and superplasticity. *Acta Metallurgica* **21**, 149–163.

Atkinson H. V. (1988) Theories of normal grain growth in pure single phase systems. *Acta Metallurgica* **36**, 469–491.

Auten T. A., Davis L. A., and Gordon R. B. (1973) Hydrostatic pressure and the mechanical properties of NaCl polycrystals. *Philosophical Magazine* **28**, 335–341.

Auten T. A., Radcliffe S. V., and Gordon R. B. (1976) Flow stress of MgO single crystals compressed along [100] at high hydrostatic pressure. *Journal of the American Ceramic Society* **59**, 40–42.

Avé Lallemant H. G. (1978) Experimental deformation of diopside and websterite. *Tectonophysics* **48**, 1–27.

Avé Lallemant H. G. and Carter N. L. (1970) Syntectonic recrystallization of olivine and modes of flow in the upper mantle. *Geological Society of America Bulletin* **81**, 2203–2220.

Avé Lallemant H. G., Mercier J.-C. C., and Carter N. L. (1980) Rheology of the upper mantle: inference from peridotite xenoliths. *Tectonophysics* **70**, 85–114.

Backus G. E. (1962) Long wave elastic anisotropy produced by horizontal layering. *Journal of Geophysical Research* **67**, 4427–4440.

Bai Q., Mackwell S. J., and Kohlstedt D. L. (1991) High temperature creep of olivine single crystals 1. Mechanical results for buffered samples. *Journal of Geophysical Research* **96**, 2441–2463.

Bai Y. L. (1982) Thermo-plastic instability in simple shear. *Journal of Mechanics and Physics of Solids* **30**, 195–207.

Bamford D. (1977) P_n velocity anisotropy in a continental upper mantle. *Geophysical Journal of Royal Astronomical Society* **57**, 397–429.

Barrat J.-L. and Hansen J.-P. (2003) *Basic Concepts for Simple and Complex Liquids*. Cambridge University Press.

Bass J. D. (1995) Elasticity of minerals, glasses, and melts. In *Mineral Physics and Crystallography: a Handbook of Physical Constants* (ed. T. J. Ahrens), pp. 46–63. American Geophysical Union.

Bass J. D., Weidner D. J., Hamaya N., Ozima M., and Akimoto S. (1984) Elasticity of the olivine and spinel polymorphs of Ni_2SiO_4. *Physics and Chemistry of Minerals* **10**, 261–272.

Beauchesne S. and Poirier J.-P. (1989) Creep of barium titanate perovskite: a contribution to a systematic approach to the viscosity of the lower mantle. *Physics of Earth and Planetary Interiors* **55**, 187–199.

Beauchesne S. and Poirier J.-P. (1990) In search of systematics for the viscosity of perovskite: creep of potassium tantalate and niobate. *Physics of Earth and Planetary Interiors* **61**, 182–198.

Becker T. W., Kellogg J. B., and O'Connell R. J. (1999) Thermal constraints on the survival of primitive blobs in the lower mantle. *Earth and Planetary Science Letters* **171**, 351–365.

Beghein C. and Trampert J. (2003a) Probability density functions for radial anisotropy: implications for the upper 1200 km of the mantle. *Earth and Planetary Science Letters* **217**, 151–162.

Beghein C. and Trampert J. (2003b) Robust normal mode constraints on inner-core anisotropy from model space search. *Science* **299**, 552–555.

Behrmann J. H. and Mainprice D. (1987) Deformation mechanisms in a high temperature quartz–feldspar mylonite: evidence for superplastic flow in the lower continental crust. *Tectonophysics* **140**, 297–305.

Béjina F., Jaoul O., and Liebermann R. C. (1999) Activation volume of Si diffusion in San Carlos olivine: implications for upper mantle rheology. *Journal of Geophysical Research* **104**, 25 529–25 542.

Bell D. R. and Rossman G. R. (1992) Water in Earth's mantle: the role of nominally anhydrous minerals. *Science* **255**, 1391–1397.

Bell D. R., Rossman G. R., Maldener J., Endisch D., and Rauch F. (2003) Hydroxide in olivine: a quantitative determination of the absolute amount and calibration of the IR spectrum. *Journal of Geophysical Research* **108**, 10.1029/2001JB000679.

Bell T. H. and Etheridge M. A. (1973) Microstructures of mylonites and their descriptive terminology. *Lithos* **6**, 337–348.

Ben Ismail W. and Mainprice D. (1998) An olivine fabric database: an overview of upper mantle fabrics and seismic anisotropy. *Tectonophysics* **296**, 145–157.

Benn K. and Allard B. (1989) Preferred mineral orientations related to magmatic flow in ophiolite layered gabbros. *Journal of Petrology* **30**, 925–946.

Bennington K. O. (1963) Some crystal growth features of sea ice. *Journal of Glaciology* **4**, 669–688.

Benz H. and Vidale J. E. (1993) Sharpness of upper-mantle discontinuities determined from high-frequency reflections. *Nature* **365**, 147–150.

Beran A. and Libowitzky E. (2006) Water in natural mantle minerals II: olivine, garnet and accessary minerals. In *Water in Nominally Anhydrous Minerals* (ed. H. Keppler and J. R. Smyth), pp. 169–191. Mineralogical Society of America.

Berckhemer H., Kampfmann W., Aulbach E., and Schmeling H. (1982) Shear modulus and Q of forsterite and dunite near partial melting from forced oscillation experiments. *Physics of Earth and Planetary Interiors* **29**, 30–41.

Bercovici D. (2003) The generation of plate tectonics from mantle convection. *Earth and Planetary Science Letters* **205**, 107–121.

Bercovici D. and Karato S. (2002) Some theoretical concepts of shear localization in the lithosphere. In *Plastic Deformation of Minerals and Rocks* (ed. S. Karato and H.-R. Wenk), pp. 387–420. American Mineralogical Society.

Bercovici D. and Karato S. (2003) Whole mantle convection and transition-zone water filter. *Nature* **425**, 39–44.

Bercovici D. and Ricard Y. (2003) Energetics of two-phase model of lithospheric damage, shear localization and plate-boundary formation. *Geophysical Journal International* **152**, 1–16.

Bercovici D. and Ricard Y. (2005) Tectonic plate generation and two-phase damage: void growth versus grain-size reduction. *Journal of Geophysical Research* **110**, 10.1029/2004JB003181.

Bercovici D., Ricard Y., and Schubert G. (2001a) A two-phase model for compaction and damage 1. General theory. *Journal of Geophysical Research* **106**, 8887–8906.

Bercovici D., Ricard Y., and Schubert G. (2001b) A two-phase model for compaction and damage 3. Applications to shear localization and plate boundary formation. *Journal of Geophysical Research* **106**, 8925–8939.

Bergman M. I. (1997) Measurements of elastic anisotropy due to solidification texturing and the implications for the Earth's inner core. *Nature* **389**, 60–63.

Bergman M. I. (1998) Estimates of the Earth's inner core grain size. *Geophysical Research Letters* **25**, 1593–1596.

Berthe D., Choukrouse P., and Jegouzo P. (1979) Orthogneiss, mylonite and non coaxial deformation of granite: the

example of the South American shear zone. *Journal of Structural Geology* **1**, 31–42.

Bethe H. A. (1935) Statistical theory of superlattice. *Proceedings of the Royal Society of London A* **150**, 552–575.

Bhattacharya J., Shearer P. M., and Masters G. (1993) Inner core attenuation for short-period PKP (BC) versus PKP (DF) waveforms. *Geophysical Journal International* **114**, 1–11.

Bilde-Sorenson J. B. and Smith D. A. (1994) Comment on 'Refutation of the relationship between denuded zones and diffusional creep'. *Scripta Metallurgica et Material* **30**, 383–386.

Billen M. I. and Gurnis M. (2001) A low viscosity wedge in subduction zones. *Earth and Planetary Science Letters* **193**, 227–236.

Billen M. I., Gurnis M., and Simons M. (2003) Multiscale dynamics of the Tonga–Kermadec subduction zone. *Geophysical Journal International* **153**, 359–388.

Billien M., Lébeque J.-J., and Trampert J. (2000) Global maps of Rayleigh wave attenuation for periods between 40 and 150 seconds. *Geophysical Research Letters* **27**, 3619–3622.

Bina C. B. and Helffrich G. (1994) Phase transition Clapeyron slopes and transition zone seismic discontinuity topography. *Journal of Geophysical Research* **99**, 15 853–15 860.

Birch F. (1952) Elasticity and constitution of the Earth's interior. *Journal of Geophysical Research* **57**, 227–286.

Birch F. (1961) The velocity of compressional waves in rocks to 10 kilobars, Part 2. *Journal of Geophysical Research* **66**, 2199–2224.

Birch F. (1964) Density and composition of mantle and core. *Journal of Geophysical Research* **69**, 4377–4388.

Blacic J. D. (1972) Effects of water in the experimental deformation of olivine. In *Flow and Fracture of Rocks* (ed. H. C. Heard, I. Y. Borg, N. L. Carter, and C. B. Raleigh), pp. 109–115. American Geophysical Union.

Blacic J. D. (1975) Plastic-deformation mechanisms of quartz: the effect of water. *Tectonophysics* **27**, 271–294.

Blackman D. K. and Kendall J.-M. (1997) Sensitivity of teleseismic body waves to mineral texture and melt in the mantle beneath a mid-ocean ridge. *Philosophical Transactions of Royal Society of London A* **355**, 217–231.

Bloomfield J. P. and Covey-Crump S. J. (1993) Correlating mechanical data with microstructural observations in deformation experiments on synthetic two-phase aggregates. *Journal of Structural Geology* **15**, 1007–1019.

Bloss F. D. (1971) *Crystallography and Crystal Chemistry*. Holt, Reinhart and Winston, Inc.

Blum J. and Shen Y. (2004) Thermal, hydrous, and mechanical states of the mantle transition zone beneath southern Africa. *Earth and Planetary Science Letters* **217**, 367–378.

Blum W., Eisenlohr P. and Breutinger F. (2002) Understanding creep – A review. *Metallurgical and Materials Transactions A* **33**, 291–303.

Boland J. N. and Tullis T. E. (1986) Deformation behaviour of wet and dry clinopyroxenite in the brittle to ductile transition region. In *Mineral and Rock Deformation: Laboratory Studies* (ed. B. E. Hobbs and H. C. Heard), pp. 35–50. American Geophysical Union.

Bolfan-Casanova N. (2005) Water in the Earth's mantle. *Mineralogical Magazine* **69**, 229–257.

Bolfan-Casanova N., Keppler H., and Rubie D. C. (2000) Water partitioning between nominally anhydrous minerals in the MgO-SiO_2-H_2O system up to 24 GPa: implications for the distribution of water in the Earth's mantle. *Earth and Planetary Science Letters* **182**, 209–221.

Bolfan-Casanova N., Keppler H., and Rubie D. C. (2003) Water partitioning at 660 km depth and evidence for very low water solubility in magnesium silicate perovskite. *Geophysical Research Letters* **30**, 10.1029/2003GL017182.

Bolfan-Casanova N., Mackwell S. J., Keppler H., McCammon C., and Rubie D. C. (2002) Pressure dependence of H solubility in magnesiowüstite up to 25 GPa: implications for the storage of water in the Earth's lower mantle. *Geophysical Research Letters* **29**, 89–1/89–4.

Bons P. D. and Cox, S. J. D. (1994) Analogue experiments and numerical modelling on the relation between microgeometry and flow properties of polyphase materials. *Materials Science and Engineering A* **175**, 237–245.

Bons P. D. and Den Brok B. (2000) Crystallographic preferred orientation development by dissolution–precipitation creep. *Journal of Structural Geology* **22**, 1713–1722.

Bons P. D. and Urai J. L. (1994) Experimental deformation of two-phase rock analogues. *Materials Science and Engineering A* **175**, 221–229.

Borch R. S. and Green H. W., II. (1987) Dependence of creep in olivine on homologous temperature and its implication for flow in the mantle. *Nature* **330**, 345–348.

Borch R. S. and Green H. W., II. (1989) Deformation of peridotite at high pressure in a new molten cell: comparison of traditional and homologous temperature treatments. *Physics of Earth and Planetary Interiors* **55**, 269–276.

Born M. (1940) On the stability of crystal lattice, 1. *Proceedings of Cambridge Philosophical Society* **36**, 160–165.

Born M. and Huang K. (1954) *Dynamical Theory of Crystal Lattice*. Clarendon Press.

Bouchez J. L., Lister G. S., and Nicolas A. (1983) Fabric asymmetry and shear sense in movement zones. *Geologische Rundschau* **72**, 401–419.

Boullier A. M. and Gueguen Y. (1975) SP-mylonites: origin of some mylonites by superplastic flow. *Contributions to Mineralogy and Petrology* **50**, 93–104.

Boysen H., Dorner B., Frey F. A., and Grimm H. (1980) Dynamic structure determination of two interacting modes at the M-point in α- and β-quartz by inelastic neutron

scattering. *Journal of Physics C: Solid State Physics* **13**, 6127–6146.

Braithwaite J. S., Wright K., and Catlow C. R. A. (2003) A theoretical study of the energetics and IR frequencies of hydroxyl defects in forsterite. *Journal of Geophysical Research* **108**, 10.1029/2002JB002126.

Braun J., Cherny J., Poliakov A. N. B., *et al*. (1999) A simple parameterization of strain localization in the ductile regime due to grain size reduction: a case study for olivine. *Journal of Geophysical Research* **104**, 25 167–25 181.

Brennan B. J. and Stacey F. D. (1977) Frequency dependence of elasticity of rock – test of seismic velocity dispersion. *Nature* **268**, 220–222.

Breuer D. and Spohn T. (1995) Possible flushing instability in mantle convection at the Archean–Proterozoic transition. *Nature* **378**, 608–610.

Brodholt J. P. and Refson K. (2000) An *ab initio* study of hydrogen in forsterite and a possible mechanism for hydrolytic weakening. *Journal of Geophysical Research* **105**, 18 977–18 982.

Bromiley G. D., Keppler H., McCammon C., Bromiley F. A., and Jacobsen S. B. (2004) Hydrogen solubility and speciation in natural, gem quality chromian diopside. *American Mineralogist* **89**, 941–949.

Brook R. J. (1969) Pore-grain boundary interactions and grain growth. *Journal of the American Ceramic Society* **52**, 65–67.

Brookes C. A., O'Neill J. B., and Redfern B. A. W. (1971) Anisotropy in the hardness of single crystals. *Proceedings of the Royal Society of London A* **322**, 73–88.

Brown A. M. and Ashby M. F. (1980) Correlations for diffusion constants. *Acta Metallurgica* **28**, 1085–1101.

Brown J. M. and McQueen R. G. (1980) Melting of iron under shock conditions. *Geophysical Research Letters* **7**, 533–536.

Brown J. M. and McQueen R. G. (1982) The equation of state for iron and the Earth's core. In *High-Pressure Research in Geophysics* (ed. S. Akimoto and M. H. Manghnani), pp. 611–623. Reidel.

Brown J. M. and Shankland T. J. (1981) Thermodynamic parameters in the Earth as determined from seismic profiles. *Geophysical Journal of Royal Astronomical Society* **66**, 579–596.

Brown L. M. (1961) Mobile charged dislocations in ionic crystals. *Physica Status Solidi* **1**, 585–599.

Bruhn D. F. and Casey M. (1997) Texture development in experimentally deformed two-phase aggregates of calcite and anhydrite. *Journal of Structural Geology* **19**, 909–925.

Bruhn D. F., Olgaard D. L., and Dell'Angelo L. N. (1999) Evidence for enhanced deformation in two-phase rocks: experiments on the rheology of calcite–anhydrite aggregates. *Journal of Geophysical Research* **104**, 707–724.

Budianski B. and O'Connell R. J. (1980) Bulk dissipation in heterogeneous media. In *Solid Earth Geophysics and Geotechnology* (ed. S. N. Nasser), pp. 1–10. American Society of Mechanical Engineering.

Buffett B. A. (1997) Geodynamic estimates of the viscosity of the Earth's inner core. *Nature* **388**, 571–573.

Buffett B. A. and Bloxham J. (2000) Deformation of Earth's inner core by electromagnetic forces. *Geophysical Research Letters* **27**, 4001–4004.

Buffett B. A., Garnero E. J., and Jeanloz R. (2000) Sediments at the top of Earth's core. *Science* **290**, 1338–1342.

Bunge H.-J. (1982) *Texture Analysis in Materials Science – Mathematical Methods*. Butterworth.

Bunge H.-P., Ricard Y., and Matas J. (2001) Non-adiabaticity in mantle convection. *Geophysical Research Letters* **28**, 879–882.

Burns R. G. (1970) *Mineralogical Applications of Crystal Field Theory*. Cambridge University Press.

Burton B. and Reynolds G. L. (1994) In defense of diffusional creep. *Materials Science and Engineering A* **191**, 135–141.

Bussod G. Y. and Christie J. C. (1991) Textural development and melt topology in spinel lherzolite experimentally deformed at hypersolidus conditions. In *Orogenic Lherzolites and Mantle Processes* (ed. M. A. Menzies, C. Dupuy, and A. Nicolas), pp. 17–39. Oxford University Press.

Bussod G. Y., Katsura T., and Rubie D. C. (1993) The large volume multi-anvil press as a high *P–T* deformation apparatus. *Pure and Applied Geophysics* **141**, 579–599.

Byerlee J. D. (1978) Friction of rocks. *Pure and Applied Geophysics* **116**, 615–626.

Bystricky M. and Mackwell S. J. (2001) Creep of dry clinopyroxene aggregates. *Journal of Geophysical Research* **106**, 13 443–13 454.

Cadek O. and Fleitout L. (2003) Effect of lateral viscosity variation in the top 300 km on the geoid and dynamic topography. *Geophysical Journal International* **152**, 566–580.

Cadek O. and van den Berg A. (1998) Radial profile of temperature and viscosity in the Earth's mantle inferred from the geoid and lateral seismic structure. *Earth and Planetary Science Letters* **164**, 607–615.

Cahn J. W. and Balluffi R. W. (1979) On diffusional mass tranport in polycrystals containing stationary or migrating boundaries. *Scripta Metallurgica* **13**, 499–502.

Cahn J. W. and Fullman R. L. (1956) On the use of lineal analysis for obtaining particle size distribution functions in opaque samples. *Transaction of AIME* **206**, 610–612.

Callen H. B. (1960) *Thermodynamics*. John Wiley and Sons.

Campbell I. H. and Taylor S. R. (1983) No water, no granites – no oceans, no continents. *Geophysical Research Letters* **10**, 1061–1064.

Cannon R. M. and Coble R. L. (1975) Review of diffusional creep of Al_2O_3. In *Deformation of Ceramic Materials* (ed. R. C. Bradt and R. E. Tressler), pp. 61–100. Plenum Press.

Cannon R. M. and Langdon T. G. (1988) Creep of ceramics, Part 2. An examination of flow mechanisms. *Journal of Materials Science* **23**, 1–20.

Cannon W. R. and Sherby O. D. (1973) Third-power stress dependence in creep of polycrystalline nonmetals. *Journal of the American Ceramic Society* **56**, 157–160.

Caristan Y. (1982) The transition from high-temperature creep to fracture in Maryland diabase. *Journal of Geophysical Research* **887**, 6781–6790.

Carlson R. W., Shirey S. B., Pearson D. G., and Boyd F. R. (1994) The mantle beneath continents. *Carnegie Institution of Washington, Yearbook* **93**, 109–117.

Carmichael I. S. E., Turner F. J., and Verhoogen J. (1974) *Igneous Petrology*. McGraw-Hill.

Carpenter M. A. (2006) Elastic properties of minerals and the influence of phase transitions. *American Mineralogist* **91**, 229–246.

Carter C. H., Jr., Stone C. A., and Davis R. F. (1980) High-temperature, multi-atmosphere, constant stress compression creep apparatus. *Review of Scientific Instruments* **51**, 1352–1357.

Carter N. L. and Avé Lallemant H. G. (1970) High temperature deformation of dunite and peridotite. *Geological Society of America Bulletin* **81**, 2181–2202.

Cathles L. M. (1975) *The Viscosity of the Earth's Mantle*. Princeton University Press.

Chaix C. and Lasalmonie A. (1981) Transformation induced plasticity in titanium. *Res Mechanica* **2**, 241–249.

Chaklader A. C. D. (1963) Deformation of quartz crystals at the transformation temperature. *Nature* **197**, 791–792.

Chakraborty S. and Ganguly J. (1992) Cation diffusion in aluminosilicate garnets: experimental determination in spessartine–almandine diffusion couples, evaluation of effective binary diffusion coefficients, and applications. *Contributions to Mineralogy and Petrology* **111**, 74–86.

Chang R. (1961) Dislocation relaxation phenomena in oxide crystals. *Journal of Applied Physics* **32**, 1127–1132.

Chen G., Miletich R., Mueller K., and Spetzler H. A. (1997) Shear and compressional mode measurements with GHz interferometry and velocity-composition systematics for the purope–almandine solid solution series. *Physics of the Earth and Planetary Interiors* **99**, 273–287.

Chen I.-W. (1982) Diffusional creep of two-phase materials. *Acta Metallurgica* **30**, 1655–1664.

Chen I.-W. and Argon A. S. (1979) Steady state power-law creep in heterogeneous alloys with coarse microstructures. *Acta Metallurgica* **27**, 785–791.

Chen I.-W. and Argon A. S. (1981) Creep cavitation in 304 steel. *Acta Metallurgica* **29**, 1321–1333.

Chen J., Inoue T., Weidner D. J., Wu Y., and Vaughan M. T. (1998) Strength and water weakening of mantle minerals, olivine, wadsleyite and ringwoodite. *Geophysical Research Letters* **25**, 575–578.

Chen J., Inoue T., Yurimoto H., and Weidner D. J. (2002a) Effect of water on olivine–wadsleyite phase boundary in the $(Mg, Fe)_2SiO_4$ system. *Geophysical Research Letters* **29**, 10.1029/2001GRL014429.

Chen J., Li L., Weidner D. J., and Vaughan M. T. (2004) Deformation experiments using synchrotron X-rays: *in situ* stress and strain measurements at high pressure and temperature. *Physics of Earth and Planetary Interiors* **143–144**, 347–356.

Chen J., Weidner D. J., and Vaughan M. T. (2002b) Strength of $Mg_{0.9}Fe_{0.1}SiO_3$ perovskite at high pressure and temperature. *Nature* **419**, 824–826.

Chen W. K. and Peterson N. L. (1973) Cation diffusion, semiconductivity and nonstoichiometry in (Co, Ni)O crystals. *Journal of Physics and Chemistry of Solids* **34**, 1093–1108.

Chen W.-P. and Molnar P. (1983) Focal depths of intracontinental and intraplate earthquakes and their implications for the thermal structure and mechanical properties of the lithosphere. *Journal of Geophysical Research* **88**, 4183–4214.

Chester F. M. (1988) The brittle–ductile transition in a deformation-mechanism map for halite. *Tectonophysics* **154**, 125–136.

Chevrot S. (2000) Multichannel analysis of shear wave splitting. *Journal of Geophysical Research* **105**, 21 579–21 590.

Chevrot S. and van der Hilst R. D. (2003) On the effects of a dipping axis of symmetry on shear wave splitting measurements in a transversely isotropic medium. *Geophysical Journal International* **152**, 497–505.

Chiang Y.-M. and Takagi T. (1990) Grain-boundary chemistry of barium titanate and strontium titanate: I. High-temperature equilibrium space charge. *Journal of American Ceramic Society* **73**, 3278–3285.

Chinh N. Q., Horvath G., Horita Z., and Langdon T. G. (2004) A new constitutive relationship for the homogeneous deformation of metals over a wide range of strain. *Acta Materialia* **52**, 3555–3563.

Chopra P. N. and Paterson M. S. (1981) The experimental deformation of dunite. *Tectonophysics* **78**, 453–573.

Chopra P. N. and Paterson M. S. (1984) The role of water in the deformation of dunite. *Journal of Geophysical Research* **89**, 7861–7876.

Christensen N. I. and Lundquist S. M. (1982) Pyroxene orientations within the upper mantle. *Geological Society of America Bulletin* **93**, 279–288.

Christensen U. R. (1989) Mantle rheology, constitution and convection. In *Mantle Convection* (ed. W. R. Peltier), pp. 595–655. Gordon and Breach.

Christensen U. R. and Hofmann A. W. (1994) Segregation of subducted oceanic crust in the convecting mantle. *Journal of Geophysical Research* **99**, 19 867–19 884.

Chung D. H. (1972) Birch's law: why is it so good? *Science* **177**, 261–263.

Clinard F. W. and Sherby O. D. (1964) Strength of iron during allotropic transformation. *Acta Metallurgica* **12**, 911–919.

Coble R. L. (1963) A model for boundary-diffusion controlled creep in polycrystalline materials. *Journal of Applied Physics* **34**, 1679–1682.

Cocks A. C. F. and Gill S. P. A. (1996) A variational approach to two dimensional grain growth – I. Theory. *Acta Materialia* **44**, 4765–4775.

Colombo L., Kataoka T., and Li J. C. M. (1982) Movement of edge dislocations in KCl by large electric fields. *Philosophical Magazine A* **46**, 211–215.

Cooper R. F. (2002) Seismic wave attenuation: energy dissipation in viscoelastic crystalline solids. In *Plastic Deformation of Minerals and Rocks* (ed. S. Karato and H.-R. Wenk), pp. 253–290. Mineralogical Society of America.

Cooper R. F. and Kohlstedt D. L. (1982) Interfacial energies in the olivine–basalt system. In *High Pressure Research in Geophysics* (ed. S. Akimoto and M. H. Manghnani), pp. 217–228. Center for Academic Publication.

Cooper R. F. and Kohlstedt D. L. (1986) Rheology and structure of olivine–basalt partial melts. *Journal of Geophysical Research* **91**, 9315–9323.

Cooper R. F., Kohlstedt D. L., and Chyung K. (1989) Solution-precipitation enhanced creep in solid–liquid aggregates which displays a non-zero dihedral angle. *Acta Metallurgica* **37**, 1759–1771.

Cordier P. (2002) Dislocations and slip systems of mantle minerals. In *Plastic Deformation of Minerals and Rocks* (ed. S. Karato and H.-R. Wenk), pp. 137–179. American Mineralogical Society.

Cordier P. and Doukhan J.-C. (1989) Water solubility in quartz and its influence on ductility. *European Journal of Mineralogy* **1**, 221–237.

Cordier P. and Doukhan J. C. (1995) Plasticity and dissociation of dislocations in water-poor quartz. *Philosophical Magazine A* **72**, 497–514.

Cordier P., Ungar T., Zsoldos L., and Tichy G. (2004) Dislocation creep in $MgSiO_3$ perovskite at conditions of the Earth's uppermost lower mantle. *Nature* **428**, 837–840.

Cormier V. F. and Li X.-D. (2002) Frequency-dependent seismic attenuation in the inner core, 2. A scattering and fabric interpretation. *Journal of Geophysical Research* **107**, 10.1029/2002JB001796.

Cormier V. F., Xu L., and Choy G. L. (1998) Seismic attenuation of the inner core: viscoelastic or stratigraphic? *Geophysical Research Letters* **25**, 4019–4022.

Cottrell A. H. (1953) *Dislocations and Plastic Flow in Crystals*. Clarendon Press.

Cottrell A. H. (1964) *The Mechanical Properties of Matter*. Wiley.

Covey-Crump S. J. and Rutter E. H. (1989) Thermally-induced grain growth of calcite marbles on Naxos Island, Greece. *Contributions to Mineralogy and Petrology* **101**, 69–86.

Crampin S. (1978) Seismic waves propagating through a cracked solid: polarization as a possible dilatancy diagnostic. *Geophysical Journal of Royal Astronomical Society* **53**, 467–496.

Crampin S. (1981) A review of wave motion in anisotropic and cracked elastic-media. *Wave Motion* **3**, 343–391.

Crampin S. (1984) An introduction to wave propagation in anisotropic media. *Geophysical Journal of Royal Astronomical Society* **76**, 17–28.

Creager K. C. (2000) Inner core anisotropy and rotation. In *Earth's Deep Interior: Mineral Physics and Tomography* (ed. S. Karato, A. M. Forte, R. C. Liebermann, G. Masters, and L. Stixrude), pp. 89–114. American Geophysical Union.

Dahlen F. A. and Tromp J. (1998) *Theoretical Global Seismology*. Princeton University Press.

Davies G. F. (1974) Elasticity, crystal structure and phase transitions. *Earth and Planetary Science Letters* **22**, 339–346.

Davis L. A. and Gordon R. B. (1968) Pressure dependence of the plastic flow stress of alkali halide single crystals. *Journal of Applied Physics* **39**, 3885–3897.

De Bresser J. H. P., Peach C. J., Reijs J. P. J., and Spiers C. J. (1998) On dynamic recrystallization during solid state flow: effects of stress and temperature. *Geophysical Research Letters* **25**, 3457–3460.

De Bresser J. H. P., ter Heege J. H., and Spiers C. J. (2001) Grain size reduction by dynamic recrystallization: can it result in major rheological weakening? *International Journal of Earth Sciences* **90**, 28–45.

de Groot S. R. and Mazur P. (1962) *Non-Equilibrium Thermodynamics*. North-Holland.

de Jong M. and Rathenau G. W. (1959) Mechanical properties of iron and some iron alloys while undergoing allotropic transformations. *Acta Metallurgica* **7**, 246–253.

de Jong M. and Rathenau G. W. (1961) Mechanical properties of an iron carbon alloy during allotropic transformation. *Acta Metallurgica* **11**, 714–720.

Debayle E., Kennett B. L. N., and Priestley K. (2005) Global azimuthal seismic anisotropy and the unique plate-motion deformation of Australia. *Nature* **433**, 509–512.

Demouchy S., Deloule E., Frost D. J., and Keppler H. (2005) Pressure and temperature-dependence of water solubility in iron-free wadsleyite. *American Mineralogist* **90**, 1084–1091.

Dennis P. F. (1984) Oxygen self-diffusion in quartz under hydrothermal conditions. *Journal of Geophysical Research* **89**, 4047–4057.

Derby B. and Ashby M. F. (1987) On dynamic recrystallization. *Scripta Metallurgica* **21**, 879–884.

Deschamps F., Snieder R., and Trampert J. (2001) The relative density-to-shear velocity scaling in the uppermost mantle. *Physics of Earth and Planetary Interiors* **124**, 193–211.

Deschamps F. and Trampert J. (2003) Mantle tomography and its relation to temperature and composition. *Physics of the Earth and Planetary Interiors* **140**, 277–291.

Deschamps F., Trampert J., and Snieder R. (2002) Anomalies of temperature and iron in the uppermost mantle inferred from gravity data and tomographic models. *Physics of Earth and Planetary Interiors* **129**, 245–264.

Deuss A. and Woodhouse J. H. (2002) A systematic search for mantle discontinuities using SS-precursors. *Geophysical Research Letters* **29**, 10.1029/2002GL014768.

Deuss A. and Woodhouse J. H. (2004) The nature of the Lehmann discontinuity from its seismological Clapeyron slope. *Earth and Planetary Science Letters* **225**, 295–304.

Dhalenne G., Dechamps M., and Revcolevschi A. (1982) Relative energies of $<011>$ tilt boundaries in NiO. *Journal of the American Ceramic Society* **65**, 611–612.

Dick H. J. B. and Sinton J. M. (1979) Compositional layering in alpine peridotites: evidence for pressure solution creep in the mantle. *Journal of Geology* **87**, 403–416.

Dieterich J. H. (1978) Time-dependent friction and mechanism of stick-slip. *Pure and Applied Geophysics* **116**, 790–806.

Dimos D., Wolfensteine J., and Kohlstedt D. L. (1988) Kinetic demixing and decomposition of multicomponent oxides due to a nonhydrostatic stress. *Acta Metallurgica* **36**, 1543–1552.

Dingley D. J. and Randle V. (1992) Microtexture determination by electron back-scatter diffraction. *Journal of Materials Sciences* **27**, 4545–4566.

Doherty R. D., Hughes D. A., Humphreys F. J., *et al.* (1997) Current issues in recrystallization: a review. *Materials Science and Engineering A* **238**, 219–274.

Doin M., Fleitout L., and Christensen U. R. (1997) Mantle convection and stability of depleted and undepleted continental lithosphere. *Journal of Geophysical Research* **102**, 2771–2787.

Doukhan J.-C. and Paterson M. S. (1986) Solubility of water in quartz. *Bulletin Mineralogie* **109**, 193–198.

Doukhan J.-C. and Trépied L. (1985) Plastic deformation of quartz single crystals. *Bulletin Mineralogie* **108**, 97–123.

Dresen G., Wang Z., and Bai Q. (1996) Kinetics of grain growth in anorthite. *Tectonophysics* **258**, 251–262.

Drury M. R. and Fitz Gerald J. D. (1996) Grain boundary melt films in an experimentally deformed olivine–pyroxene rock: implications for melt distribution in upper mantle rocks. *Geophysical Research Letters* **23**, 701–704.

Drury M. R. and Fitz Gerald J. D. (1998) Mantle rheology: insights from laboratory studies of deformation and phase transition. In *The Earth's Mantle: Composition, Structure and Evolution* (ed. I. Jackson), pp. 503–559. Cambridge University Press.

Drury M. R., Humphreys F. J. and White S. H. (1985) Large strain deformation studies using polycrystalline magnesium as a rock analogue, part II: dynamic recrystallization mechanisms at high temperature. *Physics of the Earth and Planetary Interiors* **40**, 208–222.

Drury M. R. and Urai J. (1990) Deformation-related recrystallization processes. *Tectonophysics* **172**, 235–253.

Drury M. R. and van Roermund H. L. M. (1989) Fluid assisted recrystallization in upper mantle peridotite xenoliths from kimberlite. *Journal of Petrology* **30**, 133–152.

Drury M. R., Vissers R. L. M., van der Wal D., and Hoogerduin Strating E. H. (1991) Shear localization in upper mantle peridotites. *Pure and Applied Geophysics* **137**, 439–460.

Duclos R., Doukhan N., and Escaig B. (1978) High-temperature creep behaviour of nearly stoichiometric alumina spinel. *Journal of Materials Science* **13**, 1740–1748.

Duffy T. S. and Ahrens T. H. (1992) Lateral variation in lower mantle seismic velocity. In *High-Pressure Research: Application to Earth and Planetary Sciences* (ed. Y. Syono and M. H. Manghnani), pp. 197–205. Terra Scientific Publishers.

Duffy T. S., Shen G., Heinz D. L., Shu J., Ma Y., Mao H.-K., Hemley R. J., and Singh A. K. (1999) Lattice strain in gold and rhenium under nonhydrostatic compression to 37 GPa. *Physical Review B* **60**, 15 063–15 073.

Duffy T. S., Zha C.-S., Downs R. T., Mao H.-K., and Hemley R. J. (1995) Elasticity of forsterite to 16 GPa and the composition of the upper mantle. *Nature* **378**, 170–173.

Dupas-Bruzek C., Sharp T. G., Rubie D. C., and Durham W. B. (1998) Mechanisms of transformation and deformation in $Mg_{1.8}Fe_{0.2}SiO_4$ olivine and wadsleyite under nonhydrostatic stress. *Physics of Earth and Planetary Interiors* **108**, 33–48.

Durek J. J. and Ekström G. (1995) Evidence of bulk attenuation in the asthenosphere from recordings of the Bolivia earthquake. *Geophysical Research Letters* **22**, 2309–2312.

Durek J. J. and Romanowicz B. (1999) Inner core anisotropy inferred by direct inversion of normal mode spectra. *Geophysical Journal International* **139**, 599–622.

Durham W. B., Goetze C., and Blake B. (1977) Plastic flow of oriented single crystals of olivine, 2. Observations and interpretations of the dislocation structure. *Journal of Geophysical Research* **82**, 5755–5770.

Durham W. B. and Stern L. A. (2001) Rheological properties of water ice – Applications to satellites of the outer planets. *Annual Review of Earth and Planetary Sciences* **29**, 295–330.

Durham W. B., Weidner D. J., Karato S., and Wang Y. (2002) New developments in deformation experiments at high pressure. In *Plastic Deformation of Minerals and Rocks* (ed. S. Karato and H.-R. Wenk), pp. 21–49. Mineralogical Society of America.

Durinck J., Legris A., and Cordier P. (2005a) Influence of crystal chemistry on ideal plastic shear anisotropy in forsterite: first principles calculations. *American Mineralogist* **90**, 1072–1077.

Durinck J., Legris A., and Cordier P. (2005b) Pressure sensitivity of olivine slip systems: first-principle calculations of generalised stacking faults. *Physics and Chemistry of Minerals* **32**, 646–654.

Duval P., Ashby, M. F., and Anderman, I. (1978) Anelastic behaviour of polycrystalline ice. *Journal of Glaciology* **21**, 621–628.

Duval P., Ashby M. F., and Anderman I. (1983) Rate-controlling processes in the creep of polycrystalline ice. *Journal of Physical Chemistry* **87**, 4066–4074.

Duyster J. and Stöckhert B. (2001) Grain boundary energies in olivine derived from natural microstructures. *Contributions to Mineralogy and Petrology* **140**, 567–576.

Dziewonski A. M. (1984) Mapping the lower mantle: determination of lateral heterogeneity in P velocity up to degree and order 6. *Journal of Geophysical Research* **89**, 5929–5952.

Dziewonski A. M. and Anderson D. L. (1981) Preliminary reference Earth model. *Physics of Earth and Planetary Interiors* **25**, 297–356.

Dziewonski A. M., Hager B. H., and O'Connell R. J. (1977) Large-scale heterogeneities in the lower mantle. *Journal of Geophysical Research* **82**, 239–255.

Edington J. W., Melton K. N., and Cutler C. P. (1976) Superplasticity. *Progress in Materials Sciences* **21**, 63–170.

Edmond J. M. and Paterson M. S. (1972) Volume changes during the deformation of rocks at high pressures. *International Journal of Rock Mechanics and Mining Sciences* **9**, 161–182.

Ehrenfest P. (1933) Phase conversions in a general and enhanced sense, classified according to the specific singularities of the thermodynamic potential. *Proceedings of the Koninklijke Akademie van Wetenschappen te Amsterdam* **36**, 153–157.

Einstein A. (1906) A new determination of molecular dimensions. *Annalen der Physik* **19**, 289–306.

Elliott D. (1973) Diffusion flow laws in metamorphic rocks. *Geological Society of America Bulletin* **84**, 2645–2664.

Engdahl E. R., van der Hilst R. D., and Buland R. P. (1998) Global teleseismic earthquake relocation with improved travel times and procedures for depth determination. *Bulletin of Seismological Society of America* **88**, 722–743.

Escaig B. (1968) Sur le glissement dévie des dislocations dans la structure cubique à faces centrées. *Journal de Physique* **29**, 225–239.

Eshelby J. D. (1956) The continuum theory of lattice defects. In *Solid State Physics*, Vol. 3 (ed. F. Seitz and D. Turnbull), pp. 79–144. Academic Press.

Eshelby J. D. (1957) The determination of the elastic strain field of an ellipsoidal inclusion and related problems. *Proceedings of the Royal Society of London, Ser. A* **241**, 376–396.

Eshelby J. D., Newey C. W. A., and Pratt P. L. (1958) Charged dislocations and the strength of ionic crystals. *Philosophical Magazine* **3**, 75–89.

Estrin Y. and Kubin L. (1986) Local strain hardening and nonuniformity of plastic deformation. *Acta Metallurgica* **34**, 2455–2464.

Estrin Y. and Kubin L. P. (1988) Plastic instabilities: classification and physical mechanisms. *Res Mechanica* **23**, 197–221.

Estrin Y. and Kubin L. P. (1991) Plastic instabilities: phenomenology and theory. *Materials Science and Engineering A* **137**, 125–134.

Etchecopar A. and Visseur G. (1987) A 3-D kinematic model of fabric development in polycrystalline aggregates: comparisons with experimental and natural examples. *Journal of Structural Geology* **9**, 705–717.

Etheridge M. A., Wall V. J., and Vernon R. H. (1983) The role of fluid phase during regional metamorphism and deformation. *Journal of Metamorphic Geology* **1**, 205–226.

Evans B., Fredrich J. T., and Wong T.-F. (1990) The brittle–ductile transition in rocks: recent experimental and theoretical progress. In *The Brittle–Ductile Transition in Rocks: the Heard Volume* (ed. A. G. Duba, W. B. Durham, J. W. Handin, and H. F. Wang), pp. 1–20. American Geophysical Union.

Evans B. and Goetze C. (1979) Temperature variation of hardness of olivine and its implication for polycrystalline yield stress. *Journal of Geophysical Research* **84**, 5505–5524.

Evans B., Renner J. and Hirth G. (2001) A few remarks on the kinetics of static grain growth in rocks. *International Journal of Earth Sciences* **90**, 88–103.

Evans B. and Wong T.-F. (1985) Shear localization in rocks induced by tectonic deformation. In *Mechanics of Geomaterials* (ed. Z. Bazant), pp. 189–210. John Wiley & Sons.

Eyring H. (1935) The activated complex and the absolute rate of chemical reaction. *Chemical Review* **17**, 65–82.

Fan D., Chen L.-Q., and Chen S.-P. P. (1998) Numerical simulation of Zener pinning with growing second-phase particle. *Journal of the American Ceramic Society* **81**, 526–531.

Fantozzi G., Esnouf C., Benoit W., and Ritchie I. G. (1982) Internal friction and microdeformation due to the intrinsic properties of dislocations: the Bordoni relaxation. *Progress in Materials Sciences* **27**, 311–451.

Farber D. L., Williams Q., and Ryerson F. J. (2000) Divalent cation diffusion in Mg_2SiO_4 spinel (ringwoodite), β phase (wadsleyite), and olivine: implications for the electrical conductivity of the mantle. *Journal of Geophysical Research* **105**, 513–529.

Farver J. R. and Yund R. A. (1991) Oxygen diffusion in quartz: dependence on temperature and water fugacity. *Chemical Geology* **90**, 55–70.

Faul U. H. (2001) Melt retention and segregation beneath mid-ocean ridges. *Nature* **410**, 920–923.

Faul U. H., Fitz Gerald J. D., and Jackson I. (2004) Shear-wave attenuation and dispersion in melt-bearing olivine polycrystals II. Microstructural interpretation and seismological implications. *Journal of Geophysical Research* **109**, 10.1029/2003JB002407.

Faul U. H. and Jackson I. (2005) The seismological signature of temperature and grain size variations in the upper mantle. *Earth and Planetary Science Letters* **234**, 119–134.

Faul U. H., Toomey D. R., and Waff H. S. (1994) Intergranular basaltic melt is distributed in thin, elongated inclusions. *Geophysical Research Letters* **21**, 29–32.

Fearn D. R., Loper D. E., and Roberts P. H. (1981) Structure of the Earth's inner core. *Nature* **292**, 232–233.

Fischer K. M. and Wiens D. G. (1996) The depth of mantle anisotropy beneath the Tonga subduction zone. *Earth and Planetary Science Letters* **142**, 253–260.

Flanagan M. P. and Shearer P. M. (1998) Global mapping of topography on transition zone velocity discontinuities by stacking SS precursors. *Journal of Geophysical Research* **103**, 2673–2692.

Flanagan M. P. and Wiens D. A. (1994) Radial upper mantle attenuation structure of inactive back arc basins from differential shear wave attenuation measurements. *Journal of Geophysical Research* **99**, 15 469–15 485.

Flesh L. M., Li B., and Liebermann R. C. (1998) Sound velocities of polycrystalline $MgSiO_3$-orthopyroxene to 10 GPa at room temperature. *American Mineralogist* **83**, 444–450.

Flinn D. (1962) On folding during three-dimensional progressive deformation. *Geological Society of London, Quaternary Journal* **118**, 385–433.

Flynn C. P. (1968) Atomic migration in monoatomic crystals. *Physical Review* **171**, 682–698.

Flynn C. P. (1972) *Point Defects and Diffusion*. Oxford University Press.

Foreman A. J., Jawson M. A., and Wood J. K. (1951) Factors controlling dislocation width. *Proceedings of Physical Society A* **64**, 156–163.

Forsyth D. W. (1975) The early structural evolution and anisotropy of the oceanic upper mantle. *Geophysical Journal of Royal Astronomical Society* **43**, 103–162.

Forsyth D. W. (1985) Subsurface loading and estimates of the flexural rigidity of continental lithosphere. *Journal of Geophysical Research* **90**, 12 623–12 632.

Forsyth D. W. (1992) Geophysical constraints on mantle flow and melt generation beneath mid-ocean ridge. In *Mantle Flow and Melt Generation at Mid-Ocean Ridges* (ed. J. P. Morgan, D. K. Blackman, and J. M. Sinton), pp. 1–66. American Geophysical Union.

Forte A. M. (2000) Seismic–geodynamic constraints on mantle flow: implications for layered convection, mantle viscosity, and seismic anisotropy in the deep mantle. In *Earth's Deep Interior: Mineral Physics and Seismic Tomography* (ed. S. Karato, A. M. Forte, R. C. Liebermann, G. Masters, and L. Stixrude), pp. 3–36. American Geophysical Union.

Forte A. M., Dziewonski A. M., and O'Connell R. J. (1994) Continent–ocean chemical heterogeneity in the mantle based on seismic tomography. *Science* **268**, 386–388.

Forte A. M. and Mitrovica J. X. (1996) New inferences of mantle viscosity from joint inversion of long-wavelength mantle convection and post-glacial rebound data. *Geophysical Research Letters* **23**, 1147–1150.

Forte A. M. and Mitrovica J. X. (2001) Deep-mantle high-viscosity flow and thermochemical structure inferred from seismic and geodynamic data. *Nature* **410**, 1049–1056.

Forte A. M., Woodward, R. L., and Dziewonski, A. M. (1994) Joint inversion of seismic and geodynamic data for models of three-dimensional mantle heterogeneity. *Journal of Geophysical Research* **99**, 21 857–21 877.

French J. D., Zhao J., Harmer M. P., Chan H. M., and Miller G. A. (1994) Creep of duplex microstructures. *Journal of the American Ceramic Society* **77**, 2857–2865.

Fressengas C. and Molinari A. (1987) Instability and localization of plastic flow in shear at high strain rate. *Journal of Mechanics and Physics of Solids* **35**, 185–211.

Freund F. and Wengeler H. (1982) The infrared spectrum of OH-compensated defect sites in C-doped MgO and CaO single crystals. *Journal of Physics and Chemistry of Solids* **43**, 129–145.

Frisillo A. L. and Barsch G. R. (1972) Measurement of single-crystal elastic constants of bronzite as a function of pressure and temperature. *Journal of Geophysical Research* **77**, 6360–6384.

Frost D. J., Liebske C., Langenhorst F., *et al.* (2004) Experimental evidence for the existence of iron-rich metal in the Earth's lower mantle. *Nature* **428**, 409–412.

Frost D. J. and Wood B. J. (1997a) Experimental measurements of the fugacity of CO_2 and graphite/diamond stability from 35 to 77 kbar at 925 to 1650 ºC. *Geochimica et Cosmochimica Acta* **61**, 1565–1574.

Frost D. J. and Wood B. J. (1997b) Experimental measurements of the properties of H_2O–CO_2 mixtures at high pressures and temperatures. *Geochimica et Cosmochimica Acta* **61**, 3301–3309.

Frost H. J. and Ashby M. F. (1982) *Deformation Mechanism Maps*. Pergamon Press.

Fuchs K. (1983) Recently formed elastic anisotropy and petrological models for the continental subcrustal lithosphere in southern Germany. *Physics of Earth and Planetary Interiors* **31**, 93–118.

Fujimura A., Endo S., Kato M., and Kumazawa M. (1981) Preferred orientation of β-Mn_2GeO_4. *Programme and Abstracts, The Japan Seismological Society*, **185**.

Fujino K., Nakazaki H., Momoi H., Karato S., and Kohlstedt D. L. (1992) TEM observation of dissociated dislocations with b = [010] in naturally deformed olivine. *Physics of Earth and Planetary Interiors* **78**, 131–137.

Fukao Y., Obayashi M., Inoue H., and Nenbai M. (1992) Subducting slabs stagnant in the mantle transition zone. *Journal of Geophysical Research* **97**, 4809–4822.

Fukao Y., To A., and Obayashi M. (2003) Whole mantle P wave tomography using P and PP-P data. *Journal of Geophysical Research* **108**, 10.1029/2001JB000989.

Fukao Y., Widiyantoro R. D. S., and Obayashi M. (2001) Stagnant slabs in the upper and lower mantle transition zone. *Review of Geophysics* **39**, 291–323.

Funamori N., Yagi T., and Uchida T. (1994) Deviatoric stress measurement under uniaxial compression by a powder X-ray diffraction method. *Journal of Applied Physics* **75**, 4327–4331.

Furusho M. and Kanagawa K. (1999) Reaction-induced strain localization in a lherzolite mylonite from the Hidaka metamorphic belt of central Hokkaido, Japan. *Tectonophysics* **313**, 411–432.

Gaherty J. B. (2001) Seismic evidence for hotspot-induced buoyant flow beneath the Reykjanes ridge. *Science* **293**, 1645–1647.

Gaherty J. B. and Jordan T. H. (1995) Lehmann discontinuity as the base of an anisotropic layer beneath continent. *Science* **268**, 1468–1471.

Gaherty J. B., Jordan T. H., and Gee L. S. (1996) Seismic structure of the upper mantle in a central Pacific corridor. *Journal of Geophysical Research* **101**, 22 291–22 309.

Gaherty J. B., Kato M., and Jordan T. H. (1999) Seismological structure of the upper mantle: a regional comparison of seismic layering. *Physics of Earth and Planetary Interiors* **110**, 21–41.

Gandin C.-A., Rappaz M., West D., and Adams B. L. (1995) Grain texture evolution during the columnar growth of dendritic alloys. *Metallurgical Materials Transaction A* **26**, 1543–1551.

Gannarelli C. M. S., Alfé D., and Gillan M. J. (2005) The axial ratio of hcp iron at the conditions of the Earth's inner core. *Physics of Earth and Planetary Interiors* **152**, 67–77.

Garnero E. J. (2000) Heterogeneity of the lowermost mantle. *Annual Review of Earth and Planetary Sciences* **28**, 509–537.

Garnero E. J. (2004) A new paradigm for Earth's core–mantle boundary. *Science* **304**, 834–836.

Garnero E. J. and Jeanloz R. (2000) Fuzzy patches on the Earth's core–mantle boundary? *Geophysical Research Letters* **27**, 2777–2780.

Garnero E. J., Maupin V., Lay T., and Fouch M. J. (2004) Variable azimuthal anisotropy in Earth's lowermost mantle. *Science* **306**, 259–261.

Garnero E. J., Revenaugh J., Williams Q., Lay T., and Kellogg L. H. (1998) Ultralow velocity zone at the core–mantle boundary. In *The Core–Mantle Boundary Regions* (ed. M. E. W. M. Gurnis, E. Knittle and B. A. Fuffett), pp. 319–334. American Geophysical Union.

Garofalo F. (1965) *Fundamentals of Creep and Creep-Rupture in Metals*. MacMillan.

Gay N. C. (1968) Pure shear and simple shear deformation of inhomogeneous viscous fluids. 1. Theory. *Tectonophysics* **5**, 211–234.

Getting I. C., Dutton S. J., Burnley P. C., Karato S., and Spetzler H. A. (1997) Shear attenuation and dispersion in MgO. *Physics of Earth and Planetary Interiors* **99**, 249–257.

Getting I. C. and Kennedy G. C. (1970) Effect of pressure on the EMF of chromel–alumel and platinum–platinum 10% rhodium thermocouples. *Journal of Applied Physics* **41**, 4552–4562.

Ghose S. (1985) Lattice dynamics, phase transitions and soft modes. In *Microscopic to Macroscopic* (ed. S. W. Kiefer and A. Navrotsky), pp. 127–163. Mineralogical Society of America.

Gill S. P. A. and Cocks A. C. F. (1996) A variational approach to two dimensional grain growth – II. numerical results. *Acta mater* **44**, 4777–4789.

Gilman J. J. (1985) Hardness test: a mechanical microprobe. In *Science of Hardness Testing* (ed. J. H. Westbrook and H. Conrad), pp. 51–74. American Society for Metals.

Gilman M. J. (1981) The volume of formation of defects in ionic crystals. *Philosophical Magazine A* **43**, 301–312.

Glansdorff P. and Prigogine I. (1971) *Thermodynamic Theory of Stability, Structure and Fluctuation*. John Wiley & Sons.

Gleason G. C. and Tullis J. (1995) A flow law for dislocation creep of quartz aggregates determined with the molten slat cell. *Tectonophysics* **247**, 1–23.

Goetze C. and Evans B. (1979) Stress and temperature in the bending lithosphere as constrained by experimental rock

mechanics. *Geophysical Journal of Royal Astronomical Society* **59**, 463–478.

Goldsby D. L. and Kohlstedt D. L. (2001) Superplastic deformation of ice: experimental observations. *Journal of Geophysical Research* **106**, 11 017–11 030.

Gordon R. B. (1965) Diffusion creep in the Earth's mantle. *Journal of Geophysical Research* **70**, 2413–2418.

Gordon R. B. (1971) Observation of crystal plasticity under high pressure with application to the Earth's mantle. *Journal of Geophysical Research* **76**, 1248–1254.

Gordon R. S. (1973) Mass transport in the diffusional creep of ionic solids. *Journal of the American Ceramic Society* **65**, 147–152.

Gordon R. S. and Terwillinger G. R. (1972) Transient creep in Fe-doped polycrystalline MgO. *Journal of the American Ceramic Society* **55**, 450–455.

Gottstein G. and Mecking H. (1985) Recrystallization. In *Preferred Orientation in Deformed Metals and Rocks* (ed. H.-R. Wenk), pp. 183–232. Academic Press.

Grand S. (1994) Mantle shear structure beneath Americas and surrounding oceans. *Journal of Geophysical Research* **99**, 11 591–11 621.

Green D. H. and Falloon, T. J. (1998) Pyrolite: a Ringwood concept and its current expression. In *The Earth's Mantle* (ed. I. Jackson), pp. 311–378. Cambridge University Press.

Green H. W., II. (1984) "Pressure solution" creep: some causes and mechanisms. *Journal of Geophysical Research* **89**, 4313–4318.

Green H. W., II. (1970) Diffusional flow in polycrystalline materials. *Journal of Applied Physics* **41**, 3899–3902.

Green H. W., II. and Borch R. S. (1987) The pressure dependence of creep. *Acta Metallurgica* **35**, 1301–1305.

Green H. W., II. and Houston H. (1995) The mechanics of deep earthquakes. *Annual Review of Earth and Planetary Sciences* **23**, 169–213.

Greenwood G. W. (1994) Denuded zones and diffusional creep. *Scripta Metallurgica et Material* **30**, 1527–1530.

Greenwood G. W. and Johnson R. H. (1965) The deformation of metals under small stresses during phase transformations. *Proceedings of the Royal Society of London A* **238**, 403–422.

Gribb T. T. and Cooper R. F. (1998) Low-frequency shear attenuation in polycrystalline olivine: grain boundary diffusion and the physical significance of the Andrade model for viscoelastic rheology. *Journal of Geophysical Research* **103**, 27 267–27 279.

Gribb T. T. and Cooper R. F. (2000) The effect of an equilibrated melt phase on the shear creep and attenuation behavior of polycrystalline olivine. *Geophysical Research Letters* **27**, 2341–2344.

Griggs D. T. (1967) Hydrolytic weakening of quartz and other silicates. *Geophysical Journal of Royal Astronomical Society* **14**, 19–31.

Griggs D. T. (1974) A model of hydrolytic weakening in quartz. *Journal of Geophysical Research* **79**, 1653–1661.

Griggs D. T. and Baker D. W. (1969) The origin of deep-focus earthquakes. In *Properties of Matter Under Unusual Conditions* (ed. H. Marks and S. Feshbach), pp. 23–42. Interscience.

Griggs D. T. and Blacic J. D. (1965) Quartz: anomalous weakness of synthetic crystals. *Science* **147**, 292–295.

Grimmer H. (1979) The distribution of disorientation angles if all relative orientations of neighbouring grains are equally probable. *Scripta Metallurgica* **13**, 161–164.

Grüneisen E. (1912) Theories des festen Zustands einatomiger elemente. *Annalen der Physik, Berlin* **39**, 257–306.

Gu Y. J., Dziewonski A. M., and Agee C. B. (1998) Global de-correlation of the topography of transition zone discontinuities. *Earth and Planetary Science Letters* **157**, 57–67.

Gu Y. J., Dziewonski A. M., and Ekström G. (2001) Preferential detection of the Lehmann discontinuity beneath continents. *Geophysical Research Letters* **28**, 4655–4658.

Gu Y. J., Dziewonski A. M., and Ekström G. (2003) Simultaneous inversion for mantle velocity and topography of transition zone discontinuities. *Geophysical Journal International* **154**, 559–583.

Gubbins D., Alfé D., Masters G., Price G. D., and Gillan M. J. (2003) Can the Earth's dynamo run on heat alone? *Geophysical Journal International* **155**, 609–622.

Gueguen Y., Darot M., Mazot P., and Woirgard J. (1989) Q^{-1} of forsterite single crystals. *Physics of Earth and Planetary Interiors* **55**, 254–258.

Gueguen Y. and Mercier J. M. (1973) High attenuation and low velocity zone. *Physics of Earth and Planetary Interiors* **7**, 39–46.

Gueguen Y. and Palciauskas V. (1994) *Introduction to the Physics of Rocks*. Princeton University Press.

Guillopé M. and Poirier J.-P. (1979) Dynamic recrystallization during creep of single-crystalline halite: an experimental study. *Journal of Geophysical Research* **84**, 5557–5567.

Gung Y. and Romanowicz B. (2004) Q tomography of the upper mantle using three-component long-period waveforms. *Geophysical Journal International* **157**, 813–830.

Gung Y., Romanowicz B., and Panning M. (2003) Global anisotropy and the thickness of continents. *Nature* **422**, 707–711.

Gutenberg B. (1926) Untersuchen zur Frage, bis zu welcher Tiefe die Erde kristallin ist. *Zeitschrift für Geophisik* **2**, 24–29.

Gutenberg B. (1948) On the layer of relatively low wave velocity at a depth of about 80 kilometers. *Bulletin of Seismological Society of America* **35**, 117–130.

Gutenberg B. (1954) Low-velocity layers in the Earth's mantle. *Bulletin of Seismological Society of America* **65**, 337–348.

Haasen P. (1979) Kink formation and migration as dependent on the Fermi level. *Journal de Physique C* **6**, 111–116.

Hacker B. R., Gnos E., Ratschbacher L., *et al*. (2000) Hot and dry lower crustal xenoliths from Tibet. *Science* **287**, 2463–2466.

Hager B. H. (1984) Subducted slabs and the geoid: constraints on mantle rheology and flow. *Journal of Geophysical Research* **89**, 6003–6015.

Hager B. H. and Clayton R. W. (1989) Constraints on the structure of mantle convection using seismic observations, flow models and the geoid. In *Mantle Convection* (ed. W. R. Peltier), pp. 657–763. Gordon and Breach.

Haggerty S. E. and Sautter V. (1990) Ultra deep (> 300 km) ultramafic, upper mantle xenoliths. *Science* **248**, 993–996.

Hall C. E. and Parmentier E. M. (2002) The influence of grain size evolution on a composite dislocation–diffusion creep rheology. *Journal of Geophysical Research*.

Hammond W. C. and Humphreys E. D. (2000a) Upper mantle seismic wave velocity: effects of realistic partial melt distribution. *Journal of Geophysical Research* **105**, 10 987–10 999.

Hammond W. C. and Humphreys E. D. (2000b) Upper mantle seismic wave velocity: effects of realistic partial melt geometries. *Journal of Geophysical Research* **105**, 10 975–10 986.

Handy M. R. (1989) Deformation regimes and the rheological evolution of fault zones in the lithosphere: the effects of pressure, temperature, grain size and time. *Tectonophysics* **163**, 119–152.

Handy M. R. (1994) Flow laws for rocks containing two nonlinear viscous phases: a phenomenological approach. *Journal of Structural Geology* **16**, 287–301.

Handy M. R. and Brun J. P. (2004) Seismicity, structure and strength of the continental lithosphere. *Earth and Planetary Science Letters* **223**, 427–441.

Harper J. and Dorn J. E. (1957) Viscous creep of aluminium near its melting temperature. *Acta Metallurgica* **5**, 654–665.

Harren S. V., Dève H. E., and Asaro R. J. (1988) Shear band formation in plane strain compression. *Acta Metallurgica* **36**, 2435–2480.

Harrison R. J. and Redfern S. A. T. (2002) The influence of transformation twins on the seismic-frequency elastic and anelastic properties of perovskite: dynamical mechanical analysis of single crystal $LaAlO_3$. *Physics of the Earth and Planetary Interiors* **134**, 253–272.

Hart E. W. (1967) Theory of tensile test. *Acta Metallurgica* **15**, 351–355.

Hart E. W. (1970) A phenomenological theory for plastic deformation of polycrystalline metals. *Acta Metallurgica* **18**, 599–610.

Hartmann W. K. (1999) *Moons and Planets*. Wadsworth Publishers.

Hashida T. (1989) Three-dimensional seismic attenuation structure beneath the Japanese islands and its tectonic and thermal implications. *Tectonophysics* **159**, 163–180.

Hashin Z. and Shtrikman S. (1963) A variational approach to the theory of the elastic behavior of multiphase materials. *Journal of Mechanics and Physics of Solids* **11**, 127–140.

Haskell N. A. (1935a) The motion of a viscous fluid under a surface load. *Physics* **6**, 265–269.

Haskell N. A. (1935b) The motion of a viscous fluid under a surface load. Part II. *Physics* **7**, 56–61.

Haskell N. A. (1937) The viscosity of the asthenosphere. *American Journal of Science* **33**, 22–28.

Hazen R. M. and Finger L. W. (1979) Bulk modulus–volume relationship for cation–anion polyhedra. *Journal of Geophysical Research* **84**, 6723–6728.

Heard H. C., Borg I. Y., Carter N. L., and Raleigh C. B. (1972) *Flow and Fracture of Rocks*. American Geophysical Union.

Heard H. C. and Kirby S. H. (1981) Activation volume for steady-state creep in polycrystalline CsCl: cesium chloride structure. In *Mechanical Behavior of Crustal Rocks* (ed. N. L. Carter, M. Friedman, J. M. Logan, and O. W. Stearns), pp. 83–91. American Geophysical Union.

Heggie M. and Jones R. (1986) Models of hydrolytic weakening in quartz. *Philosophical Magazine, A* **53**, L65–L70.

Heinz D. L., Jeanloz R., and O'Connell R. J. (1982) Bulk attenuation in a polycrystalline Earth. *Journal of Geophysical Research* **87**, 7772–7778.

Helffrich G. (2000) Topography of the transition zone discontinuities. *Review of Geophysics* **38**, 141–158.

Herring C. (1950) Diffusional viscosity of a polycrystalline solid. *Journal of Applied Physics* **21**, 437–445.

Hess H. H. (1964) Seismic anisotropy of the uppermost mantle under oceans. *Nature* **203**, 629–631.

Hier-Majumder S., Anderson I. M., and Kohlstedt D. L. (2005a) Influence of protons on Fe–Mg interdiffusion in olivine. *Journal of Geophysical Research* **110**, 10.1029/2004JB003292.

Hier-Majumder S., Leo P. H., and Kohlstedt D. L. (2004) On grain boundary wetting during deformation. *Acta Materialia* **52**, 3425–3433.

Hier-Majumder S., Mei S., and Kohlstedt D. L. (2005b) Water weakening of clinopyroxene in diffusion creep regime. *Journal of Geophysical Research* **110**, 10.1029/2004JB003414.

Higo Y., Inoue T., Irifune T., and Yurimoto H. (2001) Effect of water on the spinel–postspinel transformation in Mg_2SiO_4. *Geophysical Research Letters* **28**, 3505–3508.

Hill R. (1952) The elastic behaviour of a crystalline aggregate. *Proceedings of the Physical Society, London A* **65**, 349–354.

Hill R. (1958) A general theory of uniqueness and stability of elastic–plastic models. *Journal of Mechanics and Physics of Solids* **6**, 236–249.

Hill R. (1965) A self consistent mechanics of composite materials. *Journal of the Mechanics and Physics of Solids* **13**, 213–222.

Hill R. I., Campbell I. H., Davies G. F., and Griffiths R. W. (1992) Mantle plumes and continental tectonics. *Science* **256**, 186–193.

Hillert M. (1965) On the theory of normal and abnormal grain growth. *Acta Metallurgica* **13**, 227–238.

Hippertt J. F. and Hongn F. D. (1998) Deformation mechanisms in the mylonite/ultramylonite transition. *Journal of Structural Geology* **20**, 1435–1448.

Hiraga T., Anderson I. M., and Kohlstedt D. L. (2004) Grain-boundaries as reservoirs of incompatible elements in the Earth's mantle. *Nature* **427**, 699–703.

Hiraga T., Anderson I. M., Zimmerman M. E., Mei S., and Kohlstedt D. L. (2002) Structure and chemistry of grain boundaries in deformed, olivine + basalt and partially molten lherzolite aggregates: evidence of melt-free grain boundaries. *Contributions to Mineralogy and Petrology* **144**, 163–175.

Hirsch P. B. (1979) A mechanism for the effect of doping on dislocation mobility. *Journal de Physique C* **6**, 117–121.

Hirth G. (2002) Laboratory constraints on the rheology of the upper mantle. In *Plastic Deformation of Minerals and Rocks*, Vol. 51 (ed. S. Karato and H.-R. Wenk), pp. 97–120. Mineralogical Society of America.

Hirth G. and Kohlstedt D. L. (1995a) Experimental constraints on the dynamics of partially molten upper mantle: deformation in the diffusion creep regime. *Journal of Geophysical Research* **100**, 1981–2001.

Hirth G. and Kohlstedt D. L. (1995b) Experimental constraints on the dynamics of partially molten upper mantle: deformation in the dislocation creep regime. *Journal of Geophysical Research* **100**, 15 441–15 450.

Hirth G. and Kohlstedt D. L. (1996) Water in the oceanic upper mantle – implications for rheology, melt extraction and the evolution of the lithosphere. *Earth and Planetary Science Letters* **144**, 93–108.

Hirth G. and Kohlstedt D. L. (2003) Rheology of the upper mantle and the mantle wedge: a view from the experimentalists. In *Inside the Subduction Factory* (ed. J. E. Eiler), pp. 83–105. American Geophysical Union.

Hirth G., Teyssier C., and Dunlop D. J. (2001) An evaluation of quartzite flow law based on comparisons between experimentally and naturally deformed rocks. *International Journal of Earth Sciences* **90**, 77–87.

Hirth G. and Tullis J. (1992) Dislocation creep regimes in quartz aggregates. *Journal of Structural Geology* **14**, 145–159.

Hirth J. P. and Lothe J. (1982) *Theory of Dislocations*. Krieger Publishing Company.

Hitchings R. S., Paterson M. S., and Bitmead J. (1989) Effects of iron and magnetite additions in olivine–pyroxene rheology. *Physics of Earth and Planetary Interiors* **55**, 277–291.

Hobbs B. E. (1968) Recrystallization of single crystal of quartz. *Tectonophysics* **6**, 353–401.

Hobbs B. E. (1981) The influence of metamorphic environment upon the deformation of minerals. *Tectonophysics* **78**, 335–383.

Hobbs B. E. (1983) Constraints on the mechanism of deformation of olivine imposed by defect chemistry. *Tectonophysics* **92**, 35–69.

Hobbs B. E. (1984) Point defect chemistry of minerals under hydrothermal environment. *Journal of Geophysical Research* **89**, 4026–4038.

Hobbs B. E. (1985) The geological significance of microfabric analysis. In *Preferred Orientation in Deformed Metals and Rocks: an Introduction to Modern Texture Analysis* (ed. H.-R. Wenk), pp. 463–484. Academic Press.

Hobbs B. E., McLaren A. C., and Paterson M. S. (1972) Plasticity of single crystals of quartz. In *Flow and Fracture of Rocks* (ed. H. C. Heard, I. Y. Borg, N. L. Carter, and C. B. Raleigh), pp. 29–53. American Geophysical Union.

Hobbs B. E., Means W. D., and Williams P. F. (1976) *The Outline of Structural Geology*. Addison & Wiley.

Hobbs B. E., Mulhaus H.-B., and Ord A. (1990) Instability, softening and localization of deformation. In *Deformation Mechanisms, Rheology and Tectonics* (ed. R. J. Knipe and E. H. Rutter), pp. 143–165. The Geological Society.

Hobbs B. E. and Ord A. (1988) Plastic instabilities: implications for the origin of intermediate and deep focus earthquakes. *Journal of Geophysical Research* **89**, 10 521–10 540.

Hobbs B. E., Ord A., and Teyssier C. (1986) Earthquakes in the ductile regime. *Pure and Applied Geophysics* **124**, 310–336.

Hoff N. J. (1954) Approximate analysis of structures in the presence of moderately large creep deformations. *Quarterly Journal of Applied Mathematics* **12**, 49–55.

Hofmann A. W. (1997) Mantle geochemistry: the message from oceanic volcanism. *Nature* **385**, 219–228.

Hollomon J. H. (1947) The mechanical equation of state. *Trans. AIME* **171**, 535–545.

Holness M. B. (1993) Temperature and pressure dependence of quartz-aqueous fluid dihedral angles: the control of absorbed H_2O on the permeability of quartzites. *Earth and Planetary Science Letters* **117**, 363–377.

Holt D. L. (1970) Dislocation cell formation in metals. *Journal of Applied Physics* **41**, 3197–3201.

Holtzman B. K., Groebner N. J., Zimmerman M. E., Ginsberg S. B., and Kohlstedt D. L. (2003a) Stress-driven

melt segregation in partially molten rocks. *Geochemistry, Geophysics, Geosystems* **4**, 10.1029/2001GC000258.

Holtzman B. K., Kohlstedt D. L., and Phipps Morgan J. (2005) Viscous energy dissipation and strain partitioning in partially molten rocks. *Journal of Petrology* **46**, 2569–2592.

Holtzman B. K., Kohlstedt D. L., Zimmerman M. E., *et al.* (2003b) Melt segregation and strain partitioning: implications for seismic anisotropy and mantle flow. *Science* **301**, 1227–1230.

Honda S., Yuen D. A., Balachandar S., and Reuteler D. (1993) Three-dimensional instabilities of mantle convection with multiple phase transitions. *Science* **259**, 1308–1311.

Horn R. G., Smith D. T., and Haller W. (1989) Surface forces and viscosity of water measured between silica sheets. *Chemical Physics Letters* **162**, 404–408.

Houlier B., Cheraghmakni M., and Jaoul O. (1990) Silicon diffusion in San Carlos olivine. *Physics of Earth and Planetary Interiors* **62**, 329–340.

Houlier B., Jaoul O., Abel F., and Liebermann R. C. (1988) Oxygen and silicon diffusion in natural olivine at $T = 1300\,^{\circ}\mathrm{C}$. *Physics of Earth and Planetary Interiors* **50**, 240–250.

Huang X., Xu Y., and Karato S. (2005) Water content of the mantle transition zone from the electrical conductivity of wadsleyite and ringwoodite. *Nature* **434**, 746–749.

Hutchinson J. W. (1976) Bounds and self-consistent estimates for creep of polycrystalline materials. *Proceedings of the Royal Society of London A* **348**, 101–127.

Hutchinson J. W. (1977) Creep and plasticity of hexagonal polycrystals as related to single crystal slip. *Metallurgical Transactions A* **8**, 1465–1469.

Ingrin J. and Skogby H. (2000) Hydrogen in nominally anhydrous upper-mantle minerals: concentration levels and implications. *European Journal of Mineralogy* **12**, 543–570.

Inoue T., Yurimoto H., and Kudoh Y. (1995) Hydrous modified spinel, $Mg_{1.75}SiH_{0.5}O_4$: a new water reservoir in the mantle transition zone. *Geophysical Research Letters* **22**, 117–120.

Irifune T. and Ringwood A. E. (1987) Phase transformations in primitive MORB and pyrolyte composition to 25 GPa and some geophysical implications. In *High-Pressure Research in Mineral Physics* (ed. M. H. Manghnani and Y. Syono), pp. 231–242. American Geophysical Union.

Isaak D. G. (1992) High-temperature elasticity of iron-bearing olivines. *Journal of Geophysical Research* **97**, 1871–1885.

Ishii M. and Dziewonski A. M. (2002) The innermost inner core of the earth: evidence for a change in anisotropic behavior at the radius of about 300 km. *Proceedings of American Academy of Arts and Sciences* **99**, 14 026–14 030.

Ishii M. and Tromp J. (1999) Normal mode and free-air gravity constraints on lateral variation in density of Earth's mantle. *Science* **285**, 1231–1236.

Ita J. and Cohen R. E. (1997) Effects of pressure on diffusion and vacancy formation in MgO from nonempirical free-energy integration. *Physical Review Letters* **79**, 3198–3201.

Ito E. and Katsura T. (1989) A temperature profile of the mantle transition zone. *Geophysical Research Letters* **16**, 425–428.

Ito Y. and Toriumi M. (2007) Pressure effect on self-diffusion in periclase (MgO) by molecular dynamics. *Journal of Geophysical Research*, in press.

Iyer H. M. and Hirahara K. (1993) *Seismic Tomography: Theory and Practice*. Chapman and Hall.

Jackson I. (1998) Elasticity, composition and temperature of the Earth's lower mantle: a reappraisal. *Geophysical Journal International* **134**, 291–311.

Jackson I. (2000) Laboratory measurements of seismic wave dispersion and attenuation: recent progress. In *Earth's Deep Interior: Mineral Physics and Tomography from the Atomic to the Global Scale* (ed. S. Karato, A. M. Forte, R. C. Liebermann, G. Masters, and L. Stixrude), pp. 265–289. American Geophysical Union.

Jackson I., Faul U. H., Fitz Gerald J. D., and Tan B. (2004a) Shear wave attenuation and dispersion in melt-bearing olivine polycrystals: 1. Specimen fabrication and mechanical testing. *Journal of Geophysical Research* **109**, 10.1029/2003JB002406.

Jackson I., Fitz Gerald J. D., Faul U. H., and Tan B. H. (2002) Grain-size sensitive seismic-wave attenuation in polycrystalline olivine. *Journal of Geophysical Research* **107**, 10.1029/2002JB001225.

Jackson I., Fitz Gerald J. D., and Kokkonen H. (2000a) High-temperature viscoelastic relaxation in iron and its implications for the shear modulus and attenuation of the Earth's inner core. *Journal of Geophysical Research* **105**, 23 605–23 634.

Jackson I. and Niesler H. (1982) The elasticity of periclase to 3 GPa and some geophysical implications. In *High-Pressure Research in Geophysics* (ed. S. Akimoto and M. H. Manghnani), pp. 93–113. Center for Academic Publications, Japan.

Jackson I. and Paterson M. S. (1987) Shear modulus and internal friction of calcite rocks at seismic frequencies. *Physics of Earth and Planetary Interiors* **45**, 349–367.

Jackson I. and Paterson M. S. (1993) A high-pressure, high-temperature apparatus for studies of seismic wave dispersion and attenuation. *Pure and Applied Geophysics* **141**, 445–466.

Jackson I., Paterson M. S., and Fitz Gerald J. D. (1992) Seismic wave dispersion and attenuation in Åheim dunite. *Geophysical Journal International* **108**, 517–534.

Jackson J. A. (2002a) Faulting, flow, and strength of the continental lithosphere. *International Geological Review* **11**, 39–61.

Jackson J. A. (2002b) Strength of the continental lithosphere: time to abandon the jelly sandwich? *GSA Today* **12**, 4–10.

Jackson J. M., Sinogeikin S. V., and Bass J. D. (2000b) Sound velocities and elastic properties of γ-Mg_2SiO_4 to 873 K by Brillouin spectroscopy. *American Mineralogist* **85**, 296–303.

Jackson J. M., Zhang J., and Bass J. D. (2004b) Sound velocities and elasticity of aluminous $MgSiO_3$ perovskite: implications for aluminium heterogeneity in Earth's lower mantle. *Geophysical Research Letters* **31**, 10.1029/2004GL019918.

Jacobsen S. D. (2006) Effect of water on the equation of state of nominally anhydrous minerals. In *Water in Nominally Anhydrous Minerals* (ed. H. Keppler and J. R. Smyth), pp. 321–342. Mineralogical Society of America.

Jagoutz E., Palme H., Baddenhausen H., *et al.* (1979) The abundances of major, minor, and trace elements in the Earth's mantle as derived from primitive ultramafic nodules. *Proceedings of 10th Lunar and Planetary Science Conference*, 2031–2050.

Jaoul O. (1990) Multicomponent diffusion and creep in olivine. *Journal of Geophysical Research* **95**, 17631–17642.

Jaoul O. and Houlier B. (1983) Study of ^{18}O diffusion in magnesium orthosilicate by nuclear micro analysis. *Journal of Geophysical Research* **88**, 613–624.

Jaoul O., Poumellec M., Froidevaux C., and Havette A. (1981) Silicon diffusion in forsterite: a new constraint for understanding mantle deformation. In *Anelasticity in the Earth* (ed. F. D. Stacey, M. S. Paterson, and A. Nicolas). American Geophysical Union.

Jaoul O., Sautter V., and Abel F. (1991) Nuclear microanalysis: a powerful tool for measuring low atomic diffusivity with mineralogical applications. In *Diffusion, Atomic Ordering, and Mass Transport* (ed. J. Ganguly), pp. 198–220. Springer-Verlag.

Jaroslow G. E., Hirth G., and Dick H. J. B. (1996) Abyssal peridotite mylonites: implications for grain-size sensitive flow and strain localization in the oceanic lithosphere. *Tectonophysics* **256**, 17–37.

Jessel M. W. (1988a) Simulation of fabric development in recrystallizing aggregates – I. Description of the model. *Journal of Structural Geology* **10**, 771–778.

Jessel M. W. (1988b) Simulation of fabric development in recrystallizing aggregates – II. Example model runs. *Journal of Structural Geology* **10**, 779–793.

Jesser W. A. and Kuhlmann-Wilsdorf D. (1972) The flow stress and dislocation structure of nickel deformed at very high pressure. *Materials Science and Engineering* **9**, 111–117.

Ji S., Wang Z., and Wirth R. (2001) Bulk flow strength of forsterite–enstatite composites as a function of forsterite content. *Tectonophysics* **341**, 69–93.

Ji S. and Zhao P. (1993) Flow laws of multiphase rocks calculated from experimental data on the constituent phases. *Earth and Planetary Science Letters* **117**, 181–187.

Jin D., Karato S., and Obata M. (1998) Mechanisms of shear localization in the continental lithosphere: inference from the deformation microstructures of peridotites from the Ivrea zone, northern Italy. *Journal of Structural Geology* **20**, 195–209.

Jin Z. M., Green H. W., II., and Zhou Y. (1994) Melt topology in partially molten mantle peridotite during ductile deformation. *Nature* **372**, 164–167.

Jin Z. M., Zhang J., Green H. W., II., and Jin S. (2001) Eclogite rheology: implications for subducting lithosphere. *Geology* **29**, 667–670.

Joesten R. (1983) Grain growth and grain-boundary diffusion in quartz from the Christmas Mountains (Texas) contact aurole. *American Journal of Science* **283**, 233–254.

Johnson W. C. (1984) On the elastic stabilization of precipitates against coarsening under applied load. *Acta Metallurgica* **32**, 465–475.

Johnson W. C. and Cahn J. W. (1984) Elastically induced shape bifurcations of inclusions. *Acta Metallurgica* **32**, 1925–1933.

Johnson W. C. and Schmalzried H. (1992) Gibbs–Duhem and Clausius–Clapeyron type equations for elastically stressed crystals. *Acta Metallurgica et Materialia* **40**, 2337–2342.

Johnston W. G. (1962) Yield points and delay times in single crystals. *Journal of Applied Physics* **33**, 2716–2730.

Johnston W. G. and Gilman J. J. (1959) Dislocation velocities, dislocation densities, and plastic flow in lithium fluoride crystals. *Journal of Applied Physics* **30**, 129–144.

Jones R. (1980) The structure of kinks on the 90º partial in silicon and a 'strain-bond model' for dislocation motion. *Philosophical Magazine B* **42**, 213–219.

Jordan P. G. (1987) The deformation behaviour of bimineralic limestone–halite aggregates. *Tectonophysics* **135**, 185–197.

Jordan P. G. (1988) The rheology of polymineralic rocks: an approach. *Geologiches Rundschau* **77**, 285–294.

Jordan T. H. (1975) The continental tectosphere. *Review of Geophysics and Space Physics* **13**, 1–12.

Jordan T. H. (1981) Continents as a chemical boundary layer. *Philosophical Transactions of the Royal Society of London A* **301**, 359–373.

Jung H. and Karato S. (2001a) Effect of water on the size of dynamically recrystallized grains in olivine. *Journal of Structural Geology* **23**, 1337–1344.

Jung H. and Karato S. (2001b) Water-induced fabric transitions in olivine. *Science* **293**, 1460–1463.

Jung H., Katayama I., Jiang Z., Hiraga T., and Karato S. (2006) Effects of water and stress on the lattice preferred orientation in olivine. *Tectonophysics* **421**, 1–22.

Kamb W. B. (1961) The thermodynamic theory of nonhydrostatically stressed solids. *Journal of Geophysical Research* **66**, 259–271.

Kamb W. B. (1972) Experimental recrystallization of ice under stress. In *Flow and Fracture of Rocks* (ed. H. C. Heard,

I. Y. Borg, N. L. Carter, and C. B. Raleigh), pp. 211–241. American Geophysical Union.

Kaminski E. (2002) The influence of water on the development of lattice preferred orientation in olivine aggregates. *Geophysical Research Letters* **29**, 17-1/17-4.

Kaminski E. and Ribe N. M. (2001) A kinematic model for dynamic recrystallization and texture development in olivine polycrystals. *Earth and Planetary Science Letters* **189**, 253–267.

Kaminski E., Ribe N. M., and Browaeys J. T. (2004) D-rex, a program for calculation of seismic anisotropy due to crystal lattice preferred orientation in the convective upper mantle. *Geophysical Journal International* **158**, 744–752.

Kamiya S. and Kobayashi Y. (2000) Seismological evidence for the presence of serpentinized wedge mantle. *Geophysical Research Letters* **27**, 819–822.

Kampfmann W. and Berckhemer H. (1985) High temperature experiments on the elastic and anelastic behaviour of magmatic rocks. *Physics of Earth and Planetary Interiors* **40**, 223–247.

Kanamori H. and Anderson D. L. (1977) Importance of physical dispersion in surface wave and free oscillation problems: review. *Review of Geophysics and Space Physics* **15**, 105–112.

Kanamori H. and Press F. (1970) How thick is the lithosphere? *Nature* **226**, 330–331.

Kaneshima S. (1990) Origin of crustal anisotropy: shear wave splitting studies in Japan. *Journal of Geophysical Research* **95**, 11 121–11 133.

Kaneshima S. and Helffrich G. (1999) Dipping low-velocity layer in the mid-mantle: evidence for geochemical heterogeneity. *Science* **283**, 1888–1891.

Kanzaki H. (1957) Point defects in face-centred cubic lattice – I. Distortion around defects. *Journal of Physics and Chemistry of Solids* **2**, 24–36.

Karato S. (1977) *Rheological Properties of Materials Composing the Earth's Mantle*. Ph.D., University of Tokyo.

Karato S. (1978) The concentration minimum of point defects under high pressures and the viscosity of the lower mantle. *Programme and Abstracts, The Seismological Society of Japan* **1**, D31.

Karato S. (1981a) Pressure dependence of diffusion in ionic solids. *Physics of Earth and Planetary Interiors* **25**, 38–51.

Karato S. (1981b) Rheology of the lower mantle. *Physics of Earth and Planetary Interiors* **24**, 1–14.

Karato S. (1984) Grain-size distribution and rheology of the upper mantle. *Tectonophysics* **104**, 155–176.

Karato S. (1986) Does partial melting reduce the creep strength of the upper mantle? *Nature* **319**, 309–310.

Karato S. (1987a) Scanning electron microscope observation of dislocations in olivine. *Physics and Chemistry of Minerals* **14**, 245–248.

Karato S. (1987b) Seismic anisotropy due to lattice preferred orientation of minerals: kinematic or dynamic? In *High-Pressure Research in Geophysics* (ed. M. H. Manghnani and Y. Syono), pp. 455–471. American Geophysical Union.

Karato S. (1988) The role of recrystallization in the preferred orientation in olivine. *Physics of Earth and Planetary Interiors* **51**, 107–122.

Karato S. (1989a) Defects and plastic deformation in olivine. In *Rheology of Solids and of the Earth* (ed. S. Karato and M. Toriumi), pp. 176–208. Oxford University Press.

Karato S. (1989b) Grain growth kinetics in olivine aggregates. *Tectonophysics* **155**, 255–273.

Karato S. (1989c) Plasticity-crystal structure systematics in dense oxides and its implications for creep strength of the Earth's deep interior: a preliminary result. *Physics of Earth and Planetary Interiors* **55**, 234–240.

Karato S. (1990) The role of hydrogen in the electrical conductivity of the upper mantle. *Nature* **347**, 272–273.

Karato S. (1992) On the Lehmann discontinuity. *Geophysical Research Letters* **19**, 2255–2258.

Karato S. (1993a) Importance of anelasticity in the interpretation of seismic tomography. *Geophysical Research Letters* **20**, 1623–1626.

Karato S. (1993b) Inner core anisotropy due to the magnetic field-induced preferred orientation of iron. *Science* **262**, 1708–1711.

Karato S. (1995) Effects of water on seismic wave velocities in the upper mantle. *Proceedings of the Japan Academy* **71**, 61–66.

Karato S. (1997a) On the separation of crustal component from subducted oceanic lithosphere near the 660 km discontinuity. *Physics of Earth and Planetary Interiors* **99**, 103–111.

Karato S. (1997b) Phase transformations and rheological properties of mantle minerals. In *Earth's Deep Interior* (ed. D. Crossley), pp. 223–272. Gordon and Breach.

Karato S. (1998a) A dislocation model of seismic wave attenuation and velocity dispersion and microcreep of the solid Earth: Harold Jeffreys and the rheology of the solid Earth. *Pure and Applied Geophysics* **153**, 239–256.

Karato S. (1998b) Effects of pressure on plastic deformation of polycrystalline solids: some geological applications. In *High Pressure Research in Materials Sciences* (ed. R. M. Wentzcovitch, R. J. Hemley, W. J. Neillis, and P. Y. Yu), pp. 3–14. Materials Research Society.

Karato S. (1998c) Micro-physics of post glacial rebound (In *Dynamics of the Ice Age Earth* ed. P. Wu), pp. 351–364. *Trans. Tech.*

Karato S. (1998d) Seismic anisotropy in the deep mantle, boundary layers and geometry of mantle convection. *Pure and Applied Geophysics* **151**, 565–587.

Karato S. (1998e) Some remarks on seismic anisotropy in the D″ layer. *Earth, Planets, Space* **50**, 1019–1028.

Karato S. (1999) Seismic anisotropy of the Earth's inner core resulting from flow induced by Maxwell stress. *Nature* **402**, 871–873.

Karato S. (2000) Dynamics and anisotropy of the Earth's inner core. *Proceedings of Japan Academy B* **76**, 1–6.

Karato S. (2003a) *Dynamic Structure of the Deep Earth: an Interdisciplinary Approach*. Princeton University Press.

Karato S. (2003b) Mapping water content in Earth's upper mantle. In *Inside the Subduction Factory* (ed. J. E. Eiler), pp. 135–152. American Geophysical Union.

Karato S. (2006a) Influence of hydrogen-related defects on the electrical conductivity and plastic deformation of mantle minerals: a critical review. In *Earth's Deep Water Cycle* (ed. S. D. Jacobsen and S. van der Lee), pp. 113–129. American Geophysical Union.

Karato S. (2006b) Remote sensing of hydrogen in Earth's mantle. In *Water in Nominally Anhydrous Minerals* (ed. H. Keppler and J. R. Smyth), pp. 343–375. Mineralogical Society of America.

Karato S. (2007) Microscopic models for the influence of hydrogen on physical and chemical properties of minerals. In *Superplume: Beyond Plate Tectonics* (ed. D. A. Yuen, S. Maruyama, S. Karato, and B. F. Windley), 321–355. Springer-Verlag.

Karato S., Bercovici D., Leahy G., Richard G., and Jing Z. (2006) Transition zone water filter model for global material circulation: where do we stand? In *Earth's Deep Water Cycle* (ed. S. D. Jacobsen and S. van der Lee), pp. 289–313. American Geophysical Union.

Karato S., Dupas-Bruzek C., and Rubie D. C. (1998) Plastic deformation of silicate spinel under the transition zone conditions of the Earth. *Nature* **395**, 266–269.

Karato S., Ito E., and Fujino K. (1990) Plasticity of $MgSiO_3$ perovskite: the results of microhardness tests on single crystals. *Geophysical Research Letters* **17**, 13–16.

Karato S. and Jung H. (1998) Water, partial melting and the origin of seismic low velocity and high attenuation zone in the upper mantle. *Earth and Planetary Science Letters* **157**, 193–207.

Karato S. and Jung H. (2003) Effects of pressure on high-temperature dislocation creep in olivine polycrystals. *Philosophical Magazine A* **83**, 401–414.

Karato S. and Karki B. B. (2001) Origin of lateral heterogeneity of seismic wave velocities and density in Earth's deep mantle. *Journal of Geophysical Research* **106**, 21 771–21 783.

Karato S. and Lee K.-H. (1999) Stress–strain distribution in deformed olivine aggregates: inference from microstructural observations and implications for texture development. *12th International Conference on Textures of Materials*, 1546–1555.

Karato S. and Li P. (1992) Diffusion creep in the perovskite: implications for the rheology of the lower mantle. *Science* **255**, 1238–1240.

Karato S. and Murthy V. R. (1997) Core formation and chemical equilibrium in the Earth I. Physical considerations. *Physics of Earth and Planetary Interiors* **100**, 61–79.

Karato S., Paterson M. S., and Fitz Gerald J. D. (1986) Rheology of synthetic olivine aggregates: influence of grain-size and water. *Journal of Geophysical Research* **91**, 8151–8176.

Karato S., Riedel M. R., and Yuen D. A. (2001) Rheological structure and deformation of subducted slabs in the mantle transition zone: implications for mantle circulation and deep earthquakes. *Physics of Earth and Planetary Interiors* **127**, 83–108.

Karato S. and Rubie D. C. (1997) Toward experimental study of plastic deformation under deep mantle conditions: a new multianvil sample assembly for deformation experiments under high pressures and temperatures. *Journal of Geophysical Research* **102**, 20 111–20 122.

Karato S. and Sato H. (1982) The effect of oxygen partial pressure on the dislocation recovery in olivine: a new constraint on creep mechanisms. *Physics of Earth and Planetary Interiors* **28**, 312–319.

Karato S. and Spetzler H. A. (1990) Defect microdynamics in minerals and solid state mechanisms of seismic wave attenuation and velocity dispersion in the mantle. *Review of Geophysics* **28**, 399–421.

Karato S., Toriumi M., and Fujii T. (1980) Dynamic recrystallization of olivine single crystals during high temperature creep. *Geophysical Research Letters* **7**, 649–652.

Karato S., Wang Z., Liu B., and Fujino K. (1995a) Plastic deformation of garnets: systematics and implications for the rheology of the mantle transition zone. *Earth and Planetary Science Letters* **130**, 13–30.

Karato S. and Wu P. (1993) Rheology of the upper mantle: a synthesis. *Science* **260**, 771–778.

Karato S., Zhang S., and Wenk H.-R. (1995b) Superplasticity in Earth's lower mantle: evidence from seismic anisotropy and rock physics. *Science* **270**, 458–461.

Karki B. B., Stixrude L., Clark S. J., *et al*. (1997) Structure and elasticity of MgO at high pressure. *American Mineralogist* **82**, 635–639.

Karki B. B., Stixrude L., and Wentzcovitch R. M. (2001) High-pressure elastic properties of major materials of Earth's mantle from first principles. *Review of Geophysics* **39**, 507–534.

Kataoka T., Colombo L., and Li J. C. M. (1983) Dislocation charges in pure and Ca^{2+}-doped KCl in the temperature range from 82 to 294 K. *Radiation Effects* **75**, 227–234.

Kataoka T., Colombo L., and Li J. C. M. (1984a) Direct measurements of dislocation charges in Ca^{2+}-doped KCl by using large electric fields. *Philosophical Magazine A* **49**, 395–407.

Kataoka T., Colombo L., and Li J. C. M. (1984b) Dislocation charges in Ca^{2+}-doped KCl. Effects of impurity

concentration and temperature. *Philosophical Magazine A* **49**, 409–423.

Katayama I., Hirose K., Yurimoto H., and Nakashima S. (2003) Water solubility in majorite garnet in subducting oceanic crust. *Geophysical Research Letters* **30**, 10.1029/2003GL018127.

Katayama I., Jung H., and Karato S. (2004) New type of olivine fabric at modest water content and low stress. *Geology* **32**, 1045–1048.

Katayama I. and Karato S. (2006) Effects of temperature on the B- to C-type fabric transition in olivine. *Physics of the Earth and Planetary Interiors* **157**, 33–45.

Katayama I. and Karato S. (2007) The role of water and iron content on the rheological contrast between garnet and olivine. *Physics of the Earth and Planetary Interiors*, submitted.

Katayama I. and Nakashima S. (2003) Hydroxyl in clinopyroxene from the deep subducted crust: evidence for H_2O transport into the mantle. *American Mineralogist* **88**, 229–234.

Kato T. and Kumazawa M. (1985) Garnet phase of $MgSiO_3$ filling the pyroxene–ilmenite gap at very high temperature. *Nature* **316**, 803–805.

Katsura T., Mayama N., Shouno K., *et al*. (2001) Temperature derivatives of elastic moduli of $(Mg_{0.91}, Fe_{0.09})_2SiO_4$ modified spinel. *Physics of Earth and Planetary Interiors* **124**, 163–166.

Katz R. F., Spiegelman M., and Holtzman B. (2006) The dynamics of melt and shear localization in partially molten aggregates. *Nature* **442**, 676–679.

Kaula W. M. (1964) Tidal dissipation by solid friction and the resulting orbital evolution. *Review of Geophysics* **2**, 661–685.

Kawakatsu H. and Niu F. (1995) Seismic evidence for the 920-km discontinuity in the mantle. *Nature* **371**, 301–305.

Kawamoto T., Hertig R. J., and Holloway J. R. (1996) Experimental evidence for a hydrous transition zone in Earth's early mantle. *Earth and Planetary Science Letters* **142**, 587–592.

Kê T. S. (1947) Experimental evidence of the viscous behavior of grain boundaries in metals. *Physical Review* **71**, 533–546.

Kekulawala K. R. S. S., Paterson M. S., and Boland J. N. (1978) Hydrolytic weakening in quartz. *Tectonophysics* **46**, T1–T6.

Kekulawala K. R. S. S., Paterson M. S., and Boland J. N. (1981) An experimental study of the role of water in quartz deformation. In *Mechanical Behavior of Crustal Rocks: the Handin Volume* (ed. N. L. Carter, M. Friedman, J. M. Logan, and D. W. Stearns), pp. 49–60. American Geophysical Union.

Kelemen P. B., Hirth G., Shimizu N., Spiegelman M., and Dick H. J. B. (1997) A review of melt migration processes in the adiabatically upwelling mantle beneath oceanic spreading ridges. *Philosophical Transactions of the Royal Society of London* **355**, 283–318.

Kellogg L. H., Hager B. H., and van der Hilst R. D. (1999) Compositional stratification in the deep mantle. *Science* **283**, 1881–1884.

Kelly A., Tyson W. R., and Cottrell A. H. (1967) Ductile and brittle crystals. *Philosophical Magazine* **15**, 567–586.

Kendall J.-M. and Silver P. G. (1996) Constraints from seismic anisotropy on the nature of the lowermost mantle. *Nature* **381**, 409–412.

Kendall J.-M. and Silver P. G. (1998) Investigating causes of D″ anisotropy. In *The Core–Mantle Boundary Region* (ed. M. E. W. M. Gurnis, E. Knittle and B. A. Buffett), pp. 97–118. American Geophysical Union.

Kennett B. L. N., Engdahl E. R., and Buland R. P. (1995) Constraints on seismic wave velocities in the Earth from travel times. *Geophysical Journal International* **122**, 108–124.

Keppler H., Wiedenbeck M., and Shcheka S. S. (2003) Carbon solubility in olivine and the mode of carbon storage in the Earth's mantle. *Nature* **424**, 414–416.

Keyes R. W. (1963) Continuum models of the effect of pressure on activated processes. In *Solids Under Pressure* (ed. W. Paul and D. M. Warschauer), pp. 71–91. McGraw-Hill.

Khisina N. R., Wirth R., Andrut M., and Ukhanov A. V. (2001) Extrinsic and intrinsic mode of hydrogen occurrence in natural olivines: FTIR and TEM investigation. *Physics and Chemistry of Minerals* **28**, 291–301.

Kido M. and Cadek O. (1997) Inferences of viscosity from the oceanic geoid: indication of a low viscosity zone below the 660-km discontinuity. *Earth and Planetary Science Letters* **151**, 125–137.

King S. D. (1995a) Radial models of mantle viscosity: results from a genetic algorithm. *Geophysical Journal International* **122**, 725–734.

King S. D. (1995b) The viscosity structure of the mantle. *Review of Geophysics* **33**, 11–17.

Kingery W. D. (1974a) Plausible concepts necessary and sufficient for interpretation of ceramic grain-boundary phenomena: I. Grain-boundary characteristics, structure, and electrostatic potential. *Journal of the American Ceramic Society* **57**, 1–8.

Kingery W. D. (1974b) Plausible concepts necessary and sufficient for interpretation of ceramic grain-boundary phenomena: II. Solute segregation, grain-boundary diffusion, and general discussion. *Journal of the American Ceramic Society* **57**, 74–83.

Kingery W. D., Bowen H. K., and Uhlmann D. R. (1976) *Introduction to Ceramics*. John Wiley & Sons.

Kinsland G. L. and Bassett W. A. (1977) Strength of MgO and NaCl polycrystals to confining pressures of 250 kbar at 25 °C. *Journal of Applied Physics* **48**, 978–985.

Kirby S. H. (1977) The effects of the α–β phase transformation on the creep properties of hydrolytically-weakened synthetic quartz. *Geophysical Research Letters* **4**, 97–100.

Kitamura M., Kondoh S., Morimoto N., *et al*. (1987) Planar OH-bearing defects in mantle olivine. *Nature* **328**, 143–145.

Kitamura M., Matsuda H., and Morimoto N. (1986) Direct observation of the Cottrell atmosphere in olivine. *Proceedings of Japan Academy* **62**, 149–152.

Kittel C. (1986) *Introduction to Solid State Physics*. John Wiley & Sons.

Kliewer K. L. and Koehler J. S. (1965) Space charge in ionic crystals. I. General approach with application to NaCl. *Physical Review* **140**, A1226–A1240.

Kneller E. A., van Keken P. E., Karato S., and Park J. (2005) B-type olivine fabric in the mantle wedge: insights from high-resolution non-Newtonian subduction zone models. *Earth and Planetary Science Letters* **237**, 781–797.

Kocks U. F. (1970) The relation between polycrystal deformation and single crystal deformation. *Metallurgical Transactions* **1**, 1121–1143.

Kocks U. F., Argon A. S., and Ashby M. F. (1975) Thermodynamics and kinetics of slip. *Progress in Materials Sciences* **19**, 1–288.

Kocks U. F., Jonas J. J., and Mecking H. (1979) The development of strain-rate gradients. *Acta Metallurgica* **27**, 419–432.

Kocks U. F., Tomé C. N., and Wenk H.-R. (1998) *Texture and Anisotropy*. Cambridge University Press.

Kogiso T., Hirose K., and Takahashi E. (1998) Melting experiments on homogeneous mixtures of peridotites and basalts: application to the genesis of ocean island basalts. *Earth and Planetary Science Letters* **162**, 45–61.

Kohlstedt D. L. (2002) Partial melting and deformation. In *Plastic Deformation of Minerals and Rocks*, Vol. 51 (ed. S. Karato and H.-R. Wenk), pp. 121–135. Mineralogical Society of America.

Kohlstedt D. L. (2006) The role of water in high-temperature rock deformation. In *Water in Nominally Anhydrous Minerals* (ed. H. Keppler and J. R. Smyth), pp. 377–396. Mineralogical Society of America.

Kohlstedt D. L., Evans B., and Mackwell S. J. (1995) Strength of the lithosphere: constraints imposed by laboratory measurements. *Journal of Geophysical Research* **100**, 17 587–17 602.

Kohlstedt D. L. and Goetze C. (1974) Low-stress, high-temperature creep in olivine single crystals. *Journal of Geophysical Research* **79**, 2045–2051.

Kohlstedt D. L., Goetze C., and Durham W. B. (1976) A new technique for decorating dislocations in olivine. *Science* **191**, 1945–1046.

Kohlstedt D. L., Keppler H., and Rubie D. C. (1996) Solubility of water in the α, β and γ phases of $(Mg, Fe)_2SiO_4$. *Contributions to Mineralogy and Petrology* **123**, 345–357.

Kohlstedt D. L. and Mackwell S. J. (1998) Diffusion of hydrogen and intrinsic point defects in olivine. *Zeitschrift für Phisikalische Chemie* **207**, 147–162.

Kohlstedt D. L. and Mackwell S. J. (1999) Solubility and diffusion of 'water' in silicates. In *Microscopic Properties and Processes in Minerals* (ed. K. Wright and R. Catlow), pp. 539–559. Kluwer Academic Publishers.

Kohlstedt D. L. and Weathers M. S. (1980) Deformation-induced microstructures, paleopiezometers, and differential stresses in deeply eroded fault zones. *Journal of Geophysical Research* **85**, 6269–6285.

Kolsky H. (1956) The propagation of stress pulses in viscoelastic solids. *Philosophical Magazine* **1**, 693–710.

Korenaga J. (2005) Firm mantle plumes and the nature of the core–mantle region. *Earth and Planetary Science Letters* **232**, 29–37.

Korenaga J. (2007) Thermal cracking and the deep hydration of oceanic lithosphere: a key to the generation of plate tectonics? *Journal of Geophysical Research* **112**, 10.1029/2006JB004502.

Krajewski P. E., Jones J. W., and Allison J. E. (1995) The effect of particle reinforcement on the creep behavior of single-phase aluminum. *Metallurgical Materials Transactions A* **26**, 3107–3118.

Kronenberg A. K., Kirby S. H., and Aines R. D. (1986) Solubility and diffusional uptake of hydrogen in quartz at high water pressures: implications for hydrolytic weakening. *Journal of Geophysical Research* **91**, 12 723–12 744.

Kronenberg A. K. and Tullis J. (1984) Flow strength of quartz aggregates: grain size and pressure effects due to hydrolytic weakening. *Journal of Geophysical Research* **89**, 4281–4297.

Kubin L. P. (1993) Dislocation patterning. In *Materials Science and Technology*, Vol. 6 (ed. R. W. Cahn, P. Haasen, and E. J. Kramer), pp. 137–190. VCH.

Kubo T., Ohtani E., Kato T., Shinmei T., and Fujino K. (1998) Effects of water on the α–β transformation kinetics in San Carlos olivine. *Science* **281**, 85–87.

Kubo T., Ohtani E., Kato T., *et al*. (2000) Formation of metastable assemblages and mechanisms of the grain-size reduction in the postspinel transformation of Mg_2SiO_4. *Geophysical Research Letters* **27**, 807–810.

Kumazawa M. (1974) On the relation between plastic flow properties and elastic wave velocities. In *Flow of Solids: From Earth to Crystals* (ed. S. Uyeda), pp. 246–262. Tokai University Press.

Kurishita H., Yoshinaga H., and Nakashima H. (1989) The high temperature deformation mechanism in pure metals. *Acta Metallurgica* **37**, 499–505.

Kurz W. and Fischer D. J. (1998) *Fundamentals of Solidification*. Trans Tech.

Kushiro I. (1975) On the nature of silicate melt and its significance in magma genesis: regularities in the shift of the

liquidus boundaries involving olivine. *American Journal of Science* **275**, 411–431.

Kushiro I. (1976) Viscosities of basalt and andesite melts at high pressures. *Journal of Geophysical Research* **81**, 6351–6356.

Labrosse S., Poirier J.-P., and Le Mouel J.-L. (2001) The age of the inner core. *Physics of Earth and Planetary Interiors* **190**, 111–123.

Lager G. A., Armbruster T., Rotella F. J., and Rossman G. R. (1989) The OH substitution in garnets: X-ray and neutron diffraction, infrared and geometric-modelling studies. *American Mineralogist* **74**, 840–851.

Lakki A., Schaller R., Carry C., and Benoit W. (1998) High temperature anelastic and viscoelastic deformation of fine-grained MgO-doped Al_2O_3. *Acta Materialia* **46**, 689–700.

Lambeck K. and Johnston P. (1998) The viscosity of the mantle: evidence from analyses of glacial-rebound phenomena. In *The Earth's Mantle* (ed. I. Jackson), pp. 461–502. Cambridge University Press.

Landau L. D. and Lifshitz E. M. (1959) *Theory of Elasticity*. Pergamon Press.

Landau L. D. and Lifshitz E. M. (1964) *Statistical Physics*. Pergamon Press.

Landau L. D. and Lifshitz E. M. (1987) *Fluid Dynamics*. Pergamon Press.

Langdon T. G., Dehghan A., and Sammis C. G. (1982) Deformation of olivine, and the application to lunar and planetary interiors. *Strength of Metals and Alloys, Proceedings of the 6th International Conference*, pp. 757–762 Pergamon Press.

Langdon T. G. and Yavari P. (1982) An investigation of Harper–Dorn creep – II. The flow process. *Acta Metallurgica* **30**, 881–887.

Langmuir J. W., Klein E. M., and Plank T. (1992) Petrological systematics of mid-ocean ridge basalt: constraints on melt generation beneath ocean ridges. In *Mantle Flow and Melt Generation at Mid-Ocean Ridges* (ed. J. P. Morgan, D. K. Blackman, and J. M. Sinton), pp. 183–280. American Geophysical Union.

Lasaga A. C. (1997) *Kinetic Theory in Earth Sciences*. Princeton University Press.

Lawlis J. D. (1998) *High Temperature Creep of Synthetic Olivine-Enstatite Aggregates*. Ph.D., The Pennsylvania State University.

Lawrence J. F. and Wysession M. E. (2005) QLM9: a new radial quality factor (Q) model for the mantle. *Earth and Planetary Science Letters* **241**, 962–971.

Lawrence J. F. and Wysession M. E. (2006) Seismic evidence for subduction-transported water in the lower mantle. In *Earth's Deep Water Cycle* (ed. S. D. Jacobsen and S. v. d. Lee), pp. 251–261. American Geophysical Union.

Lay T., Garnero E. J., and Williams Q. (2004) Partial melting in a thermo-chemical boundary layer at the base of the mantle. *Physics of Earth and Planetary Interiors* **146**, 441–467.

Lay T., Heinz D. L., Ishii M., *et al.* (2005) Multidisciplinary impact of the deep mantle phase transition in perovskite structure. *EOS, Transactions of American Geophysical Union* **86**, 1–5.

Lay T. and Wallace T. C. (1995) *Modern Global Seismology*. Academic Press.

Lay T., Williams Q., and Garnero E. J. (1998) The core–mantle boundary layer and deep Earth dynamics. *Nature* **392**, 461–468.

Lebensohn R. A. and Tomé C. N. (1993) A self-consistent anisotropic approach for the simulation of plastic deformation and texture development of polycrystals: application to zirconium alloys. *Acta Metallurgica et Materials* **41**, 2611–2624.

Lee D.-C. and Halliday A. N. (1995) Hafnium–tungsten chronometry and the timing of terrestrial core formation. *Nature* **392**, 771–774.

Lee K.-H., Jiang Z., and Karato S. (2002) A scanning electron microscope study of effects of dynamic recrystallization on the lattice preferred orientation in olivine. *Tectonophysics* **351**, 331–341.

Lemaire C., Kohn S. C., and Brooker R. A. (2004) The effect of silica activity on the incorporation mechanisms of water in synthetic forsterite: a polarized infrared spectroscopic study. *Contributions to Mineralogy and Petrology* **147**, 48–57.

Lenardic A. and Moresi L. N. (1999) Some thoughts on the stability of cratonic lithosphere: effects of buoyancy and viscosity. *Journal of Geophysical Research* **104**, 12 747–12 759.

Levien L. and Prewitt C. T. (1981) High-pressure structural study of diopside. *American Mineralogist* **66**, 315–323.

Lewis J. S. (1974) Chemical composition of the solar system. *Scientific American* **230**, 50–65.

Li B., Liebermann R. C., and Weidner D. J. (1998) Elastic moduli of wadsleyite (β-Mg_2SiO_4) to 7 GPa and 873 K. *Science* **281**, 675–677.

Li J., Hadidiacos C., Mao H.-K., Fei Y., and Hemley R. J. (2003a) Behavior of thermocouples under high pressure in a multi-anvil apparatus. *High Pressure Research* **23**, 389–401.

Li J. C. M. (1963) A dislocation mechanism of transient creep. *Acta Metallurgica* **11**, 1269–1270.

Li L., Raterron P., Weidner D. J., and Long H. (2006) Plastic flow of pyrope at mantle pressure and temperature. *American Mineralogist* **91**, 517–525.

Li L., Ratteron P., Weidner D. J., and Chen J. (2003b) Olivine flow mechanisms at 8 GPa. *Physics of Earth and Planetary Interiors* **138**, 113–129.

Li L., Weidner D. J., Chen J., *et al.* (2004a) X-ray strain analysis at high pressure: effect of plastic deformation in MgO. *Journal of Applied Physics* **95**, 8357–8365.

Li L., Weidner D. J., Ratteron P., Chen J., and Vaughan M. T. (2004b) Stress measurements of deforming olivine at high pressure. *Physics of Earth and Planetary Interiors* **143/144**, 357–367.

Li P., Karato S., and Wang Z. (1996) High-temperature creep in fine-grained polycrystalline $CaTiO_3$, an analogue material of $(Mg, Fe)SiO_3$ perovskite. *Physics of Earth and Planetary Interiors* **95**, 19–36.

Li X. and Cormier V. F. (2002) Frequency-dependent seismic attenuation in the inner core 1. A viscoelastic interpretation. *Journal of Geophysical Research* **107**, 10.1029/2002JB001795.

Li Y. and Langdon T. G. (1998) High strain rate superplasticity in metal matrix composites: the role of load transfer. *Acta Materialia* **46**, 3937–3948.

Lidiard A. B. (1981) The volume of formation of Schottky defects in ionic solids. *Philosophical Magazine A* **43**, 292–300.

Liebermann R. C. (1982) Elasticity of minerals at high pressure and temperature. In *High Pressure Research in Geosciences* (ed. W. Schreyer), pp. 1–14. Schweizerbartsche.

Liebermann R. C. (2000) Elasticity of mantle minerals (experimental studies). In *Earth's Deep Interior: Mineral Physics and Tomography* (ed. S. Karato, A. M. Forte, R. C. Liebermann, G. Masters, and L. Stixrude), pp. 181–199. American Geophysical Union.

Liebermann R. C. and Ringwood A. E. (1973) Birch's law and polymorphic phase transformations. *Journal of Geophysical Research* **78**, 6926–6932.

Lifshitz I. M. (1963) On the theory of diffusion–viscous flow of polycrystalline bodies. *Soviet Physics JETP* **17**, 909–920.

Lifshitz I. M. and Shikin V. B. (1965) The theory of diffusional viscous flow of polycrystalline solids. *Soviet Physics, Solid State* **6**, 2211–2218.

Lin J.-F., Sturhahn W., Zhao J., *et al.* (2005) Sound velocities of hot dense iron: Birch's law revisited. *Science* **308**, 1892–1894.

Lindemann F. A. (1910) Über die Berechnung Molecular Eigenfrequnzen. *Physikalische Zeitschrift* **11**, 609–612.

Linker M. F. and Kirby S. H. (1981) Anisotropy in the rheology of hydrolytically weakened quartz crystals. In *Mechanical Behavior of Crustal Rocks* (ed. N. L. Carter, M. Friedman, J. M. Logan, and D. W. Stearns), pp. 29–48. American Geophysical Union.

Linker M. F., Kirby S. H., Ord A., and Christie J. M. (1984) Effects of compression direction on the plasticity and rheology of hydrolytically weakened synthetic quartz crystals at atmospheric pressure. *Journal of Geophysical Research* **89**, 4241–4255.

Lister G. S. (1979) Fabric transitions in plastically deformed quartzites: competition between basal, prism and rhomb systems. *Bulletin Mineralogie* **102**, 232–241.

Lister G. S. and Hobbs B. E. (1980) The simulation of fabric development during plastic deformation and its application to quartzite: the influence of deformation history. *Journal of Structural Geology* **2**, 355–370.

Lister G. S. and Paterson M. S. (1979) The simulation of fabric development during plastic deformation and its application to quartzite: fabric transition. *Journal of Structural Geology* **1**, 99–115.

Lister G. S., Paterson M. S., and Hobbs B. E. (1978) The simulation of fabric development during plastic deformation and its application to quartzite: the model. *Tectonophysics* **45**, 107–158.

Lister G. S. and Snoke A. W. (1984) S-C mylonite. *Journal of Structural Geology* **6**, 617–638.

Litasov K., Ohtani E., Langenhorst F., *et al.* (2003) Water solubility in Mg-perovskite and water storage capacity in the lower mantle. *Earth and Planetary Science Letters* **211**, 189–203.

Lithgow-Bertelloni C. and Silver P. G. (1998) Dynamic topography, plate driving forces and the African superswell. *Nature* **395**, 269–272.

Long M., Xiao X., Jiang Z., Evans B., and Karato S. (2006) Lattice preferred orientation in deformed polycrystalline (Mg, Fe)O and implications for seismic anisotropy in D″. *Physics of Earth and Planetary Interiors* **156**, 75–88.

Long M. D. and van der Hilst R. D. (2005) Upper mantle anisotropy beneath Japan from shear wave splitting. *Physics of Earth and Planetary Interiors* **151**, 206–222.

Loper D. E. and Fearn D. R. (1983) A seismic model of a partially molten inner core. *Journal of Geophysical Research* **88**, 1235–1242.

Louat N. P. and Duesbery M. S. (1994) On the theory of normal grain growth. *Philosophical Magazine A* **69**, 841–854.

Louchet F. and George A. (1983) Dislocation mobility measurements: an essential tool for understanding the atomic and electronic core structures of dislocations in semiconductors. *Journal de Physique C* **4**, 51–58.

Lu R. and Keppler H. (1997) Water solubility in pyrope to 100 kbar. *Contributions to Mineralogy and Petrology* **129**, 35–42.

Luan F. C. and Paterson M. S. (1992) Preparation and deformation of synthetic aggregates of quartz. *Journal of Geophysical Research* **97**, 301–320.

Luton M. J. and Sellars C. M. (1969) Dynamic recrystallization in nickel and nickel–iron alloys during high temperature deformation. *Acta Metallurgica* **17**, 1033–1043.

Mackwell S. J. (1991) High-temperature rheology of enstatite: implications for creep in the upper mantle. *Geophysical Research Letters* **18**, 2027–2030.

Mackwell S. J. and Kohlstedt D. L. (1990) Diffusion of hydrogen in olivine: implications for water in the mantle. *Journal of Geophysical Research* **95**, 5079–5088.

Mackwell S. J., Kohlstedt D. L., and Paterson M. S. (1985) The role of water in the deformation of olivine single crystals. *Journal of Geophysical Research* **90**, 11 319–11 333.

Mackwell S. J. and Paterson M. S. (1985) Water-related diffusion and deformation effects in quartz at pressure of 1500 and 300 MPa. In *Point Defects in Minerals* (ed. R. N. Schock), pp. 141–150. American Geophysical Union.

Mackwell S. J., Zimmerman M. E., and Kohlstedt D. L. (1998) High-temperature deformation of dry diabase with application to tectonics on Venus. *Journal of Geophysical Research* **103**, 975–984.

Mainprice D. H. and Nicolas A. (1989) Development of shape and lattice preferred orientations: application to the seismic anisotropy of the lower crust. *Journal of Structural Geology* **11**, 175–189.

Mainprice D. H. and Paterson M. S. (1984) Experimental studies on the role of water in the plasticity of quartzite. *Journal of Geophysical Research* **89**, 4257–4269.

Mainprice D. H. and Silver P. G. (1993) Interpretation of SKS-waves using samples from the subcontinental lithosphere. *Physics of Earth and Planetary Interiors* **78**, 257–280.

Malvern L. E. (1969) *Introduction to the Mechanics of a Continuous Medium*. Prentice-Hall.

Manga M. (1996) Mixing of heterogeneities in the mantle: effect of viscosity differences. *Geophysical Research Letters* **23**, 403–406.

Mao H.-K., Shu J., Shen G., *et al.* (1998) Elasticity and rheology of iron above 200 GPa and the nature of the Earth's inner core. *Nature* **396**, 741–743.

Maradudin A. A., Montroll E. W., Weiss G. H., and Ipanova I. P. (1971) *Theory of Lattice Dynamics in the Harmonic Approximation*. Academic Press.

March N. H. and Tosi M. P. (2002) *Introduction to Liquid State Physics*. World Scientific.

Marone C. (1998) Laboratory-derived friction laws and their application to seismic faulting. *Annual Review of Earth and Planetary Sciences* **26**, 643–696.

Martin R. F. and Donnay G. (1972) Hydroxyl in the mantle. *American Mineralogist* **57**, 554–570.

Mase G. E. (1970) *Continuum Mechanics*. McGraw-Hill.

Masters G. and Gubbins D. (2003) On the resolution of density within the Earth. *Physics of the Earth and Planetary Interior* **139**, 159–167.

Masters G., Laske G., Bolton H., and Dziewonski A. M. (2000) The relative behavior of shear velocity, bulk sound speed, and compressional velocity in the mantle: implications for chemical and thermal structure. In *Earth's Deep Interior* (ed. S. Karato, A. M. Forte, R. C. Liebermann, G. Masters, and L. Stixrude), pp. 63–87. American Geophysical Union.

Matsukage K. N., Nishihara Y., and Karato S. (2005) Seismological signature of chemical evolution of Earth's upper mantle. *Journal of Geophysical Research* **110**, 10.1029/2004JB003504.

Matthies S. and Wagner F. (1996) On a $1/n$ law in texture related single orientation analysis. *Physica Status Solidi* **196**, K11–K15.

Mavko G. M. (1980) Velocity and attenuation in partially molten rocks. *Journal of Geophysical Research* **85**, 5173–5189.

Mavko G. M. and Nur A. (1975) Melt squirt in the asthenosphere. *Journal of Geophysical Research* **80**, 1444–1448.

Mayama N., Suzuki I., and Saito T. (2004) Temperature dependence of elastic moduli of β-$(Mg, Fe)_2SiO_4$. *Geophysical Research Letters* **31**, 10.1029/2003GL019247.

McBirney A. R. and Murase T. (1984) Rheological properties of magmas. *Annual Review of Earth and Planetary Sciences* **12**, 337–357.

McCartney L. N. (1976) No time-gentlemen please! *Philosophical Magazine* **33**, 689–695.

McDonnell R. D., Peach C. J., van Roemund H. L. M., and Spiers C. J. (2000) Effect of varying enstatite content on the deformation behavior of fine-grained synthetic peridotite under wet conditions. *Journal of Geophysical Research* **105**, 13 535–13 553.

McDonough W. F. and Sun S.-S. (1995) The composition of the Earth. *Chemical Geology* **120**, 223–253.

McGovern P. J. and Schubert G. (1989) Thermal evolution of the Earth: effects of volatile exchange between atmosphere and interior. *Earth and Planetary Science Letters* **96**, 27–37.

McKenzie D. P. (1969) Speculations on the consequences and cause of plate motion. *Geophysical Journal of Royal Astronomical Society* **18**, 1–32.

McKenzie D. P. (1984) The generation and compaction of partially molten rocks. *Journal of Petrology* **25**, 713–765.

McKenzie D. P. (2003) Estimating T_e in the presence of internal loads. *Journal of Geophysical Research* **108**, 10.1029/JB001766.

McLaren A. C., Cook R. F., Hyde S. T., and Tobin R. C. (1983) The mechanisms of the formation and growth of water bubbles and associated dislocation loops in synthetic quartz. *Physics and Chemistry of Minerals* **9**, 79–94.

McLaren A. C., Fitz Gerald J. D., and Gerretsen J. (1989) Dislocation nucleation and multiplication in synthetic quartz: relevance to water weakening. *Physics and Chemistry of Minerals* **16**, 465–482.

McNamara A., Karato S., and van Keken P. E. (2001) Localization of dislocation creep in Earth's lower mantle: implications for seismic anisotropy. *Earth and Planetary Science Letters* **191**, 85–99.

McNamara A., van Keken P. E., and Karato S. (2002) Development of anisotropic structure by solid-state convection in the Earth's lower mantle. *Nature* **416**, 310–314.

McNamara A., van Keken P. E., and Karato S. (2003) Development of finite strain in the convecting lower mantle

and its implications for seismic anisotropy. *Journal of Geophysical Research* **108**, 10.1029/2002JB001970, 2003.

McNutt M. K. (1998) Superswells. *Review of Geophysics* **36**, 211–244.

Meade C. and Jeanloz R. (1988) Yield strength of the B1 and B2 phases of NaCl. *Journal of Geophysical Research* **93**, 3270–3274.

Meade C. and Jeanloz R. (1990) The strength of mantle silicates at high pressures and room temperature: implications for the viscosity of the mantle. *Nature* **348**, 533–535.

Meade C., Reffner J. A., and Ito E. (1993) Synchrotron infrared absorbance measurements of hydrogen in $MgSiO_3$ perovskite. *Science* **264**, 1558–1560.

Meade C., Silver P. G., and Kaneshima S. (1995) Laboratory and seismological observations of lower mantle isotropy. *Geophysical Research Letters* **22**, 1293–1296.

Means W. D. (1976) *Stress and Strain*. Springer-Verlag.

Mecklenburgh J. and Rutter E. H. (2003) On the rheology of partially molten synthetic granite. *Journal of Structural Geology* **25**, 1575–1585.

Mehl L., Hacker B. R., and Hirth G. (2003) Arc-parallel flow within the mantle wedge: evidence from the accreted Talkeetna arc, south central Alaska. *Journal of Geophysical Research* **108**, 10.1029/2002JB002233.

Mei S., Bai W., Hiraga T., and Kohlstedt D. L. (2002) Influence of melt on the creep behavior of olivine–basalt aggregates under hydrous conditions. *Earth and Planetary Science Letters* **201**, 491–507.

Mei S. and Kohlstedt D. L. (2000a) Influence of water on plastic deformation of olivine aggregates, 1. Diffusion creep regime. *Journal of Geophysical Research* **105**, 21 457–21 469.

Mei S. and Kohlstedt D. L. (2000b) Influence of water on plastic deformation of olivine aggregates, 2. Dislocation creep regime. *Journal of Geophysical Research* **105**, 21 471–21 481.

Meike A. (1993) A critical review of investigation into transformational plasticity. In *Defects and Processes in the Solid States* (ed. J. N. Boland and J. D. Fitz Gerald), pp. 5–25. Elsevier.

Meissner R. and Mooney W. D. (1998) Weakness of lower continental crust: a condition for delamination, uplift, and escape. *Tectonophysics* **296**, 47–60.

Mendelson M. I. (1969) Average grain size in polycrystalline ceramics. *Journal of the American Ceramic Society* **55**, 19–24.

Mercier J.-C. C. (1980) Magnitude of the continental lithospheric stresses inferred from rheomorphic petrology. *Journal of Geophysical Research* **85**, 6293–6303.

Merkel S., Wenk H.-R., Badro J., *et al*. (2003) Deformation of $(Mg_{0.9}, Fe_{0.1})SiO_3$ perovskite aggregates up to 32 GPa. *Earth and Planetary Science Letters* **209**, 351–360.

Merkel S., Wenk H.-R., Gillet P., Mao H.-K., and Hemley R. J. (2004) Deformation of polycrystalline iron up to 30 GPa and 1000 K. *Physics of Earth and Planetary Interiors* **145**, 239–251.

Merkel S., Wenk H.-R., Shu J., *et al*. (2002) Deformation of polycrystalline MgO at pressures of the lower mantle. *Journal of Geophysical Research* **107**, 10.1029/2001JB000920.

Merrill R. T., McElhinny M. W., and McFaddon P. L. (1998) *The Magnetic Field of the Earth*. Academic Press.

Mibe K., Fujii T., and Yasuda A. (1998) Connectivity of aqueous fluid in the Earth's upper mantle. *Geophysical Research Letters* **25**, 1233–1236.

Minster J. B. and Anderson D. L. (1980) Dislocations and nonelastic processes in the mantle. *Journal of Geophysical Research* **85**, 6347–6352.

Minster J. B. and Anderson D. L. (1981) A model of dislocation-controlled rheology for the mantle. *Philosophical Transaction of Royal Society of London A* **299**, 319–356.

Misener D. J. (1974) Cationic diffusion in olivine to 1400 °C and 35 kbar. In *Geochemistry and Reaction Kinetics* (ed. A. W. Hofmann, B. J. Giletti, J. H. S. Yorder, and R. A. Yund), pp. 117–129. Carnegie Institution of Washington.

Mistler R. E. and Coble R. L. (1974) Grain-boundary diffusion and boundary widths in metals and ceramics. *Journal of Applied Physics* **45**, 1507–1509.

Mitrovica J. X. (1996) Haskell [1935] revisited. *Journal of Geophysical Research* **101**, 555–569.

Mitrovica J. X. and Peltier W. R. (1991a) A complete formalism for the inversion of postglacial rebound data: resolving power analysis. *Geophysical Journal International* **104**, 267–288.

Mitrovica J. X. and Peltier W. R. (1991b) Radial resolution in the inference of mantle viscosity from observations of glacial isostatic adjustment. In *Glacial Isostasy, Sea-Level and Mantle Rheology* (ed. R. Sabadini, K. Lambeck, and E. Boschi), pp. 63–78. Kluwer Academic Publisher.

Mizutani H. and Kanamori H. (1964) Variation in elastic wave velocity and attenuative property near the melting temperature. *Journal of Physics of the Earth* **12**, 43–49.

Molinari A., Canova G. R., and Ahzi S. (1987) A self-consistent approach of the large deformation polycrystal viscoplasticity. *Acta Metallurgica* **35**, 2983–2994.

Möller H.-J. (1978) The movement of dissociated dislocations in the diamond-cubic structure. *Acta Metallurgica* **26**, 963–973.

Montagner J.-P. (1998) Where can seismic anisotropy be detected in the Earth's mantle? In boundary layers .... *Pure and Applied Geophysics* **151**, 223–256.

Montagner J.-P. (2002) Upper mantle low anisotropy channels below the Pacific Plate. *Earth and Planetary Science Letters* **202**, 263–274.

Montagner J.-P., Griot-Pommera D.-A., and Lavé J. (2000) How to relate body wave and surface wave anisotropy? *Journal of Geophysical Research* **105**, 19 015–19 028.

Montagner J.-P. and Guillot L. (2000) Seismic anisotropy in the Earth's mantle. In *Problems in Geophysics for the*

New Millennium (ed. E. Boschi, G. Ekström, and A. Morelli), pp. 217–253. Editrice Compositori.

Montagner J.-P. and Guillot L. (2002) Seismic anisotropy and global geodynamics. In *Plastic Deformation of Minerals and Rocks*, Vol. 51 (ed. S. Karato and H.-R. Wenk), pp. 353–385. Mineralogical Society of America.

Montagner J.-P. and Kennett B. L. N. (1996) How to reconcile body-wave and normal-mode reference Earth models. *Geophysical Journal International* **125**, 229–248.

Montagner J.-P. and Nataf H.-C. (1986) A simple method for inverting the azimuthal anisotropy of surface waves. *Journal of Geophysical Research* **91**, 511–520.

Montagner J.-P. and Ritsema J. (2001) Interactions between ridges and plumes. *Science* **294**, 1472–1473.

Montagner J.-P. and Tanimoto T. (1990) Global anisotropy in the upper mantle inferred from the regionalization of phase velocities. *Journal of Geophysical Research* **95**, 4797–4819.

Montagner J.-P. and Tanimoto T. (1991) Global upper mantle tomography of seismic wave velocities and anisotropies. *Journal of Geophysical Research* **96**, 20337–20351.

Montelli R., Nolet G., Dahlen F. A., *et al*. (2004) Finite-frequency tomography reveals a variety of plumes in the mantle. *Science* **303**, 338–343.

Montési L. and Hirth G. (2003) Grain size evolution and the rheology of ductile shear zone: from laboratory experiments to postseismic creep. *Earth and Planetary Science Letters* **211**, 97–110.

Montési L. and Zuber M. T. (2002) A unified description of localization for application to large-scale tectonics. *Journal of Geophysical Research* **107**, 1/1–1/21.

Morelli A., Dziewonski A. M., and Woodhouse J. H. (1986) Anisotropy of the inner core inferred from PKIKP travel times. *Geophysical Research Letters* **13**, 1545–1548.

Mosenfelder J. L., Connelly J. A. D., Rubie D. C., and Liu M. (2000) Strength of $(Mg, Fe)_2SiO_4$ wadsleyite determined by relaxation of transformational stress. *Physics of Earth and Planetary Interiors* **120**, 63–78.

Mott N. F. and Littleton M. J. (1938) Conduction in polar crystals: I. Electrolytic conduction in solid salts. *Transactions of Faraday Society* **34**, 485–491.

Mukherjee A. K. (1971) The rate controlling mechanism in superplasticity. *Materials Science and Engineering* **8**, 83–89.

Murakami M., Hirose K., Kawamura K., Sata N., and Ohnishi Y. (2004) Post-perovskite phase transition in $MgSiO_3$. *Science* **304**, 855–858.

Murakami M., Hirose K., Yurimoto H., Nakashima S., and Takafuji N. (2002) Water in Earth's lower mantle. *Science* **295**, 1885–1887.

Nabarro F. R. N. (1948) Deformation of crystals by the motion of single ions. *Report of a Conference on Strength of Solids*, 75–90.

Nabarro F. R. N. (1967a) Steady state diffusional creep. *Philosophical Magazine* **16**, 231–237.

Nabarro F. R. N. (1967b) *Theory of Crystal Dislocations*. Oxford University Press.

Nabarro F. R. N. (1989) The mechanism of Harper-Dorn creep. *Acta Metallurgica* **37**, 2217–2222.

Nakada M. (1986) Holocene sea levels in oceanic islands: implications for the rheological structure of the Earth's mantle. *Tectonophysics* **121**, 263–276.

Nakada M. and Lambeck K. (1987) Glacial rebound and relative sea level variations: a new appraisal. *Geophysical Journal of Royal Astronomical Society* **90**, 171–224.

Nakada M. and Lambeck K. (1989) Late Pleistocene and Holocene sea-level change in the Australian region and mantle rheology. *Geophysical Journal International* **96**, 497–517.

Nakada M. and Lambeck K. (1991) Late Pleistocene and Holocene sea-level change: evidence for lateral mantle viscosity variation? In *Glacial Isostasy, Sea Level and Mantle Rheology* (ed. R. Sabadini, K. Lambeck, and E. Boschi), pp. 79–94. Kluwer Academic.

Nakajima J. and Hasegawa A. (2004) Shear-wave polarization anisotropy and subduction-induced flow in the mantle wedge of northern Japan. *Earth and Planetary Science Letters* **225**, 365–377.

Nakashima S. (1995) Diffusivity of ions in pore water as a quantitative basis for rock deformation rate estimate. *Tectonophysics* **245**, 185–203.

Nakashima S., De Meer S., and Spiers C. J. (2004) Distribution of thin film water in grain boundaries of crustal rocks and implications for crustal strength. In *Physicochemistry of Water in Geological and Biological Systems* (ed. S. Nakashima, C. J. Spiers, L. Mercury, P. A. Fenter, and M. F. M. F. Hochella, Jr.), pp. 159–178. Universal Academy Press, Inc.

Nakatani M. (2001) Conceptual and physical clarification of rate and state friction: frictional sliding and thermally activated rheology. *Journal of Geophysical Research* **106**, 13 347–13 380.

Nataf H.-C., Nakanishi I., and Anderson D. L. (1984) Anisotropy and shear wave heterogeneities in the upper mantle. *Geophysical Research Letters* **11**, 109–112.

Nataf H.-C., Nakanishi I., and Anderson D. L. (1986) Measurement of mantle wave velocities and inversion for lateral heterogeneities and anisotropy, 3. Inversion. *Journal of Geophysical Research* **91**, 7261–7307.

Navrotsky A. (1994) *Physics and Chemistry of Earth Materials*. Cambridge University Press.

Nes E., Hirsch J., and Lücke K. (1984) On the origin of the cube recrystallization texture in directionally solidified aluminium. *Seventh International Conference on Texture of Materials*, 663–674.

Newman J., Lamb W. M., Drury M. R., and Vissers R. L. M. (1999) Deformation processes in a peridotite shear zone: reaction-softening by a H_2O-deficit, continuous net transfer reaction. *Tectonophysics* **303**, 193–222.

Nicolas A. (1978) Stress estimates from structural studies in some mantle peridotites. *Philosophical Transactions of the Royal Society of London A* **288**, 49–57.

Nicolas A. (1993) Why fast polarization direction of SKS seismic waves are parallel to mountain belts. *Physics of Earth and Planetary Interiors* **78**, 337–342.

Nicolas A. and Christensen N. I. (1987) Formation of anisotropy in upper mantle peridotite: a review. In *Composition, Structure and Dynamics of the Lithosphere–Asthenosphere System* (ed. K. Fuchs and C. Foridevaux), pp. 111–123. American Geophysical Union.

Nieh T. G., Wadsworth J., and Sherby O. D. (1997) *Superplasticity in Metals and Ceramics*. Cambridge University Press.

Nimmo F., Price G. D., Brodholt J. P., and Gubbins D. (2004) The influence of potassium on core and geodynamo evolution. *Geophysical Journal International* **156**, 363–376.

Nishihara Y., Shinmei T., and Karato S. (2006) Grain-growth kinetics in wadsleyite: effects of chemical environment. *Physics of Earth and Planetary Interiors* **154**, 30–43.

Nishihara Y., Shinmei T., and Karato S. (2007a) Effects of chemical environments on the hydrogen-defects in wadsleyite. *American Mineralogist* in press.

Nishihara Y., Tinker D., Xu Y., *et al*. (2007b) Plastic deformation of wadsleyite and olivine at high-pressures and high-temperatures using a rotational Drickamer apparatus (RDA). *Physics of the Earth and Planetary Interiors* submitted.

Nitsan U. (1974) Stability field of olivine with respect to oxidation and reduction. *Journal of Geophysical Research* **79**, 706–711.

Nixon P. H. and Boyd F. R. (1973) Petrogenesis of the granular and sheared ultrabasic nodule site in kimberlites. In *Lesotho Kimberlites* (ed. P. H. Nixon), pp. 48–56. Lesotho National Development.

Nolet G. (1987a) *Seismic Tomography*. Reidel Publishing Company.

Nolet G. (1987b) Waveform tomography. In *Seismic Tomography* (ed. G. Nolet), pp. 301–322. Reidel Publishing Company.

Nolet G. (2000) Interpreting seismic waveforms: forward and inverse problems for heterogeneous media. In *Problems in Geophysics for the New Millennium* (ed. E. Boschi, G. Ekström, and A. Morelli), pp. 373–401. Edrice Compositori.

Nolet G. and Dahlen F. A. (2000) Wave front healing and the evolution of seismic delay times. *Journal of Geophysical Research* **105**, 19 043–19 054.

Nolet G. and Zielhuis A. (1994) Low S velocities under the Tornquist–Teisseyre zone: evidence for water injection into the transition zone by subduction. *Journal of Geophysical Research* **99**, 15 813–15 820.

Nowick A. S. and Berry B. S. (1972) *Anelastic Relaxation in Crystalline Solids*. Academic Press.

Nye J. F. and Mae S. (1972) The effect of non-hydrostatic stress on intergranular water veins and lenses in ice. *Journal of Glaciology* **11**, 81–101.

O'Connell R. J. (1977) On the scale of mantle convection. *Tectonophysics* **38**, 119–136.

O'Connell R. J. and Budianski B. (1974) Seismic velocities in dry and saturated cracked solids. *Journal of Geophysical Research* **79**, 5412–5426.

O'Connell R. J. and Budianski B. (1977) Viscoelastic properties of fluid-saturated cracked solids. *Journal of Geophysical Research* **82**, 5719–5735.

O'Neill H. S. C., McCammon C. A., Canil D., *et al*. (1993) Mössbauer spectroscopy of mantle transition zone phases and determination of minimum Fe^{3+} content. *American Mineralogist* **78**, 456–460.

Obata M. and Karato S. (1995) Ultramafic pseudotachylyte from Balmuccia peridotite, Ivrea–Verbana zone, northern Italy. *Tectonophysics* **242**, 313–328.

Oganov A. R., Martonak R., Laio A., Raiteri P., and Parrinello M. (2005) Anisotropy of Earth's D″ layer and stacking faults in the $MgSiO_3$ post-perovskite phase. *Nature* **438**, 1142–1144.

Oganov A. R. and Ono S. (2004) Theoretical and experimental evidence for a post-perovskite phase of $MgSiO_3$ in Earth's D″ layer. *Nature* **430**, 445–448.

Ogawa M. (1987) Shear instability in a viscoelastic material as the cause for deep earthquakes. *Journal of Geophysical Research* **92**, 13 801–13 810.

Ohtani E. (1988) Chemical stratification of the mantle formed by melting in the early stage of the terrestrial evolution. *Tectonophysics* **154**, 201–210.

Ohtani E., Mizobata H., and Yurimoto H. (2000) Stability of dense hydrous magnesium silicate phases in the system Mg_2SiO_4–H_2O and $MgSiO_3$–H_2O at pressures up to 27 GPa. *Physics and Chemistry of Minerals* **27**, 533–544.

Ohuchi T. and Nakamura M. (2006) Grain growth in the forsterite–diopside system. *Physics of the Earth and Planetary Interiors* **160**, 1–21.

Oki S. (2006) *Whole mantle Vp/Vs tomography*, University of Tokyo.

Omori S., Kamiya S., Maruyama S., and Zhao D. (2002) Morphology of the intraslab seismic zone and devolatilization phase equilibria of the subducting slab peridotite. *Bulletin of Earthquake Research Institute* **76**, 455–478.

Orowan E. (1934) Zur Kristallplastizität. *Zeitschrift für Phisik* **89**, 605–659.

Ozawa K. (1989) Stress induced Al-Cr zoning of spinel in deformed peridotite. *Nature* **338**, 141–144.

Panasyuk S. V. and Hager B. H. (1998) A model of transformational superplasticity in the upper mantle. *Geophysical Journal International* **133**, 741–755.

Panning M. and Romanowicz B. (2004) Inferences on flow at the base of the Earth's mantle based on seismic anisotropy. *Science* **303**, 351–353.

Park J. and Levin V. (2002) Seismic anisotropy: tracing plate dynamics in the mantle. *Science* **296**, 485–489.

Park K. T. and Mohamed F. A. (1995) Creep strengthening in a discontinuous SiC–Al composite. *Metallurgical Materials Transaction A* **26**, 3119–3129.

Parmentier E. M. (1981) A possible mantle instability due to superplastic deformation associated with phase transitions. *Geophysical Research Letters* **8**, 143–146.

Pasteris J. D. (1984) Kimberlites: complex mantle melts. *Annual Review of Earth and Planetary Sciences* **12**, 133–153.

Paterson M. S. (1970) A high temperature high pressure apparatus for rock deformation. *International Journal of Rock Mechanics and Mining Sciences* **7**, 517–526.

Paterson M. S. (1973) Non-hydrostatic thermodynamics and its geologic applications. *Review of Geophysics and Space Physics* **11**, 355–389.

Paterson M. S. (1982) The determination of hydroxyl by infrared absorption in quartz, silicate glass and similar materials. *Bulletin Mineralogie* **105**, 20–29.

Paterson M. S. (1983) Creep of transforming materials. *Mechanics of Materials* **2**, 103–109.

Paterson M. S. (1989) The interaction of water with quartz and its influence in dislocation flow – an overview. In *Rheology of Solids and of the Earth* (ed. S. Karato and M. Toriumi), pp. 107–142. Oxford University Press.

Paterson M. S. (1990) Rock deformation experimentation. In *The Brittle–Ductile Transition in Rocks: the Heard Volume* (ed. A. G. Duba, W. B. Durham, J. W. Handin, and H. F. Wang), pp. 187–194. American Geophysical Union.

Paterson M. S. and Kekulawala K. R. S. S. (1979) The role of water in quartz deformation. *Bulletin Mineralogie* **102**, 92–98.

Paterson M. S. and Olgaard D. L. (2000) Rock deformation tests to large shear strains in torsion. *Journal of Structural Geology* **22**, 1341–1358.

Paterson M. S. and Weiss L. E. (1961) Symmetry concepts in the structural analysis of deformed rocks. *Geological Society of America Bulletin* **72**, 841–882.

Paterson M. S. and Wong T.-F. (2005) *Experimental Rock Deformation – The Brittle Field*. Springer-Verlag.

Pauling L. (1960) *The Nature of the Chemical Bonds*. Cornell University Press.

Pearson D. G. (1999) Evolution of cratonic lithospheric mantle: an isotopic perspective. In *Mantle petrology: Field Observations and High Pressure Experimentation* (ed. Y. Fei, C. M. Bertka, and B. O. Mysen), pp. 57–78. The Geochemical Society.

Peltier W. R. (1984) The thickness of the continental lithosphere. *Journal of Geophysical Research* **89**, 11303–11316.

Peltier W. R. (1985a) New constraints on transient lower mantle rheology and internal mantle buoyancy from glacial rebound data. *Nature* **318**, 614–617.

Peltier W. R. (1985b) The LAGEOS constraint on deep mantle viscosity: results from a new normal mode method for the inversion of viscoelastic spectra. *Journal of Geophysical Research* **90**, 9411–9421.

Peltier W. R. (1989) Mantle viscosity. In *Mantle Convection* (ed. W. R. Peltier), pp. 389–478. Gordon & Breach.

Peltier W. R. (1998) Postglacial variation in the level of the sea: implications for climate dynamics and solid-Earth geophysics. *Review of Geophysics* **36**, 603–689.

Pharr G. M. and Ashby M. F. (1983) On creep enhanced by a liquid phase. *Acta Metallurgica* **31**, 129–138.

Phipps Morgan J. and Shearer P. M. (1993) Seismic constraints on mantle flow and topography of the 660-km discontinuity. *Nature* **365**, 506–511.

Pieri M., Kunze K., Burlini L., Stretton I., Olgaard D. L., Burg J.-P., and Wenk H.-R. (2001) Texture development of calcite by deformation and dynamic recrystallization at 1000 K during torsion experiments of marble to large strains. *Tectonophysics* **330**, 119–142.

Pitzer K. S. and Sterner S. M. (1994) Equations of state valid continuously from zero to extreme pressures for H_2O and CO_2. *Journal of Chemical Physics* **101**, 3111–3116.

Plank T. and Langmuir A. H. (1992) Effects of melting regime on the composition of the oceanic crust. *Journal of Geophysical Research* **97**, 19 749–19 770.

Poirier J.-P. (1976a) On the symmetrical role of cross-slip of screw dislocations and climb of edge dislocations as recovery processes controlling high-temperature creep. *Revue de Physique Appliquée* **11**, 731–738.

Poirier J.-P. (1976b) *Plasticité a Haute Température des Solides Cristallins*. Editions Eyrolles.

Poirier J.-P. (1980) Shear localization and shear instability in materials in the ductile field. *Journal of Structural Geology* **2**, 135–142.

Poirier J.-P. (1982) On transformation plasticity. *Journal of Geophysical Research* **87**, 6791–6797.

Poirier J.-P. (1985) *Creep of Crystals*. Cambridge University Press.

Poirier J.-P. (1988) Transport properties of liquid metals and viscosity of the Earth's core. *Geophysical Journal of Royal Astronomical Society* **92**, 99–105.

Poirier J.-P. (1994) Light elements in the Earth's outer core: a critical review. *Physics of Earth and Planetary Interiors* **85**, 319–337.

Poirier J.-P. (2000) *Introduction to the Physics of Earth's Interior*. Cambridge University Press.

Poirier J.-P. and Guillopé M. (1979) Deformation induced recrystallization of minerals. *Bulletin Mineralogie* **102**, 67–74.

Poirier J.-P. and Liebermann R. C. (1984) On the activation volume for creep and its variation with depth in the Earth's lower mantle. *Physics of Earth and Planetary Interiors* **35**, 283–293.

Poirier J.-P., Peyronneau J., Gesland J. Y., and Brebec G. (1983) Viscosity and conductivity of the lower mantle: and experimental study on a $MgSiO_3$ analogue, $KZnF_3$. *Physics of Earth and Planetary Interiors* **32**, 273–287.

Poirier J.-P., Peyronneau J., Madon M., Guyot F., and Revcoleshi A. (1986) Eutectoid phase transformation of olivine and spinel into perovskite and rock salt structures. *Nature* **321**, 603–605.

Poirier J.-P., Sotin C., and Peyronneau J. (1981) Viscosity of high-pressure ice VI and evolution and dynamics of Ganymede. *Nature* **292**, 225–227.

Poirier J.-P. and Vergobbi B. (1978) Splitting of dislocations in olivine, cross-slip controlled creep and mantle rheology. *Physics of Earth and Planetary Interiors* **16**, 370–378.

Polanyi M. (1934) Über eine Art Gitterstörung, die einen Kristall plastisch machen könnte. *Zeitschrift für Physik* **89**, 660–664.

Pollack H. K. (1986) Cratonization and the thermal evolution of the mantle. *Earth and Planetary Science Letters* **80**, 175–182.

Pollack H. K., Hurter S. J., and Johnson J. R. (1993) Heat flow from the Earth's interior: analysis of the global data. *Review of Geophysics* **31**, 267–280.

Ponte Castañeda P. and Willis J. R. (1988) On the overall properties of nonlinearly viscous composites. *Proceedings of the Royal Society of London A* **416**, 217–244.

Post A. and Tullis J. A. (1999) A recrystallized grain size piezometer for experimentally deformed feldspar. *Tectonophysics* **303**, 159–173.

Post A. D., Tullis J., and Yund R. A. (1996) Effects of chemical environment on dislocation creep of quartzite. *Journal of Geophysical Research* **101**, 22 143–22 155.

Post R. L. (1977) High-temperature creep of Mt. Burnett dunite. *Tectonophysics* **42**, 75–110.

Prigogine I. and Defay R. (1950) *Thermodynamique Chemique*. Editions Desoer.

Prior D. and Wheeler J. (1999) Feldspar fabrics in a greenshist facies albite-rich mylonite from electron backscatter diffraction. *Tectonophysics* **303**, 29–49.

Przystupa M. A. and Ardell A. J. (2002) Predictive capabilities of the dislocation-network theory of Harper–Dorn creep. *Metallurgical and Materials Transactions A* **33**, 231–239.

Raitt R. W., Shor G. G., Francis T. J. G., and Morris G. B. (1969) Anisotropy of the Pacific upper mantle. *Journal of Geophysical Research* **74**, 3095–3109.

Raj R. (1982) Separation of cavitation-strain and creep strain during deformation. *Journal of the American Ceramic Society* **65**, 46–48.

Raj R. (1986) Unstable spreading of a film inclusion in a grain boundary under normal stress. *Journal of the American Ceramic Society* **69**, 708–712.

Raj R. and Ashby M. F. (1971) On grain boundary sliding and diffusional creep. *Metallurgical Transactions* **2**, 1113–1127.

Raj R. and Chung C. K. (1981) Solution-precipitation creep in glass ceramics. *Acta Metallurgica* **29**, 159–166.

Raleigh C. B., Kirby S. H., Carter N. L., and Avé Lallemant H. G. (1971) Slip and the clinoenstatite transformation as competing processes in enstatite. *Journal of Geophysical Research* **76**, 4011–4022.

Raleigh C. B. and Paterson M. S. (1965) Experimental deformation of serpentine and its tectonic implications. *Journal of Geophysical Research* **70**, 3965–3985.

Randle V. (2003) *Microtexture Determination and its Applications*. The Institute of Materials, Minerals and Mining.

Rauch M. and Keppler H. (2002) Water solubility in orthopyroxene. *Contributions to Mineralogy and Petrology* **143**, 525–536.

Regan J. and Anderson D. L. (1984) Anisotropic models of the upper mantle. *Physics of Earth and Planetary Interiors* **35**, 227–263.

Regenauer-Lieb K. and Yuen D. A. (2003) Modeling shear zones in geological and planetary sciences: solid- and fluid-mechanical approaches. *Review of Earth Sciences* **63**, 295–349.

Renner J., Stöckhert B., Zerbian A., Roller K., and Rummel F. (2001) An experimental study into the rheology of synthetic polycrystalline coesite aggregates. *Journal of Geophysical Research* **106**, 19 411–19 429.

Reppich B., Haasen P., and Ilschner B. (1964) Kriechen von Silizium-Einkristallen. *Acta Metallurgica* **12**, 1283–1288.

Revenaugh J. and Jordan T. H. (1991) Mantle layering from ScS reverberations, 3. Upper mantle. *Journal of Geophysical Research* **96**, 19 781–19 810.

Revenaugh J. and Sipkin S. A. (1994) Seismic evidence for silicate melt atop the 410-km mantle discontinuity. *Nature* **369**, 474–476.

Ribe N. M. (1989a) A continuum theory for lattice preferred orientation. *Geophysical Journal* **97**, 199–207.

Ribe N. M. (1989b) Seismic anisotropy and mantle flow. *Journal of Geophysical Research* **94**, 4213–4223.

Ribe N. M. and Yu Y. (1991) A theory of plastic deformation and textural evolution of olivine polycrystals. *Journal of Geophysical Research* **96**, 8325–8335.

Ricard Y., Bercovici D., and Schubert G. (2001) A two-phase model for compaction and damage 2. Applications to compaction, deformation, and the role of interfacial tension. *Journal of Geophysical Research* **106**, 8907–8924.

Rice J. R. (1976) The localization of plastic deformation. In *Theoretical and Applied Mechanics* (ed. W. T. Koitier), pp. 207–220. North-Holland.

Richard G., Monnereau M., and Ingrin J. (2002) Is the transition zone an empty water reservoir? Inference from numerical model of mantle dynamics. *Earth and Planetary Science Letters* **205**, 37–51.

Richards M. A. and Hager B. H. (1984) Geoid anomalies in the dynamic Earth. *Journal of Geophysical Research* **89**, 5987–6002.

Richards M. A., Yang W. S., Baumgardnner J. R., and Bunge H.-P. (2001) Role of a low-viscosity zone in stabilizing plate tectonics: implications for comparative planetology. *Geochemistry, Geophysics, Geosystems* **2**, 2000GC000115.

Ricoult D. L. and Kohlstedt D. L. (1983) Structural width of low-angle grain boundaries in olivine. *Physics and Chemistry of Minerals* **9**, 133–138.

Riedel M. R. and Karato S. (1996) Microstructural development during nucleation and growth. *Geophysical Journal International* **125**, 397–414.

Riedel M. R. and Karato S. (1997) Grain-size evolution in subducted oceanic lithosphere associated with the olivine-spinel transformation and its effects on rheology. *Earth and Planetary Science Letters* **148**, 27–43.

Ringwood A. E. (1975) *Composition and Structure of the Earth's Mantle*. McGraw-Hill.

Ritsema J., van Heijst H. J., and Woodhouse J. H. (1999) Complex shear wave velocity structure imaged beneath Africa and Iceland. *Science* **286**, 1925–1928.

Rogers H. C. (1979) Adiabatic plastic deformation. *Annual Review of Materials Science* **9**, 283–311.

Rokosky J. M., Lay T., Garnero E. J., and Russell S. A. (2004) High-resolution investigation of shear wave anisotropy in D″ beneath the Cocos Plate. *Geophysical Research Letters* **31**, 10.1029/2003GL018902.

Romanowicz B. (1994) Anelastic tomography: a new perspective on upper mantle thermal structure. *Earth and Planetary Science Letters* **128**, 113–121.

Romanowicz B. (1995) A global tomographic model of shear attenuation in the upper mantle. *Journal of Geophysical Research* **100**, 12 375–12 394.

Romanowicz B. (2003) Global mantle tomography: progress status in the past 10 years. *Annual Review of Earth and Planetary Sciences* **31**, 303–328.

Romanowicz B. and Durek J. J. (2000) Seismological constraints on attenuation in the Earth: a review. In *Earth's Deep Interior* (ed. S. Karato, A. M. Forte, R. C. Liebermann, G. Masters, and L. Stixrude), pp. 161–179. American Geophysical Union.

Roscoe R. (1952) The viscosity of suspensions of rigid spheres. *British Journal of Applied Physics* **3**, 267–269.

Ross J. V., Avé Lallemant H. G., and Carter N. L. (1979) Activation volume for creep in the upper mantle. *Science* **203**, 261–263.

Ross J. V., Avé Lallemant H. G., and Carter N. L. (1980) Stress dependence of recrystallized grain and subgrain size in olivine. *Tectonophysics* **70**, 39–61.

Ross J. V., Bauer S. J., and Hansen F. D. (1987) Textural evolution of synthetic anhydrite–halite mylonites. *Tectonophysics* **140**, 307–326.

Ross J. V. and Nielsen K. C. (1978) High-temperature flow of wet polycrystalline enstatite. *Tectonophysics* **44**, 233–261.

Rossman G. R. and Aines R. D. (1991) The hydrous components in garnets: grossular-hydrogrossular. *American Mineralogist* **76**, 1153–1164.

Rossman G. R., Beran A., and Lange M. A. (1989) The hydrous component of pyrope from the Dora Maira Massif, western Alps. *European Journal of Mineralogy* **1**, 151–154.

Roth E. G., Wiens D. A., Dorman L. M., Hildebrand J., and Webb S. C. (1999) Seismic attenuation tomography of the Toga-Fiji region using phase pair methods. *Journal of Geophysical Research* **104**, 4795–4809.

Royden L. H., Burchfiel B. C., King R. W., Chen Z., Shen F., and Liu Y. (1997) Surface deformation and lower crust flow in eastern Tibet. *Science* **276**, 788–790.

Ruano O. A., Wadsworth J., Wolfensteine J., and Sherby O. D. (1993) Evidence for Nabarro–Herring creep in metals: fiction or reality? *Materials Science and Engineering A* **165**, 133–141.

Rubie D. C. (1983) Reaction-enhanced ductility: the role of solid–solid univariant reactions in deformation of the crust and mantle. *Tectonophysics* **96**, 331–352.

Rubie D. C. (1984) The olivine –> spinel transformation and the rheology of subducting lithosphere. *Nature* **308**, 505–508.

Rubie D. C., Karato S., Yan H., and O'Neill H. S. C. (1993) Low differential stress and controlled chemical environment in multianvil high-pressure experiments. *Physics and Chemistry of Minerals* **20**, 315–322.

Rubie D. C. and Ross C. R., II. (1994) Kinetics of the olivine–spinel transformation in subducting lithosphere: experimental constraints and implications for deep slab processes. *Physics of Earth and Planetary Interiors* **86**, 223–241.

Rudnick R. L. and Fountain D. M. (1995) Nature and composition of the continental lower crust: the lower crustal perspective. *Review of Geophysics and Space Physics* **33**, 267–309.

Rudnick R. L., McDonough W. F., and O'Connell R. J. (1998) Thermal structure, thickness and compopsition of continental lithosphere. *Chemical Geology* **145**, 395–411.

Rudnicki J. W. and Rice J. R. (1975) Conditions for localization of deformation in pressure-sensitive dilatant materials. *Journal of Mechanics and Physics of Solids* **23**, 371–394.

Ruina A. (1983) Slip instability and state variable friction laws. *Journal of Geophysical Research* **88**, 10 359–10 370.

Ruoff A. L. (1965) Mass transfer problems in ionic crystals with charge neutrality. *Journal of Applied Physics* **36**, 2903–2907.

Rüpke L. H., Phipps Morgan J., Hort M., and Connolly J. A. D. (2004) Serpentine and the subduction zone water cycle. *Earth and Planetary Science Letters* **223**, 17–34.

Russo R. and Silver P. G. (1994) Trench-parallel flow beneath the Nazca plate from seismic anisotropy. *Science* **263**, 1105–1111.

Rutter E. H. (1972) The influence of interstitial water on the rheological behaviour of calcite rocks. *Tectonophysics* **14**, 13–33.

Rutter E. H. (1976) The kinetics of rock deformation by pressure solution. *Philosophical Transactions of the Royal Society of London A* **283**, 203–219.

Rutter E. H. (1983) Pressure solution in nature, theory and experiment. *Journal of the Geological Society of London* **140**, 725–740.

Rutter E. H. (1986) On the nomenclature of failure transitions in rocks. *Tectonophysics* **122**, 381–387.

Rutter E. H. (1995) Experimental study of the influence of stress, temperature, and strain on the dynamic recrystallization of Carrara marble. *Journal of Geophysical Research* **100**, 24 651–24 663.

Rutter E. H. (1998) Use of extension testing to investigate the influence of finite strain on the rheological behaviour of marble. *Journal of Structural Geology* **20**, 243–254.

Rutter E. H. and Brodie K. (1988) The role of tectonic grainsize reduction in the rheological stratification of the lithosphere. *Geologische Rundschau* **77**, 295–308.

Rutter E. H. and Brodie K. H. (1992) Rheology of the lower crust. In *Continental Lower Crust* (ed. D. M. Fountain, R. Arculus, and R. W. Key), pp. 201–267. Elsevier.

Rutter E. H. and Brodie K. H. (2004) Experimental grain size-sensitive flow of hot-pressed Brasilian quartz aggregates. *Journal of Structural Geology* **26**, 2011–2023.

Rutter E. H., Casey M., and Burlini L. (1994) Preferred crystallographic orientation development during the plastic and superplastic flow of calcite rocks. *Journal of Structural Geology* **16**, 1431–1446.

Rybacki E. and Dresen G. (2000) Dislocation and diffusion creep of synthetic anorthite aggregates. *Journal of Geophysical Research* **105**, 26 017–26 036.

Rybacki E. and Dresen G. (2004) Deformation mechanism maps for feldspar rocks. *Tectonophysics* **382**, 173–187.

Rybacki E., Gootschalk M., Wirth R., and Dresen G. (2006) Influence of water fugacity and activation volume on the flow properties of fine-grained anorthite aggregates. *Journal of Geophysical Research* **111**, 10.1029/2005JB003663.

Rybacki E., Paterson M. S., Wirth R., and Dreibus G. (2003) Rheology of calcite–quartz aggregates deformed to large strain in torsion. *Journal of Geophysical Research* **108**, 10.1029/2002JB001833.

Rychert C. A., Fischer K. M., and Rodenay S. (2005) A sharp lithosphere–asthenosphere boundary imaged beneath eastern North America. *Nature* **434**, 542–545.

Ryerson F. J., Weed H. C., and Piwinskii A. J. (1988) Rheology of subliquidus magmas 1. Picritic compositions. *Journal of Geophysical Research* **93**, 3421–3436.

Sabadini R., Smith B. K., and Yuen D. A. (1987) Consequences of experimental transient rheology. *Geophysical Research Letters* **14**, 816–819.

Sakai T. and Jonas J. J. (1984) Dynamic recrystallization: mechanical and microstructural considerations. *Acta Metallurgica* **32**, 189–209.

Saltzer R. L., Gaherty J. B., and Jordan T. H. (2000) How are vertical shear wave splitting measurements affected by variations in the orientation of azimuthal anisotropy with depth? *Geophysical Journal International* **141**, 374–390.

Saltzer R. L., van der Hilst R. D., and Karason H. (2001) Comparing P and S wave heterogeneity in the mantle. *Geophysical Research Letters* **28**, 1335–1338.

Sammis C. G. and Dein J. L. (1974) On the possibility of transformational superplasticity in the Earth's mantle. *Journal of Geophysical Research* **79**, 2961–2965.

Sammis C. G., Smith J. C., and Schubert G. (1981) A critical assessment of estimation methods for activation volume. *Journal of Geophysical Research* **86**, 10 707–10 718.

Sammis C. G., Smith J. C., Schubert G., and Yuen D. A. (1977) Viscosity depth profile of the Earth's mantle: effect of polymorphic transitions. *Journal of Geophysical Research* **82**, 3747–3761.

Sandström R. (1977) Subgrain growth occurring by boundary migration. *Acta Metallurgica* **25**, 905–911.

Sato H., Sacks I. S., Murase T., Munchill G., and Fukuyama H. (1989) Q_p-melting temperature relation in peridotite at high pressure and temperature: attenuation mechanism and implications for the mechanical properties of the upper mantle. *Journal of Geophysical Research* **94**, 10 647–10 661.

Sato M. (1971) Electrochemical measurements and control of oxygen fugacity and other gaseous fugacities with solid electrolyte sensors. In *Research Techniques for High Pressure and High Temperature* (ed. G. C. Ulmer), pp. 43–99. Springer-Verlag.

Savage M. K. (1999) Seismic anisotropy and mantle deformation: what have we learned from shear wave splitting? *Review of Geophysics* **37**, 65–106.

Saxena S. K., Dubrovinski L. S., and Lazor P. (1996) Stability of perovskite ($MgSiO_3$) in the Earth's lower mantle. *Science* **274**, 1357–1359.

Schmalzried H. (1995) *Chemical Kinetics of Solids*. VCH.

Schmeling H. (1985) Numerical models on the influence of partial melt on elastic, anelastic and electric properties of

rocks. Part I: elasticity and anelasticity. *Physics of Earth and Planetary Interiors* **41**, 34–57.

Schmeling H. (1987) On the interaction between small- and large-scale convection and postglacial rebound flow in a power-law mantle. *Earth and Planetary Science Letters* **84**, 254–262.

Schmid S. M. and Casey M. (1986) Complete fabric analysis of some commonly observed quartz c-axis patterns. In *Mineral and Rock Deformation: Laboratory Studies, The Paterson Volume* (ed. B. E. Hobbs and H. C. Heard), pp. 263–286. American Geophysical Union.

Schmidt C., Bruhn D., and Wirth R. (2003) Experimental evidence of transformation plasticity in silicates: mimimum of creep strength in quartz. *Earth and Planetary Science Letters* **205**, 273–280.

Scholz C. H. (2002) *The Mechanics of Earthquake and Faulting*. Cambridge University Press.

Schubert G., Turcotte D. L., and Olson P. (2001) *Mantle Convection in the Earth and Planets*. Cambridge University Press.

Schutt D. L. and Lesher C. E. (2006) Effects of melt depletion on the density and seismic velocity of garnet and spinel lherzolite. *Journal of Geophysical Research* **111**, 10.1029/2003JB002950.

Sclater J. C., Parsons B., and Jaupart C. (1981) Oceans and continents: similarities and differences in the mechanisms of heat loss. *Journal of Geophysical Research* **86**, 11535–11552.

Sclater J. G., Jaupart C., and Galson D. (1980) The heat flow through the oceanic and continental crust and the heat loss of the earth. *Review of Geophysics and Space Physics* **18**, 269–312.

Scott D. R. and Stevenson D. J. (1984) Magma solitons. *Geophysical Research Letters* **11**, 1161–1164.

Scott T. and Kohlstedt D. L. (2006) The effect of large melt fraction on the deformation behavior of peridotite. *Earth and Planetary Science Letters* **246**, 177–187.

Secco R. A. (1995) Viscosity of the outer core. In *Mineral Physics & Crystallography* (ed. T. H. Ahrens), pp. 218–226. American Geophysical Union.

Seeger A. and Schiller P. (1966) Kinks in dislocation lines and their effects on the internal friction in crystals. In *Physical Acoustics*, Vol. III – Part A (ed. W. P. Mason), pp. 361–495. Academic Press.

Selitser S. I. and Morris J. W., Jr. (1994) Substructure formation during plastic deformation. *Acta Metallurgica et Materials* **42**, 3985–3991.

Shankland T. J. (1977) Elastic properties, chemical composition, and crystal structures of minerals. *Geophysical Survey* **3**, 69–100.

Shankland T. J., O'Connell R. J., and Waff H. S. (1981) Geophysical constraints on partial melt in the upper mantle. *Review of Geophysics and Space Physics* **19**, 394–406.

Sharp T. G., Bussod G. Y., and Katsura T. (1994) Misrostructures in beta-$Mg_{1.8}Fe_{0.2}SiO_4$ experimentally deformed at transition-zone conditions. *Physics of Earth and Planetary Interiors* **86**, 69–83.

Shearer P. M. (2000) Upper mantle discontinuities. In *Earth's Deep Interior: Mineral Physics and Tomography from the Atomic to the Global Scales* (ed. S. Karato, A. M. Forte, R. C. Liebermann, G. Masters, and L. Stixrude), pp. 115–131. American Geophysical Union.

Shearer P. M. and Masters G. (1992) Global mapping of topography on the 660-km discontinuity. *Nature* **355**, 791–796.

Shen G., Mao H.-K., Hemley R. J., and Duffy T. S. (1998) Melting and crystal structure of iron at high pressures and temperatures. *Geophysical Research Letters* **25**, 373–376.

Shen Y. and Blum J. (2003) Seismic evidence for accumulated oceanic crust above the 660-km discontinuity beneath southern Africa. *Geophysical Research Letters* **30**, 10.1029/2003GL017991.

Sherby O. D., Klundt R. H., and Miller A. L. (1977) Flow-stress, subgrain size and subgrain stability at elevated temperatures. *Metallurgical Transactions A* **8**, 843–850.

Sherby O. D., Robbins J. L., and Goldberg A. (1970) Calculation of activation volumes for self-diffusion and creep at high temperatures. *Journal of Applied Physics* **41**, 3961–3968.

Shewmon P. G. (1989) *Diffusion in Solids*. The Minerals, Metals & Materials Society.

Shieh S. R., Duffy T. S., and Li B. (2002) Strength and elasticity of SiO_2 across the stishovite–$CaCl_2$-type phase boundary. *Physical Review Letters* **89**, 10.1103/PhysRevLett. 89.255507.

Shim S.-H., Duffy T. S., and Shen G. (2001) Stability and structure of $MgSiO_3$ perovskite to 2300-kilometer depth in Earth's mantle. *Science* **293**, 2437–2440.

Shimamoto T. and Logan J. M. (1981) Effects of simulated gouges on the sliding behavior of Tennessee sandstone. *Tectonophysics* **75**, 243–255.

Shimamura H., Asada T., Suyehiro K., Yamada T., and Inatani H. (1983) Longshot experiments to study velocity anisotropy in the oceanic lithosphere of the northwestern Pacific. *Physics of Earth and Planetary Interiors* **31**, 348–362.

Shimazu Y. (1954) Equation of state of materials composing the Earth's interior. *Journal of Earth Science, Nagoya University* **2**, 15–172.

Shimizu I. (1992) Nonhydrostatic and nonequilibrium thermodynamics of deformable materials. *Journal of Geophysical Research* **97**, 4587–4597.

Shimizu I. (1994) Rock deformation by pressure solution and its implications to the rheology of lithosphere: a review. *Structural Geology* **39**, 153–164.

Shimizu I. (1998) Stress and temperature dependence of recrystallized grain size: a subgrain misorientation model. *Geophysical Research Letters* **25**, 4237–4240.

Shimozuru D. (1963) On the possibility of the existence of the molten portion in the upper mantle of the earth. *Journal of Physics of the Earth* **11**, 49–55.

Shinmei T., Tomioka N., Fujino K., Kuroda K., and Irifune T. (1999) *In situ* X-ray diffraction of enstatite up to 12 GPa and 1473 K and equation of state. *American Mineralogist* **84**, 1588–1594.

Shito A., Karato S., Matsukage K. N., and Nishihara Y. (2006) Toward mapping water content, temperature and major element chemistry in Earth's upper mantle from seismic tomography. In *Earth's Deep Water Cycle* (ed. S. D. Jacobsen and S. van der Lee), pp. 225–236. American Geophysical Union.

Shito A., Karato S., and Park J. (2004) Frequency dependence of Q in Earth's upper mantle inferred from continuous spectra of body wave. *Geophysical Research Letters* **31**, 10.1029/2004GL019582.

Shito A. and Shibutani T. (2003a) Anelastic structure of the upper mantle beneath the northern Philippine Sea. *Physics of Earth and Planetary Interiors* **140**, 319–329.

Shito A. and Shibutani T. (2003b) Nature of heterogeneity of the upper mantle beneath the northern Philippine Sea as inferred from attenuation and velocity tomography. *Physics of Earth and Planetary Interiors* **140**, 331–341.

Sibson R. H. (1975) Generation of pseudotachylyte by ancient seismic faulting. *Geophysical Journal of Royal Astronomical Society* **43**, 775–794.

Sibson R. H. (1977) Fault rocks and fault mechanics. *Journal of Geological Society of London* **133**, 191–213.

Siegesmund S., Takeshita T., and Kern H. (1989) Anisotropy of V_p and V_s in an amphibolite of the deeper crust and its relationship to the mineralogical, microstructural and textural characteristics of the rock. *Tectonophysics* **157**, 25–38.

Silver P. G. (1996) Seismic anisotropy and mantle deformation: probing the depths of geology. *Annual Review of Earth and Planetary Sciences* **24**, 385–432.

Silver P. G., Mainprice D., Ben Ismail W., Tommasi A., and Barroul G. (1999) Mantle structural geology from seismic anisotropy. In *Mantle Petrology: Field Observations and High Pressure Experimentation* (ed. Y. Fei, C. M. Bertka, and B. O. Mysen), pp. 79–103. The Geochemical Society.

Simpson C. and Schmid S. (1983) An evaluation of criteria to deduce the sense of movement in sheared rocks. *Geological Society of America Bulletin* **94**, 1281–1288.

Singh A. K. (1993) The lattice strain in a specimen (cubic system) compressed nonhydrostatically in an opposed anvil device. *Journal of Applied Physics* **73**, 4278–4286.

Singh A. K., Mao H.-K., Shu J., and Hemley R. J. (1998) Estimation of single-crystal elastic moduli from polycrystalline X-ray diffraction at high pressure: application to FeO and iron. *Physical Review Letters* **80**, 2157–2160.

Singh S. C., Taylor M. A. J., and Montagner J.-P. (2000) On the presence of liquid in Earth's inner core. *Science* **287**, 2471–2474.

Sinogeikin S. V. and Bass J. D. (1999) Single-crystal elasticity of MgO at high pressure. *Physical Review B* **59**, R14 141–R14 144.

Sinogeikin S. V. and Bass J. D. (2002) Elasticity of majorite and a majorite–pyrope solid solution to high pressure: implications for the transition zone. *Geophysical Research Letters* **29**, 10.1029/2001GL013937.

Sinogeikin S. V., Bass J. D., and Katsura T. (2003) Single-crystal elasticity of ringwoodite to high pressures and high temperatures: implications for 520 km seismic discontinuity. *Physics of Earth and Planetary Interiors* **136**, 41–66.

Sinogeikin S. V., Chen G., Neuville D. R., Vaughan M. T., and Lierbermann R. C. (1998) Ultrasonic shear wave velocities of $MgSiO_3$ perovskite at 8 GPa and 800 K and lower mantle composition. *Science* **281**, 677–679.

Sipkin S. and Jordan T. H. (1979) Frequency dependence of Q_{ScS}. *Bulletin of Seismological Society of America* **69**, 1055–1079.

Skemer P. A., Katayama I., Jiang Z., and Karato S. (2005) The misorientation index: development of a new method for calculating the strength of lattice-preferred orientation. *Tectonophysics* **411**, 157–167.

Skemer P. A., Katayama I., and Karato S. (2006) Deformation fabrics of a peridotite from Cima di Gagnone, central Alps, Switzerland: evidence of deformation under water-rich condition at low temperatures. *Contributions to Mineralogy and Petrology* **152**, 43–51.

Skinner B. J., Porter S. C., and Park J. (2004) *Dynamic Earth: an Introduction to Physical Geology*. John Wiley & Sons.

Skogby H. (1994) OH incorporation in synthetic clinopyroxene. *American Mineralogist* **79**, 240–249.

Skogby H., Bell D. R., and Rossman G. R. (1990) Hydroxide in pyroxene: variations in the natural environment. *American Mineralogist* **75**, 764–774.

Skogby H. and Rossman G. R. (1989) OH^- in pyroxene: an experimental study of incorporation mechanisms and stability. *American Mineralogist* **74**, 1059–1069.

Smith B. K. (1985) The influence of defect crystallography on some properties of orthosilicates. In *Metamorphic Reactions, Kinetics, Textures and Deformation* (ed. T. A. B. and D. C. Rubie), pp. 98–117. Springer-Verlag.

Smith B. K. and Carpenter F. O. (1987) Transient creep in orthosilicates. *Physics of Earth and Planetary Interiors* **49**, 314–324.

Smith G. P., Wiens D. A., Fischer K. M., Dorman L. M., and Hildebrand J. A. (2001) A complex pattern of mantle flow in the Lau back-arc. *Science* **292**, 713–716.

Smith M. F. and Dahlen F. A. (1981) The period and Q of the Chandler wobble. *Geophysical Journal of Royal Astronomical Society* **64**, 223–281.

Smith M. L. and Dahlen F. A. (1973) The azimuthal dependence of Love and Rayleigh wave propagation in a slightly anisotropic medium. *Journal of Geophysical Research* **78**, 3321–3333.

Smyth J. R., Bell D. R., and Rossman G. R. (1991) Incorporation of hydroxyl in upper-mantle clinopyroxenes. *Nature* **351**, 732–735.

Smyth J. R. and Frost D. J. (2002) The effect of water on the 410-km discontinuity: an experimental study. *Geophysical Research Letters* **29**, 10.129/2001GL014418.

Solomatov V. S. (1996) Can hot mantle be stronger than cold mantle? *Geophysical Research Letters* **23**, 937–940.

Solomatov V. S. (2001) Grain size-dependent viscosity convection and the thermal evolution of the Earth. *Earth and Planetary Science Letters* **191**, 203–212.

Solomatov V. S., El-Khozondar R., and Tikare V. (2002) Grain size in the lower mantle: constraints from numerical modeling of grain growth in two-phase systems. *Physics of Earth and Planetary Interiors* **129**, 265–282.

Solomatov V. S. and Moresi L. N. (1996) Stagnant lid convection on Venus. *Journal of Geophysical Research* **101**, 4737–4753.

Solomon S. C. (1972) Seismic wave attenuation and partial melting in the upper mantle of North America. *Journal of Geophysical Research* **77**, 1483–1502.

Solomon S. C., Head J. W., Kaula W. M., *et al.* (1991) Venus tectonics: initial analysis from Magellan. *Science* **252**, 297–312.

Song T.-R. A., Helmberger D. V., and Grand S. P. (2004) Low-velocity zone atop the 410-km seismic discontinuity in the northwestern United States. *Nature* **427**, 530–533.

Song X. (1997) Anisotropy of the Earth's inner core. *Review of Geophysics* **35**, 297–313.

Song X. and Helmberger D. V. (1998) Seismic evidence for an inner core transition zone. *Science* **282**, 924–927.

Song X. and Richards P. G. (1996) Seismic evidence for the rotation of the inner core. *Nature* **382**, 221–224.

Souriau A. (1998) Earth's inner core: is the rotation real? *Science* **281**, 55–56.

Souriau A. and Poupinet G. (2002) Inner core rotation: a critical appraisal. In *Earth's Core: Dynamics, Structure, Rotation* (ed. V. Dehant, K. C. Creager, S. Karato, and S. Zatman), pp. 65–82.

Souriau A. and Roudil P. (1995) Attenuation in the uppermost inner core from broadband Geoscope PKP data. *Geophysical Journal International* **123**, 572–587.

Spetzler H. A. and Anderson D. L. (1968) The effect of temperature and partial melting on velocity and attenuation in a simple binary system. *Journal of Geophysical Research* **73**, 6051–6060.

Speziale S., Jiang F., and Duffy T. S. (2005) Compositional dependence of the elastic wave velocities of mantle minerals: implications for seismic properties of mantle rocks. In *Earth's Deep Mantle* (ed. R. D. v. d. Hilst, J. D. Bass, J. Matas, and J. Trampert), pp. 301–320. American Geophysical Union.

Spiegelman M. (2003) Linear analysis of melt band formation by simple shear. *Geochemical Geophysical Geosystems* **4**, 10.1029/2002GC000499.

Spiegelman M. and Elliott T. (1993) Consequences of melt transport for uranium series disequilibrium in young lavas. *Earth and Planetary Science Letters* **118**, 1–20.

Spiegelman M. and Kenyon P. M. (1992) The requirement of chemical disequilibrium during magma migration. *Earth and Planetary Science Letters* **109**, 611–620.

Spiers C. J., De Meer S., Niemeijer A. R., and Zhang X. (2004) Kinetics of rock deformation by pressure solution and the role of thin aqueous films. In *Physicochemistry of Water in Geological and Biological Systems* (ed. S. Nakashima, C. J. Spiers, L. Mercury, P. A. Fenter, and J. M. F. Hochella), pp. 129–158. Universal Academy Press.

Spiers C. J., Schutjens P. M. T. M., Brezesowsky P. H., *et al.* (1990) Experimental determination of constitutive parameters governing creep of rocksalt by pressure solution. In *Deformation Mechanisms, Rheology and Tectonics* (ed. R. J. Knipe and E. H. Rutter), pp. 215–227. The Geological Society.

Spingarn J. R., Barnett D. M., and Nix W. D. (1979) Theoretical description of climb controlled steady state creep at high and intermediate temperatures. *Acta Metallurgica* **27**, 1549–1562.

Spingarn J. R. and Nix W. D. (1978) Diffusional creep and diffusionally accommodated grain rearrangement. *Acta Metallurgica* **26**, 1388–1398.

Spray J. G. (1987) Artificial generation of pseudotachylyte using friction welding apparatus: simulation of melting on a fault plane. *Journal of Structural Geology* **9**, 49–60.

Srolovitz D. J. and Davis S. H. (2001) Do stresses modify wetting angles? *Acta Materialia* **49**, 1005–1007.

Stacey F. D. (1992) *Physics of the Earth*. Brookfield Press.

Stauffer D. and Aharony A. (1992) *Introduction to Percolation Theory*. Taylor and Francis.

Steinle-Neumann G., Stixrude L., Cohen R. E., and Gülseren O. (2001) Elasticity of iron at the temperature of the Earth's inner core. *Nature* **413**, 57–60.

Stevenson D. J. (1989) Spontaneous small-scale melt segregation in partial melts undergoing deformation. *Geophysical Research Letters* **16**, 1067–1070.

Stipp M. and Tullis J. (2003) The recrystallized grain size piezometer for quartz. *Geophysical Research Letters* **30**, 10.1029/2003GL018444.

Stipp M., Tullis J., and Behrens H. (2006) Dislocation creep of quartz: the effect of water on flow stress and microstructure. *Journal of Geophysical Research* **111**, 10.1029/2005JB003852.

Stixrude L. and Lithgow-Bertelloni C. (2005a) Mineralogy and elasticity of the oceanic upper mantle: origin of the low-velocity zone. *Journal of Geophysical Research* **110**, 10.1029/2004JB002965.

Stixrude L. and Lithgow-Bertelloni C. (2005b) Thermodynamics of mantle minerals – I. Physical properties. *Geophysical Journal International* **162**, 610–632.

Stocker R. L. and Ashby M. F. (1973) Rheology of the upper mantle. *Review of Geophysics and Space Physics* **11**, 391–426.

Stroh A. N. (1954) The formation of cracks as a result of plastic flow. *Proceedings of the Royal Society of London A* **223**, 404–414.

Stroh A. N. (1955) The formation of cracks in plastic flow II. *Proceedings of the Royal Society of London A* **232**, 548–560.

Stünitz H., Fitz Gerald J. D., and Tullis J. (2003) Dislocation generation, slip systems, and dynamic recrystallization in experimentally deformed plagioclase single crystals. *Tectonophysics* **372**, 215–233.

Stünitz H. and Tullis J. (2001) Weakening and strain localization produced by syn-deformational reaction of plagioclase. *International Journal of Earth Sciences* **90**, 136–148.

Sturhahn W., Toellner T. S., Alp E. E., *et al*. (1995) Phonon density of states measured by inelastic nuclear resonant scattering. *Physical Review Letters* **74**, 3832–3835.

Su W.-J., Dziewonski A. M., and Jeanloz R. (1996) Planet within a planet – rotation of the inner core of the Earth. *Science* **274**, 1883–1887.

Suetsugu D., Inoue T., Yamada A., Zhao D., and Obayashi M. (2006) Towards mapping three-dimensional distribution of water in the transition zone from P-wave velocity tomography and 660-km discontinuity depths. In *Earth's Deep Water Cycle* (ed. S. D. Jacobsen and S. van der Lee), pp. 237–249. American Geophysical Union.

Sumino K. (1974) A model for the dynamical state of dislocations in crystals. *Materials Science and Engineering* **13**, 269–275.

Sumita I., Yoshida H., Hamano Y., and Kumazawa M. (1996) A model for sedimentary compaction in a viscous medium and its application to inner-core growth. *Geophysical Journal International* **124**, 502–524.

Sung C.-M., Goetze C., and Mao H.-K. (1977) Pressure distribution in the diamond anvil press and shear strength of fayalite. *Review of Scientific Instruments* **48**, 1386–1391.

Suzuki H. (1962) Segregation of solute atoms to stacking faults. *Journal of Physical Society of Japan* **17**, 322–325.

Tackley P. J. (2000a) Self-consistent generation of tectonic plates in time-dependent, three dimensional mantle convection simulations, 1. Pseudoplastic yielding. *Geochemistry, Geophysics, Geosystems* **1**, 2000GC000, 036.

Tackley P. J. (2000b) Self-consistent generation of tectonic plates in time-dependent, three dimensional mantle convection simulations, 2. Strain weakening and asthenosphere. *Geochemistry, Geophysics, Geosystems* **1**, 2000GC000, 043.

Tackley P. J., Stevenson D. J., Glatzmaier G. A., and Schubert G. (1993) Effects of endothermic phase transition at 670 km depth in a spherical model of mantle convection in the Earth's mantle. *Nature* **361**, 699–704.

Tada R. and Siever R. (1986) Experimental knife-edge pressure solution of halite. *Geochemica et Cosmochemica Acta* **50**, 29–36.

Tada R. and Siever R. (1987) A new mechanism for pressure solution in porous quartzose sandstone. *Geochemica et Cosmochemica Acta* **51**, 2295–2301.

Takanami T., Sacks I. S., and Hasegawa A. (2000) Attenuation structure beneath the volcanic front in northeastern Japan from broad-band seismograms. *Physics of Earth and Planetary Interiors* **121**, 339–357.

Takei Y. (1998) Constitutive mechanical relations of solid–liquid composites in terms of grain-boundary contiguity. *Journal of Geophysical Research* **103**, 18 183–18 203.

Takei Y. (2000) Acoustic properties of partially molten media studied on a simple binary system with a controllable dihedral angle. *Journal of Geophysical Research* **105**, 16 665–16 682.

Takei Y. (2002) Effect of pore geometry on Vp/Vs: from equilibrium geometry to crack. *Journal of Geophysical Research* **107**, 10.1029/2001JB000522.

Takeshita T. (1989) Plastic anisotropy in textured mineral aggregates: theories and geological applications. In *Rheology of Solids and of the Earth* (ed. S. Karato and M. Toriumi), pp. 237–262. Oxford University Press.

Takeshita T. and Wenk H.-R. (1988) Plastic anisotropy and geometric hardening in quartzites. *Tectonophysics* **149**, 345–361.

Takeshita T., Wenk H.-R., Molinari A., and Canova G. (1990) Simulation of dislocation assisted plastic deformation in olivine polycrystals. In *Deformation Processes in Minerals, Ceramics and Rocks* (ed. D. J. Barber and P. G. Meredith), pp. 365–377. Unwin Hyman.

Takeuchi S. and Argon A. S. (1976) Steady-state creep of alloys due to viscous motion of dislocations. *Acta Metallurgica* **24**, 883–889.

Takeuchi S. and Suzuki T. (1988) Deformation of crystals controlled by the Peierls mechanism. *Strength of Metals and Alloys (ICSMA 8)*, 161–166.

Tan B., Jackson I., and Fitz Gerald J. D. (1997) Shear wave dispersion and attenuation in fine-grained synthetic olivine aggregates: preliminary results. *Geophysical Research Letters* **24**, 1055–1058.

Tan B., Jackson I., and Fitz Gerald J. D. (2001) High-temperature viscoelasticity of fine-grained polycrystalline olivine. *Physics and Chemistry of Minerals* **28**, 641–664.

Tanaka S. and Hamaguchi H. (1997) Degree one heterogeneity and hemispherical variation of anisotropy in the inner core from PKP(BC)-PKP(DF) times. *Journal of Geophysical Research* **102**, 2925–2938.

Tanimoto T. and Anderson D. L. (1984) Mapping mantle convection. *Geophysical Research Letters* **11**, 287–290.

Tanimoto T. and Anderson D. L. (1985) Lateral heterogeneities and azimuthal anisotropy of the upper mantle: Love and Rayleigh waves 100–250 s. *Journal of Geophysical Research* **90**, 1842–1858.

Tanimoto T. and Anderson D. L. (1990) Long-wavelength S-wave velocity structure throughout the mantle. *Geophysical Journal International* **100**, 327–336.

Tapponnier P. and Francheteau J. (1978) Necking of the lithosphere and the mechanics of accreting plate boundaries. *Journal of Geophysical Research* **83**, 3955–3970.

Tarits P., Hautot S., and Perrier F. (2004) Water in the mantle: results from electrical conductivity beneath the French Alps. *Geophysical Research Letters* **31**, 10.1029/2003GL019277.

Taylor G. I. (1934) The mechanism of plastic deformation of crystals. *Proceedings of the Royal Society A* **145**, 362–415.

Tharp T. M. (1983) Analogies between the high-temperature deformation of polyphase rocks and the mechanical behavior of porous powder metal. *Tectonophysics* **96**, T1–T11.

Thompson A. B. (1992) Water in the Earth's upper mantle. *Nature* **358**, 295–302.

Thoraval C. and Richards M. A. (1997) The geoid constraint in global geodynamics: viscosity structure, mantle heterogeneity models and boundary conditions. *Geophysical Journal International* **131**, 1–8.

Thurel E. and Cordier P. (2003) Plastic deformation of wadsleyite: I. High-pressure deformation in compression. *Physics and Chemistry of Minerals* **30**, 256–266.

Thurel E., Cordier P., Frost D. J., and Karato S. (2003a) Plastic deformation of wadsleyite: II. High-pressure deformation in shear. *Physics and Chemistry of Minerals* **30**, 267–270.

Thurel E., Douin J., and Cordier P. (2003b) Plastic deformation of wadsleyite: III. Interpretation of dislocation slip systems. *Physics and Chemistry of Minerals* **30**, 271–279.

Tingle T. N., Green H. W., II., Young T. E., and Koczynski T. A. (1993) Improvements to Griggs-type apparatus for mechanical testing at high pressures and temperatures. *Pure and Applied Geophysics* **141**, 523–543.

Tommasi A., Mainprice D., Canova G., and Chastel Y. (2000) Viscoelastic self-consistent and equilibrium-based modeling of olivine preferred orientations: implications for the upper mantle seismic anisotropy. *Journal of Geophysical Research* **105**, 7893–7908.

Tommasi A., Mainprice D., Cordier P., Thoraval C., and Couvy H. (2004) Strain-induced seismic anisotropy of wadsleyite polycrystals and flow patterns in the mantle transition zone. *Journal of Geophysical Research* **109**, 10.1029/2004JB003158.

Toomey D. R., Wilcock W. S. D., Solomon S. C., Hammond W. C., and Orcott J. A. (1998) Mantle structure beneath the MELT region of the East Pacific Rise from P and S wave tomography. *Science* **280**, 1224–1227.

Toramaru A. and Fujii N. (1986) Connectivity of melt phase in a partially molten peridotite. *Journal of Geophysical Research* **91**, 9239–9252.

Toriumi M. (1982) Grain boundary migration in olivine at atmospheric pressure. *Physics of Earth and Planetary Interiors* **30**, 26–35.

Toriumi M. and Karato S. (1985) Preferred orientation development of dynamically recrystallized olivine during high temperature creep. *Journal of Geology* **93**, 407–417.

Tosi M. P. (1964) Cohesion of ionic solids in the Born model. *Solid State Physics* **16**, 1–120.

Trampert J., Deschamps F., Resovsky J. S., and Yuen D. A. (2004) Probabilistic tomography maps chemical heterogeneities throughout the lower mantle. *Science* **306**, 853–856.

Trampert J., Vacher P., and Vlaar N. J. (2001) Sensitivities of seismic velocities to temperature, pressure and composition in the lower-mantle. *Physics of Earth and Planetary Interiors* **124**, 255–267.

Trampert J. and van Heijst H. J. (2002) Global azimuthal anisotropy in the transition zone. *Science* **296**, 1297–1299.

Treagus S. H. (2002) Modelling the bulk viscosity of two-phase mixtures in terms of clast shape. *Journal of Structural Geology* **24**, 57–76.

Treagus S. H. (2003) Viscous anisotropy of two-phase composites, and applications to rocks and structures. *Tectonophysics* **372**, 121–133.

Tromp J. (2001) Inner-core anisotropy and rotation. *Review of Earth and Planetary Sciences* **29**, 47–69.

Tsenn M. C. and Carter N. L. (1987) Upper limits of power law creep of rocks. *Tectonophysics* **136**, 1–26.

Tsuchiya T., Tsuchiya J., Umemoto K., and Wentzcovitch R. M. (2004a) Elasticity of post-perovskite $MgSiO_3$. *Geophysical Research Letters* **31**, 10.1029/2004GL020278.

Tsuchiya T., Tsuchiya J., Umemoto K., and Wentzcovitch R. M. (2004b) Phase transition in $MgSiO_3$ in the Earth's lower mantle. *Earth and Planetary Science Letters* **224**, 241–248.

Tsumura N., Matsumoto S., Horiuchi S., and Hasegawa A. (2000) Three-dimensional attenuation structure beneath the northeastern Japan arc estimated from spectra of small earthquakes. *Tectonophysics* **319**, 241–260.

Tsutsumi A. and Shimamoto T. (1997) High-velocity frictional properties of gabbro. *Geophysical Research Letters* **24**, 699–702.

Tullis J. (2002) Deformation of granitic rocks: Experimental studies and natural examples. In *Plastic Deformation of Minerals and Rocks*, Vol. 51 (ed. S. Karato and H.-R. Wenk), pp. 51–95. Mineralogical Society of America.

Tullis J., Christie J. M., and Griggs D. T. (1973) Microstructure and preferred orientations of experimentally deformed quartzites. *Geological Society of America Bulletin* **84**, 297–314.

Tullis J., Shelton G. L., and Yund R. A. (1979) Pressure dependence of rock strength: implications for hydrolytic weakening. *Bulletin Mineralogie* **102**, 110–114.

Tullis J. and Yund R. A. (1980) Hydrolytic weakening of experimentally deformed Westerly granite and Hale albite rock. *Journal of Structural Geology* **2**, 439–451.

Tullis J. and Yund R. A. (1982) Grain growth kinetics of quartz and calcite aggregates. *Journal of Geology* **90**, 301–318.

Tullis J. and Yund R. A. (1985) Dynamic recrystallization of feldspar: a mechanism of shear zone formation. *Geology* **13**, 238–241.

Tullis T. E., Horowitz F. G., and Tullis J. (1991) Flow laws of polyphase aggregates from end-member flow laws. *Journal of Geophysical Research* **96**, 8081–8096.

Tullis T. E. and Tullis J. (1986) Experimental rock deformation. In *Mineral and Rock Deformation* (ed. B. E. Hobbs and H. C. Heard), pp. 297–324. American Geophysical Union.

Tungatt P. D. and Humphreys F. J. (1984) The plastic deformation and dynamic recrystallization of polycrystalline sodium nitrate. *Acta Metallurgica* **32**, 1625–1635.

Turcotte D. L. and Schubert G. (1982) *Geodynamics: Applications of Continuum Physics to Geological Problems*. John Wiley & Sons.

Twiss R. J. (1977) Theory and applicability of a recrystallized grain size paleopiezometer. *Pure and Applied Geophysics* **115**, 227–244.

Uchida T., Funamori N., and Yagi T. (1996) Lattice strains in crystals under uniaxial stress field. *Journal of Applied Physics* **80**, 739–746.

Underwood E. E. (1969) *Quantitative Stereology*. Addison-Wesley.

Urai J. L. (1983) Water-assisted dynamic recrystallization and weakening in polycrystalline bischofite. *Tectonophysics* **96**, 125–157.

Urai J. L. (1987) Development of microstructure during deformation of carnalite and bischofite in transmitted light. *Tectonophysics* **135**, 251–263.

Urai J. L., Means W. D., and Lister G. S. (1986a) Dynamic recrystallization in minerals. In *Mineral and Rock Deformation: Laboratory Studies* (ed. B. E. Hobbs and H. C. Heard), pp. 166–199. American Geophysical Union.

Urai J. L., Spiers C. J., Zwart H. J., and Lister G. S. (1986b) Water weakening in rock salt during long-term creep. *Nature* **324**, 554–557.

van der Hilst R. D. and Kárason H. (1999) Compositional heterogeneity in the bottom 1000 kilometers of Earth's mantle: toward a hybrid convection model. *Science* **283**, 1885–1888.

van der Hilst R. D., Widiyantoro R. D. S., and Engdahl E. R. (1997) Evidence for deep mantle circulation from global tomography. *Nature* **386**, 578–584.

van der Meijde M., Marone F., Giardini D., and van der Lee S. (2003) Seismic evidence for water deep in Earth's upper mantle. *Science* **300**, 1556–1558.

van der Molen I. and Paterson M. S. (1979) Experimental deformation of partially-melted granite. *Contributions to Mineralogy and Petrology* **70**, 299–318.

van der Wal D., Chopra P. N., Drury M., and Fitz Gerald J. D. (1993) Relationships between dynamically recrystallized grain size and deformation conditions in experimentally deformed olivine rocks. *Geophysical Research Letters* **20**, 1479–1482.

van Houtte P. and Wagner F. (1985) Development of texture by slip and twinning. In *Preferred Orientation in Deformed Metals and Rocks* (ed. H.-R. Wenk), pp. 233–258. Academic Press.

Van Orman J. A. (2004) On the viscosity and creep mechanism of Earth's inner core. *Geophysical Research Letters* **31**, 10.1029/2004GL021209.

Van Orman J. A., Fei Y., Hauri E. H., and Wang J. (2003) Diffusion in MgO at high pressure: constraints on deformation mechanisms and chemical transport at the core–mantle boundary. *Geophysical Research Letters* **30**, 10.1029/2002GL016343.

Vauchez A. and Nicolas A. (1991) Mountain building: strike-parallel motion and mantle anisotropy. *Tectonophysics* **185**, 183–191.

Vaughan P. J. and Coe R. S. (1978) Geometric flow properties of the germanate analog of forsterite. *Tectonophysics* **46**, 187–196.

Vaughan P. J. and Coe R. S. (1981) Creep mechanisms in Mg_2GeO_4: effects of a phase transition. *Journal of Geophysical Research* **86**, 389–404.

Vidale J. E., Dodge D. A., and Earle P. S. (2000) Slow differential rotation of the Earth's inner core indicated by temporal change in scattering. *Nature* **405**, 445–448.

Vidale J. E. and Earle P. S. (2000) Fine-scale heterogeneity in the Earth's inner core. *Nature* **404**, 273–275.

Vineyard G. H. (1957) Frequency factors and isotope effects in solid state rate processes. *Journal of Physics and Chemistry of Solids* **3**, 121–127.

Vinnik L., Breger L., and Romanowicz. (1998) Anisotropic structures at the base of the Earth's mantle. *Nature* **393**, 564–567.

Vinnik L. and Montagner J.-P. (1996) Shear wave splitting in the mantle from Ps phases. *Geophysical Research Letters* **23**, 2449–2452.

Vinnik L., Romanowicz B., Le Stunff Y., and Makayeva L. I. (1995) Seismic anisotropy in D″-layer. *Geophysical Research Letters* **22**, 1657–1660.

Voce E. (1948) The relationship between stress and strain for homogeneous deformation. *Journal of Institute of Metals* **74**, 537–562.

von Mises R. (1928) Mechanik der plastischen Formändern von Kristallen. *Zeitschrift für Angewandte Mathematik und Mechanik* **8**, 161–185.

Voorhees P. W. (1985) The theory of Ostwald ripening. *Journal of Statistical Physics* **38**, 231–252.

Voorhees P. W. (1992) Ostwald ripening of 2-phase mixtures. *Annual Review of Materials Science* **22**, 197–215.

Waff H. S. and Blau J. R. (1979) Equilibrium fluid distribution in an ultramafic partial melt under hydrostatic stress conditions. *Journal of Geophysical Research* **84**, 6109–6114.

Waff H. S. and Blau J. R. (1982) Experimental determination of near equilibrium textures in partially molten silicates at high pressures. In *High-pressure Research in Geophysics* (ed. S. Akimoto and M. H. Manghnani), pp. 229–236. Center for Academic Publication.

Walcott R. I. (1970) Flexural rigidity, thickness, and viscosity of the lithosphere. *Journal of Geophysical Research* **75**, 3941–3954.

Walker K. T., Bokelmann G. H., and Klemperer S. L. (2001) Shear-wave splitting to test mantle deformation models around Hawaii. *Geophysical Research Letters* **28**, 4319–4322.

Wall A. and Price G. D. (1989) Electrical conductivity of the lower mantle: a molecular dynamics simulation of $MgSiO_3$. *Physics of Earth and Planetary Interiors* **58**, 192–204.

Wallace D. C. (1972) *Thermodynamics of Crystals*. Wiley.

Walsh J. B. (1968) Attenuation in partially molten material. *Journal of Geophysical Research* **73**, 2209–2216.

Walsh J. B. (1969) New analysis of attenuation in partially molten rock. *Journal of Geophysical Research* **74**, 4333–4337.

Wang D., Mookherjee M., Xu Y., and Karato S. (2006) The effect of water on the electrical conductivity in olivine. *Nature* **443**, 977–980.

Wang J. N. (1994) Harper–Dorn creep in olivine. *Materials Science and Engineering A* **183**, 267–272.

Wang J. N., Hobbs B. E., Ord A., Shimamoto T., and Toriumi M. (1994) Newtonian dislocation creep in quartzites: implications for the rheology of the lower crust. *Science* **265**, 1203–1205.

Wang J. N. and Nieh T. G. (1995) Effects of the Peierls stress on the transition from power-law creep to Harper–Dorn creep. *Acta Metallurgica et Materialia* **43**, 1415–1419.

Wang Y., Durham W. B., Getting I. C., and Weidner D. J. (2003) The deformation-DIA: a new apparatus for high temperature triaxial deformation to pressures up to 15 GPa. *Review of Scientific Instruments* **74**, 3002–3011.

Wang Y., Guyot F., and Liebermann R. C. (1992) Electron microscopy of $(Mg, Fe)SiO_3$ perovskite: evidence for structural phase transitions and implications for the lower mantle. *Journal of Geophysical Research* **97**, 12 327–12 347.

Wang Z. and Ji S. (2000) Diffusion creep of fine-grained garnetite: implications for the flow strength of subducting slabs. *Geophysical Research Letters* **27**, 2333–2336.

Wang Z., Karato S., and Fujino K. (1993) High temperature creep of single crystal strontium titanate: a contribution to creep systematics in perovskites. *Physics of Earth and Planetary Interiors* **79**, 299–312.

Wang Z., Karato S., and Fujino K. (1996) High temperature creep of single crystal gadolinium gallium garnet. *Physics and Chemistry of Minerals* **23**, 73–80.

Wang Z., Mei S., Karato S., and Wirth R. (1999) Grain growth in $CaTiO_3$–perovskite + FeO–wüstite aggregates. *Physics and Chemistry of Minerals* **27**, 11–19.

Watson E. B. and Brenan J. M. (1987) Fluids in the lithosphere 1. Experimentally-determined wetting characteristics of CO_2–H_2O fluids and their implications for fluid transport, host-rock physical-properties, and fluid inclusion formation. *Earth and Planetary Science Letters* **85**, 497–515.

Watt J. P., Davies G. F., and O'Connell R. J. (1976) The elastic properties of composite materials. *Review of Geophysics and Space Physics* **14**, 541–563.

Webb S. and Jackson I. (1990) Polyhedral rationalization of variation among the single crystal elastic moduli for upper-mantle silicates: garnets, olivine and orthopyroxene. *American Mineralogist* **75**, 731–738.

Webb S. and Jackson I. (2003) Anelasticity and microcreep in polycrystalline MgO at high temperature: an exploratory study. *Physics and Chemistry of Minerals* **30**, 157–166.

Webb S., Jackson I., and Fitz Gerald J. (1999) Viscoelasticity of the titanate perovskite $CaTiO_3$ and $SrTiO_3$ at high temperature. *Physics of Earth and Planetary Interiors* **115**, 259–291.

Webster G. A. (1966a) A widely applicable dislocation model of creep. *Philosophical Magazine* **14**, 775–783.

Webster G. A. (1966b) In support of a model of creep based on dislocation dynamics. *Philosophical Magazine* **14**, 1303–1307.

Weertman J. (1957) Steady state creep of crystals. *Journal of Applied Physics* **28**, 1185–1191.

Weertman J. (1968) Dislocation climb theory of steady state creep. *Transactions of the American Society of Metals* **61**, 681–694.

Weertman J. (1970) The creep strength of the Earth's mantle. *Review of Geophysics and Space Physics* **8**, 145–168.

Weertman J. (1978) Creep laws for the mantle of the Earth. *Philosophical Transactions of the Royal Society of London A* **228**, 9–26.

Weertman J. and Blacic J. D. (1984) Harper–Dorn creep; an artifact of low-amplitude temperature cycling? *Geophysical Research Letters* **11**, 117–120.

Weertman J. and Weertman J. R. (1975) High temperature creep of rock and mantle viscosity. *Annual Review of Earth and Planetary Sciences* **3**, 293–315.

Weidner D. J. (1987) Elastic properties of rocks and minerals. In *Methods of Experimental Physics*, Vol. 1–30 (ed. C. G. Sammis and T. L. Henyey). Academic Press.

Weidner D. J. (1998) Rheological studies at high pressure. In *Ultrahigh-Pressure Mineralogy* (ed. R. J. Hemley), pp. 492–524. The Mineralogical Society of America.

Weidner D. J., Li L., Davis M., and Chen J. (2004) Effect of plasticity on elastic modulus measurements. *Geophysical Research Letters* **31**, 10.1029/2003GL019090.

Weidner D. J. and Wang Y. (2000) Phase transformations: implications for mantle structure. In *Earth's Deep Interior: Mineral Physics and Tomography* (ed. S. Karato, A. M. Forte, R. C. Liebermann, G. Masters, and L. Stixrude), pp. 215–235. American Geophysical Union.

Weidner D. J., Wang Y., Chen G., Ando J., and Vaughan M. T. (1998) Rheology measurements at high pressure and temperature. In *Properties of Earth and Planetary Materials at High Pressure and Temperature* (ed. M. H. Manghnani and T. Yagi), pp. 473–480. American Geophysical Union.

Weiss L. E. and Wenk H.-R. (1985) Symmetry of pole figures and textures. In *Preferred Orientation in Deformed Metals and Rocks: an Introduction to Modern Texture Analysis* (ed. H.-R. Wenk), pp. 49–72. Academic Press.

Wen L. (2001) Seismic evidence for a rapidly varying compositional anomaly at the base of the Earth's mantle beneath the Indian Ocean. *Earth and Planetary Science Letters* **194**, 83–95.

Wen L. and Anderson D. L. (1997) Layered mantle convection: a model for geoid and topography. *Earth and Planetary Science Letters* **146**, 367–377.

Wen L. and Niu F. (2002) Seismic velocity and attenuation structures in the top of the Earth's inner core. *Journal of Geophysical Research* **107**, 10.1029/2001JB000170.

Wen L., Silver P. G., James D. E., and Kuehnel R. (2001) Seismic evidence of a thermo-chemical boundary at the base of the Earth's mantle. *Earth and Planetary Science Letters* **189**, 141–153.

Wenk H.-R. (1985) *Preferred Orientation in Deformed Metals and Rocks: an Introduction to Modern Texture Analysis*. Academic Press.

Wenk H.-R. (2002) Texture and anisotropy. In *Plastic Deformation of Minerals and Rocks*, Vol. 51 (ed. S. Karato and H.-R. Wenk), pp. 291–329. The Mineralogical Society of America.

Wenk H.-R., Bennett K., Canova G., and Molinari A. (1991) Modelling plastic deformation of peridotite with the self-consistent theory. *Journal of Geophysical Research* **96**, 8337–8349.

Wenk H.-R., Canova G., Molinari A., and Mecking H. (1989) Texture development in halite: comparison of Taylor model and self-consistent theory. *Acta Metallurgica* **37**, 2017–2029.

Wenk H.-R., Canova G. C., Brechet Y., and Flandin L. (1997) A deformation-based model for recrystallization of anisotropic materials. *Acta Mater* **45**, 3283–3296.

Wenk H.-R. and Christie J. M. (1991) Comments on the interpretation of deformation textures in rocks. *Journal of Structural Geology* **13**, 1091–1110.

Wenk H.-R., Lonardelli I., Pehl J., Devine J. D., Prakapenka V., Shen G., and Mao H.-K. (2004) *In situ* observation of texture development in olivine, ringwoodite, magnesiowüstite and silicate perovskite at high pressure. *Earth and Planetary Science Letters* **226**, 507–519.

Wenk H.-R., Matthius S., Hemley R. J., Mao H.-K., and Shu J. (2000) The plastic deformation of iron at pressures of the Earth's inner core. *Nature* **405**, 1044–1047.

Wettlaufer J. S., Worster M. G., and Huppert H. E. (1997) Natural convection during solidification of an alloy from above with application to the evolution of sea ice. *Journal of Fluid Dynamics* **344**, 291–316.

Wheeler J. (1992) Importance of pressure solution and Coble creep in the deformation of polymineralic rocks. *Journal of Geophysical Research* **97**, 4579–4586.

Wheeler J., Prior D. J., Jiang Z., Spiess R., and Trimbly P. W. (2001) The petrological significance of misorientations between grains. *Contributions to Mineralogy and Petrology* **141**, 109–124.

White S. H. (1979) Grain and sub-grain size variations across a mylonite shear zone. *Contributions to Mineralogy and Petrology* **70**, 193–202.

White S. H., Burrows S. E., Carreras J., Shaw N. D., and Humphreys F. J. (1980) On mylonites in ductile shear zones. *Journal of Structural Geology* **2**, 175–187.

White S. H. and Knipe R. J. (1978) Transformation- and reaction-induced ductility in rocks. *Journal of the Geological Society of London* **135**, 513–516.

Whitehead J. A., Jr. and Luther P. S. (1975) Dynamics of laboratory diapir and plume models. *Journal of Geophysical Research* **80**, 705–717.

Williams D. B. and Carter C. B. (1996) *Transmission Electron Microscopy*. Plenum Press.

Williams Q. and Garnero E. J. (1996) Seismic evidence for partial melt at the base of Earth's mantle. *Science* **273**, 1528–1530.

Williams Q. and Hemley R. J. (2001) Hydrogen in the deep Earth. *Annual Review of Earth and Planetary Sciences* **29**, 365–418.

Winger L. A., Bradt R. C., and Hoke J. H. (1980) Transformational superplasticity of Bi_2WO_6 and Bi_2MoO_6. *Journal of the American Ceramic Society* **63**, 291–294.

Withers A. C., Wood B. J., and Carroll M. R. (1998) The OH content of pyrope at high pressure. *Chemical Geology* **147**, 161–171.

Woirgard J., Rivière A., and De Fouquet J. (1981) Experimental and theoretical aspect of the high temperature damping of pure metals. *Journal de Physique Colloque C* **5**, 407–419.

Wolf G. H. and Jeanloz R. (1984) Lindemann melting law: anharmonic correction and test of its validity for minerals. *Journal of Geophysical Research* **89**, 7821–7835.

Wolfe C. J. and Solomon S. C. (1998) Shear-wave splitting and implications for mantle flow beneath the MELT region of the East Pacific. *Science* **280**, 1230–1232.

Wolfenstein J., Ruano O. A., Wadsworth J., and Sherby O. D. (1993) Refutation of the relationship between denuded zones and diffusional creep. *Scripta Metallurgica et Material* **29**, 515–520.

Wood B. J. (1995) The effect of H_2O on the 410-kilometer seismic discontinuity. *Science* **268**, 74–76.

Wood B. J. and Fraser D. G. (1976) *Elementary Thermodynamics for Geologists*. Oxford University Press.

Wood B. J. and Haliday A. N. (2005) Cooling of the Earth and core formation after the giant impact. *Nature* **437**, 1345–1348.

Wood B. J., Pawley A. R., and Frost D. R. (1996) Water and carbon in the Earth's mantle. *Philosophical Transactions of the Royal Society of London* **354**, 1495–1511.

Wood B. J., Walter M. J., and Wade J. (2006) Accretion of the Earth and segregation of its core. *Nature* **441**, 825–833.

Woodhouse J. H. and Dziewonski A. M. (1984) Mapping the upper mantle: three-dimensional modeling of Earth structure by inversion of seismic waveforms. *Journal of Geophysical Research* **89**, 5953–5986.

Woodhouse J. H. and Dziewonski A. M. (1989) Seismic modelling of the Earth's large-scale three-dimensional structure. *Philosophical Transactions of the Royal Society of London A* **328**, 291–308.

Woodhouse J. H., Giardini D., and Li X. D. (1986) Evidence for inner core anisotropy from free oscillations. *Geophysical Research Letters* **13**, 1549–1552.

Wookey J. and Kendall J.-M. (2004) Evidence of midmantle anisotropy from shear wave splitting and the influence of shear-coupled P waves. *Journal of Geophysical Research* **109**, 10.1029/2003JB002871.

Wookey J., Kendall J. M., and Barruol G. (2002) Mid-mantle deformation inferred from seismic anisotropy. *Nature* **415**, 777–780.

Wright K. and Price G. D. (1993) Computer simulation of defects and diffusion in perovskites. *Journal of Geophysical Research* **98**, 22 245–22 253.

Wyllie P. J. and Huang W. L. (1976) Carbonation and melting reactions in the system CaO-MgO-SiO_2-CO_2 at mantle pressure with geophysical and petrological applications. *Contributions to Mineralogy and Petrology* **54**, 79–107.

Xiao X., Wirth R., and Dresen G. (2002) Diffusion creep of anorthite–quartz aggregates. *Journal of Geophysical Research* **107**, 10.1029/2001JB000789.

Xie Y., Wenk H.-R., and Matthies S. (2003) Plagioclase preferred orientation by TOF neutron diffraction and SEM-EBSD. *Tectonophysics* **370**, 269–286.

Xu Y., Nishihara Y., and Karato S. (2005) Development of a rotational Drickamer apparatus for large-strain deformation experiments under deep Earth conditions. In *Frontiers in High-pressure Research: Applications to Geophysics* (ed. J. Chen, Y. Wang, T. S. Duffy, G. Shen, and L. F. Dobrzhinetskaya), pp. 167–182. Elsevier.

Xu Y., Weidner D. J., Chen J., Vaughan M. T., Wang Y., and Uchida T. (2003) Flow-law for ringwoodite at subduction zone conditions. *Physics of Earth and Planetary Interiors* **136**, 3–9.

Yamazaki D., Inoue T., Okamoto M., and Irifune T. (2005) Grain growth kinetics of ringwoodite and its implication for rheology of the subducting slab. *Earth and Planetary Science Letters* **236**, 871–881.

Yamazaki D. and Irifune T. (2003) Fe–Mg interdiffusion in magnesiowüstite up to 35 GPa. *Earth and Planetary Science Letters* **216**, 301–311.

Yamazaki D. and Karato S. (2001a) High pressure rotational deformation apparatus to 15 GPa. *Review of Scientific Instruments* **72**, 4207–4211.

Yamazaki D. and Karato S. (2001b) Some mineral physics constraints on the rheology and geothermal structure of Earth's lower mantle. *American Mineralogist* **86**, 385–391.

Yamazaki D. and Karato S. (2002) Fabric development in (Mg, Fe)O during large strain, shear deformation: implications for seismic anisotropy in Earth's lower mantle. *Physics of Earth and Planetary Interiors* **131**, 251–267.

Yamazaki D., Kato T., Ohtani E., and Toriumi M. (1996) Grain growth rates of $MgSiO_3$ perovskite and periclase under lower mantle conditions. *Science* **274**, 2052–2054.

Yamazaki D., Kato T., Toriumi M., and Ohtani E. (2001) Silicon self-diffusion in $MgSiO_3$ perovskite at 25 GPa. *Physics of Earth and Planetary Interiors* **119**, 299–309.

Yamazaki D., Yishino T., Ohfuji H., Ando J., and Yoneda A. (2006) Origin of seismic anisotropy in the D″ layer inferred from shear deformation experiments on post-perovskite phase. *Earth and Planetary Science Letters*.

Yan H. (1992) Dislocation Recovery in Olivine. Master of Science, University of Minnesota.

Yan M. F., Cannon R. F., and Bowen H. K. (1977) Grain boundary migration in ceramics. In *Ceramic Microstructures '76* (ed. R. M. Fulrath and J. A. Pask), pp. 276–307. Westview Press.

Yan M. F., Cannon R. M., and Bowen H. K. (1983) Space charge, elastic field and dipole contributions to equilibrium solute segregation at interfaces. *Journal of Applied Physics* **54**, 764–777.

Yokobori T. (1968) Criteria for nearly brittle fracture. *The International Journal of Fracture Mechanics* **4**, 179–205.

Yoon C. K. and Chen I.-W. (1990) Superplastic flow of two-phase ceramics containing rigid inclusions: zirconia/mullite composites. *Journal of the American Ceramic Society* **73**, 1555–1565.

Yoon D. N. and Lazarus D. (1972) Pressure dependence of ionic conductivity in KCl, NaCl, KBr and NaBr. *Physical Review B* **5**, 4935–4945.

Yoshida H., Ikuhara Y., and Sakuma T. (2002) Grain boundary electronic structure related to the high-temperature creep resistance in polycrystalline Al_2O_3. *Acta Materialia* **50**, 2955–2966.

Yoshida S., Sumita I., and Kumazawa M. (1996) Growth model of the inner core coupled with the outer core dynamics and the resulting elastic anisotropy. *Journal of Geophysical Research* **101**, 28 085–28 103.

Yoshii T. (1973) Upper mantle structure beneath the north Pacific and marginal seas. *Journal of Physics of the Earth* **21**, 313–328.

Yoshii T., Kono Y., and Ito K. (1976) Thickening of the oceanic lithosphere. In *The Geophysics of the Pacific Ocean Basin and Its Margin* (ed. G. H. Sutton, M. H. Manghnani, and R. Moberly), pp. 423–430. American Geophysical Union.

Yoshino T., Nishihara Y., and Karato S. (2007) Complete wetting of olivine grain-boundaries by a hydrous melt near the mantle transition zone. *Earth and Planetary Science Letters* **256**, 466–472.

Yoshinobu A. S. and Hirth G. (2002) Microstructural and experimental constraints on the rheology of partially molten gabbro beneath oceanic spreading centers. *Journal of Structural Geology* **24**, 1101–1107.

Yuen D. A., Sabadini R., and Boschi E. V. (1982) Viscosity of the lower mantle as inferred from rotational data. *Journal of Geophysical Research* **87**, 10 745–10 762.

Zamora M. and Poirier J.-P. (1983) Experiments in anisothermal transformation plasticity: the case of cobalt. Geophysical implications. *Mechanics of Materials* **2**, 193–202.

Zener C. (1942) Theory of lattice expansion introduced by cold-work. *Transactions of the Metallurgical Society of AIME* **147**, 104–110.

Zener C. (1948a) *Elasticity and Anelasticiy of Metals*. University of Chicago Press.

Zener C. (1948b) The micro-mechanism of fracture. In *Fracturing of Metals* (ed. F. Johnson, W. P. Roop, and R. T. Bayles), pp. 3–31. ASM.

Zener C. and Hollomon J. H. (1946) Problems in non-elastic deformation of metals. *Journal of Applied Physics* **17**, 69–82.

Zeuch D. H. (1982) Ductile faulting, dynamic recrystallization and grain-size-sensitive flow in olivine. *Tectonophysics* **83**, 293–308.

Zeuch D. H. (1983) On the inter-relationship between grain-size sensitive creep and dynamic recrystallization of olivine. *Tectonophysics* **93**, 151–168.

Zha C.-S., Duffy T. S., Downs R. T., *et al*. (1998) Brillouin scattering and X-ray diffraction of San Carlos olivine: direct pressure determination to 32 GPa. *Earth and Planetary Science Letters* **159**, 25–33.

Zhang S. and Christensen U. R. (1993) Some effects of lateral viscosity variations on geoid and surface velocities induced by density anomalies in the mantle. *Geophysical Journal International* **114**, 531–547.

Zhang S. and Karato S. (1995) Lattice preferred orientation of olivine aggregates deformed in simple shear. *Nature* **375**, 774–777.

Zhang S., Karato S., Fitz Gerald J., Faul U. H., and Zhou Y. (2000) Simple shear deformation of olivine aggregates. *Tectonophysics* **316**, 133–152.

Zhang Y. and Xu Z. (1995) Atomic radii of noble gas elements in condensed phases. *American Mineralogist* **80**, 670–675.

Zhang Y. S. and Tanimoto T. (1992) Ridges, hotspots and their interactions as observed in seismic velocity maps. *Nature* **355**, 45–49.

Zhang Y. S. and Tanimoto T. (1993) High-resolution global upper mantle structure and plate tectonics. *Journal of Geophysical Research* **98**, 9793–9823.

Zhao D. (2004) Global tomographic images of mantle plumes and subducting slabs: insights into deep mantle dynamics. *Physics of the Earth and Planetary Interiors* **146**, 3–34.

Zhao Y.-H., Ginsberg S. B., and Kohlstedt D. L. (2004) Solubility of hydrogen in olivine: dependence on temperature and iron content. *Contributions to Mineralogy and Petrology* **147**, 155–161.

Zimmerman M. E. and Kohlstedt D. L. (2004) Rheological properties of partially molten lherzolite. *Journal of Petrology* **45**, 275–298.

Zimmerman M. R., Zhang S., Kohlstedt D. L., and Karato S. (1999) Melt distribution in mantle rocks deformed in shear. *Geophysical Research Letters* **26**, 1505–1508.

Materials index

Ag, 55
akimotoite, 409
Al_2O_3, 127, 134, 142, 375, 378
albite, 27, 53
alkali halide, 54, 171
anorthite, 27, 172, 241
Au, 55

basalt, 254, 315, 317, 345

$CaIrO_3$, 410
calcite, 62, 190, 209, 226, 245, 266, 378
carbon, 193
carbon dioxide, 20, 102
carbonaceous chondrite, 316
$CaTiO_3$, 209
  $CaTiO_3$ perovskite, 410
clinopyroxene, 84, 186, 190, 345, 351
cobalt, 275
coesite, 272
corundum, 65
CsCl, 171, 172, 274
Cu, 55

diabase, 254, 345, 346, 348
diopside, 53, 241, 347
dunite, 189

eclogite, 314, 318, 348, 405
enstatite, 55, 65, 347

Fe_2SiO_4, 26
feldspar, 190, 215, 245, 347
forsterite, 55, 65

gabbro, 254, 317, 345
garnet, 26, 53, 69, 84, 172, 186, 190, 215, 318, 319, 347
garnetite, 405
granite, 317

H_2O, 274, 275
halite, 187
hydrogen, 104, 127, 129, 144, 149, 181, 183, 193, 195, 209, 287
  hydrogen-related defect, 82
hydrous mineral, 318

ice, 53, 55, 274, 275
iron, 23, 28, 209, 275, 316
  α–iron, 55, 209
  ε-iron, 53, 362, 410
  ferric iron, 28, 128
  ferrous iron, 28, 128

KBr, 172
KCl, 55, 172

lherzolite, 241
  garnet lherzolite, 319
  spinel lherzolite, 319

magnesiowüstite, 27, 215, 274, 282, 386, 405, 409
magnetite, 28
majorite, 319, 359, 375, 409
  majorite-pyrope, 69
metal
  bcc metal, 84
  fcc metal, 84
  hcp metal, 71, 84
meteorite, 305
Mg, 245
Mg_2SiO_4, 26, 70, 71, 81, 127, 134, 203
MgO, 53, 54, 81, 82, 126, 132, 133, 134, 142, 171, 172, 209, 337, 375, 378, 406
$MgSiO_3$, 26, 81, 82
mica, 215
mid-ocean ridge basalt, 315
  MORB, 315
mylonite, 232, 246, 295, 300, 317, 346
  ultra-mylonite, 232

NaBr, 172
NaCl, 55, 83, 172, 245, 274

$NaNO_3$, 245
Ni, 245

olivine, 21, 23, 26, 27, 28, 53, 69, 70, 71, 79, 83, 84, 91, 108, 126, 134, 135, 149, 171, 172, 173, 181, 182, 185, 186, 187, 189, 190, 192, 193, 200, 201, 203, 208, 209, 215, 225, 234, 240, 241, 245, 254, 269, 272, 274, 282, 286, 298, 318, 319, 337, 338, 345, 347, 350, 359, 375, 378, 386, 406, 407, 408, 409
  A-type fabric, 408, 409
  B-type fabric, 409
  C-type fabric, 409
  metastable olivine, 23, 24
  olivine + melt, 212
  olivine-spinel phase transformation, 359
orthopyroxene, 53, 69, 82, 84, 162, 186, 215, 254, 318, 350, 351, 409

periclase, 55, 65
peridotite, 23, 26, 28, 55, 65, 190, 209, 215, 241, 266, 274, 278, 279, 282, 287, 320, 341, 360, 375, 378, 381, 386, 405, 409, 410
perovskite, 23, 26, 28, 55, 65, 190, 209, 215, 241, 266, 274, 278, 279, 282, 287, 320, 341, 360, 375, 378, 381, 386, 405, 409, 410
  $CaTiO_3$ perovskite, 410
  perovskite ($CaTiO_3$), 84
  perovskite (cubic), 84
  $MgSiO_3$ perovskite, 53
  orthorhombic perovskite, 162
plagioclase, 23, 27, 187, 317
post-perovskite, 381, 410
  post-perovskite phase, 361, 390, 410
proton, 128, 129, 182, 190
pseudotachylyte, 122, 295
pyrolite, 315, 316, 382
  pyrolite model, 315, 316
pyrope, 55, 65, 134, 375
pyroxene, 26, 190, 314, 317, 318

quartz, 23, 84, 135, 149, 157, 162, 181, 182, 186, 187, 188, 189, 190, 191, 192, 195, 196, 215, 226, 240, 241, 245, 269, 272, 317, 345, 347
  α-quartz, 53
  β-quartz, 53, 55

ringwoodite, 26, 53, 55, 65, 69, 182, 185, 187, 190, 241, 273, 274, 282, 319, 359, 375, 386, 409

SiO_2, 81, 134, 181
serpentine, 318, 351
sheared lherzolite, 318
spinel, 54, 55, 65, 84, 272
$SrTiO_3$, 209
stishovite, 53, 74, 272, 279, 287

titanium, 275

wadsleyite, 23, 26, 53, 55, 65, 69, 84, 182, 185, 186, 187, 190, 239, 240, 241, 242, 272, 273, 274, 282, 286, 319, 359, 375, 386, 409
water, 20, 22, 100, 102, 127, 144, 168, 169, 171, 181–196, 209, 272, 273, 287, 317, 319, 322, 342, 346, 354, 355, 356, 357, 359, 361, 366, 383, 386, 387, 388
  water content, 317, 320, 322, 338, 340, 341, 346, 350, 354, 357, 358, 361
  water fugacity, 22, 33, 104, 268, 277, 345
  water-related defect, 75
wüstite, 28

xenolith, 318, 385

Subject index

"O" ring, 102
$(Mg, Fe)_2SiO_4$, 82, 91, 225
(Mg, Fe)O, 82, 85, 92, 129, 225, 320, 341, 360, 410
$(Mg, Fe)SiO_3$, 225, 390, 410
$(Mg, Fe)SiO_3$ perovskite, 360, 410
410-km discontinuity, 358, 386, 389
660-km discontinuity, 369, 386

absolute rate theory, 32, 33
absorption band model, 326
acoustic wave, 64
activation
  activation energy, 47, 130, 144
  activation enthalpy, 33, 47, 109, 137–139, 221, 340, 379
  activation volume, 47, 109, 130, 168, 169, 170, 171, 174, 175, 176–181
activity, 17–20, 28
  activity coefficient, 18, 21
actuator, 99, 104
Adams–Williamson equation, 306, 309
adiabatic
  adiabatic compression, 313
  adiabatic elastic constant, 55, 58
  adiabatic instability, 289, 294, 295
  adiabatic temperature gradient, 312, 356
ak135, 318
aliovalent ion, 76
analog material, 272, 275, 276
Anderson–Grüneisen parameter, 66
Andrade creep, 39, 157
anelasticity, 39, 42, 44, 57, 199, 200, 201, 202, 357, 370, 378, 379, 380
  anelastic behavior, 205
  anelastic deformation, 34
  anelastic relaxation, 210
anharmonicity, 51, 63, 64, 357, 374
  anharmonic effect, 378
  anharmonic parameter, 63, 65
  anharmonic properties, 375
anisotropy, 318, 320, 322, 351, 362
  amplitude of anisotropy, 401
  azimuthal anisotropy, 393, 395, 397, 398–399, 409
  polarization anisotropy, 393, 399–401, 409
  radial anisotropy, 404
apparatus distortion, 109
asthenosphere, 317, 325, 327, 354, 409
athermal motion, 33
atmosphere, 314, 317
attenuation, 41, 326, 363
  attenuation coefficient, 200
  attenuation of seismic wave, 199, 323
  attenuation tomography, 365, 382, 387
  bulk attenuation, 208, 211, 212, 384, 385
  seismic wave attenuation, 34, 199, 199–213, 321, 323, 324, 337, 372, 373
Avogadro number, 16, 77
Avrami
  Avrami equation, 252
  Avrami length, 252
  Avrami time, 252

B1 structure, 72
B2 structure, 72
back-stress, 34, 44
bending, 352
Bethe lattice, 223, 224
Bi (NaCl-type), 84
bifurcation, 290
Birch's law, 51, 59, 59–67, 73, 280, 374
  Birch's law of correspondent state, 61
body force, 4
body wave, 351, 364
Boltzmann constant, 16
bond
  bond length, 71
  bond percolation, 223
  bond strength, 70
Bordoni peak, 206
Born–Meyer type interatomic potential, 68, 69
boundary condition, 336
boundary layer, 144, 337, 360, 410
Brillouin scattering, 58

brittle
  brittle deformation, 114
  brittle failure, 288, 339, 340, 342
  brittle faulting, 293
  brittle fracture, 35, 114, 115, 115–118, 119, 121, 188
  brittle to plastic transition, 114
  brittle–ductile transition, 115
  brittle–plastic transition, 114, 122, 342–345
B-type fabric, 409
bulk modulus, 25, 52, 61, 63, 66
bulk sound wave velocity, 372
bulk viscosity, 228
Bullen parameter, 313, 320
Burgers model, 43, 44
Burgers vector, 83, 85, 86, 88, 102, 126, 145, 164, 169, 175, 191, 204
Byerlee's law, 116–117

cataclastic
  cataclastic deformation, 114
  cataclastic flow, 115
Cauchy relation, 54–55
cavitation, 102
Chandler wobble, 202, 323, 324
charge neutrality condition, 80, 92, 128, 129, 185, 186
chemical
  chemical bonding, 51, 271, 272, 278
  chemical composition, 67–70, 381, 382
  chemical defect, 76
  chemical environment, 103–104
  chemical equilibrium, 13, 21, 77
  chemical heterogeneity, 370, 381, 388, 390
  chemical layering, 319
  chemical potential, 13, 14, 17, 18, 21, 24, 25, 27, 31, 32, 123, 125, 183
  chemical reaction, 21, 22
  chemical stress, 160
chondrite model, 316
Christoffel equation, 393, 396
circum-Pacific high velocity anomaly, 366
Clapeyron
  Clapeyron slope, 13, 22–24, 381, 386, 388
  Clapeyron–Clausius relation, 24
climb, 85, 152–153, 158
  climb control model, 158–160
coarse microstructure approximation, 217
Coble creep, 130–132, 135, 142, 229, 254
coincident-site-lattice, 95
compaction, 136, 228, 410
  compaction length, 228
complex compliance, 46
condensation, 316
constitutive relation, 34, 36–38, 339–342
continent
  continental crust, 317, 345, 346
  continental lithosphere, 168, 311, 353, 358
  continental lower crust, 408
  continental root, 353, 357, 388
  continental upper crust, 408
  continental upper mantle, 357
  deep continent, 358
  deep continental root, 357
convective flow, 334
converted wave, 400
coordination polyhedron, 71
core, 306, 314, 316, 320
  core–mantle boundary, 390, 410
  CMB, 390
Cottrell drag, 151
Coulombic interaction, 69
Coulomb–Navier criterion, 118
Coulomb–Navier law, 116–118, 119, 120, 293
CPO, 255, 256
crack, 114, 115, 121, 288, 345, 408
  crack-tip, 121
craton, 352
  Archean craton, 352, 357
creep
  creep compliance function, 40, 42
  creep response function, 39, 40
  diffusional creep, 123, 129–142, 143, 166, 173, 175, 176, 189, 191, 203, 229, 232, 263, 266, 278, 296, 330, 340, 345, 358, 359, 360
  dislocation creep, 130, 143, 144, 162–164, 191–193, 330, 341, 354, 358, 359, 360, 362, 406, 411
  dissolution–precipitation creep, 135
  long-term creep, 325, 326
  steady-state creep, 136
  transient creep, 38, 46, 143, 146, 156, 326, 329–330, 337
  transient diffusional creep, 203
  transient dislocation creep, 204
cross slip, 149, 152–154
crust, 306, 317, 408
crystal
  crystal chemistry, 71
  crystal plasticity, 114
  crystal structure, 51, 70–72, 271, 272, 280
  crystal surface, 29
crystalline defect, 75
crystallographic orientation, 100
crystallographic preferred orientation, 255
CSL, 95
C-type fabric, 409

D″ layer, 213, 314, 320, 366, 381, 386, 402, 405, 408, 410
dead weight
  dead weight creep apparatus, 106
  dead weight loading, 104
Debye model, 51, 59, 61, 64, 67
  Debye frequency, 17, 59, 175, 277

Debye model (cont.)
Debye temperature, 59, 66
Debye–Hückel atmosphere, 97
Debye–Hückel length, 98
decoration, 91
deep mantle, 338
defect, 76
defect mobility, 168
deformation
coaxial deformation, 11, 112
deformation gradient tensor, 3, 11
deformation mechanism map, 165–167, 269
deformation-DIA, 105, 106
irrotational deformation, 3, 11
non-coaxial deformation, 12
non-elastic deformation, 34, 35, 39
delamination, 319
density, 59, 61
density anomaly, 336, 370, 372
denuded zone, 141
diagenesis, 136
diamond anvil cell, 274, 275
dielectric constant, 74, 92, 177
diffusion, 32, 123, 125–126, 143, 149, 173–174, 188, 190, 235, 342
chemical diffusion, 126, 127
chemical diffusion coefficient, 127
diffusion coefficient, 30, 123, 124, 125, 187, 195, 360
diffusion flux, 32
diffusional creep, 123, 129–142, 130–136, 139, 141, 143, 166, 173, 175, 176, 189, 191, 203, 229, 232, 263, 266, 278, 296, 330, 340, 345, 358, 359, 360
self diffusion, 126
self diffusion coefficient, 127, 128
tracer diffusion coefficient, 127
dihedral angle, 97, 117, 135, 227, 230, 356, 357
dimensional analysis, 327
dislocation, 31, 33, 75, 76, 82–94, 121, 126, 136, 143, 204, 345
dislocation climb, 86, 152–154, 159, 192, 205, 263
dislocation creep, 130, 143, 144, 162–164, 191–193, 330, 341, 354, 358, 359, 360, 362, 406, 411
dislocation density, 29, 89, 93–94, 108, 145, 233, 266
dislocation dipole, 153, 159
dislocation energy, 233
dislocation glide, 205, 267
dislocation microstructure, 35, 36, 164
dislocation mobility, 191
dislocation multiplication, 154–155, 191
dislocation network model, 161
dislocation node, 154
dislocation pinning, 205
dislocation recovery, 158, 188, 192, 285
dislocation splitting, 88, 91
dislocation velocity, 145
dissociation of a dislocation, 88–89
edge dislocation, 82
geometrically necessary dislocation, 90, 248, 266, 284
mixed dislocation, 83
screw dislocation, 83, 154
partial dislocation, 83, 88–89, 149
displacement gradient tensor, 7, 8
δ_K, 373
δ_μ, 373
ductile fault, 120
ductile faulting, 115, 120
ductile flow, 35
ductile regime, 345
Dufour effect, 31
dynamic recrystallization, 90, 101, 141, 155, 188, 190, 232, 233, 243–249, 253, 265, 266, 267, 268, 270, 276, 296, 298, 301, 342, 362
dynamically recrystallized grain-size, 245, 248
dynamic topography, 333–335, 336

Earth's interior, 294–295, 305–322
See also: continent, crust, upper mantle, transition zone, lower mantle, core
earthquake, 300
deep and intermediate earthquake, 114, 295, 361
EBSD, 256, 259, 260, 269
Ehrenfest relation, 24
Ehrenfest slope, 22–24
Einstein formula, 229
elastic
elastic anisotropy, 70–71, 71–72
elastic constant, 23, 51, 52–53, 57, 59, 61, 74
elastic constant tensor, 392
elastic deformation, 29, 34, 51, 52, 75
elastic lithosphere, 332
elastic material, 43
elastic strain energy model, 177
elasticity, 51
electric
electric charge, 91, 92–93
electrical conductivity, 185, 189–190, 383, 384
electron backscattered diffraction, 255, 256
electrostatic energy, 177
energy, 63
energy dissipation, 32
enthalpy, 14
entropy, 14, 15, 16, 17, 18, 23, 29, 30
configurational entropy, 16, 27
entropy production, 14, 32
equation of motion, 392
equation of state, 18
error function, 311
etch pit, 93
Euler angle, 258, 259, 260
exponential flow, 340, 345
extensive quantity, 16

extensive variable, 17, 31
extrinsic defect, 76

fabric, 255
  fabric development, 190
  fabric diagram, 268–269
  fabric transition, 268
fault, 115
faulting, 115–116
Fick's law, 30, 31, 123–124
  Fick's first law, 123
  Fick's second law, 124
film, 211
finite amplitude instability, 290–292
first principle of thermodynamics, 13
first-order phase transformation, 23, 72, 271, 280, 286
first-order transformation, 23, 272
flexural rigidity, 328, 352
Flinn diagram, 10, 11
flow law, 164
fluctuation, 29
foliation, 11, 257
  foliation plane, 11
  foliation/lineation, 11
four-grain junction, 138, 141
Fourier's law, 30, 309
Frank energy criterion, 88
Frank-Read source, 155, 329
free oscillation, 324, 364, 400, 410
Frenkel pair, 79, 79–80, 81
frequency-dependent modulus, 201
frequency-dependent phase-lag, 201
friction
  friction coefficient, 116, 117
  frictional heating, 310
FT-IR, 196
fugacity, 17, 18, 18–20, 28, 168, 182
  fugacity coefficient, 18, 22
  fugacity of water, 20, 21, 22

gas-medium apparatus, 102, 106
generalized force, 30, 30–32
geochemical reservoir, 361
geodetic observation, 306
geoid, 332, 333
  geoid anomaly, 332, 334, 335, 336, 337
  geoid kernel, 334
geometrical hardening, 299
geometry of partial melt, 227
Gibbs free energy, 14, 15, 18, 21, 23, 24, 25, 29, 77, 87
Gibbs phase rule, 24, 27
Gibbs–Duhem relation, 16
glide control model, 160, 192
glide plane, 102
Goetze criterion, 120

grain boundary, 29, 31, 75, 76, 94–98, 126, 132, 134, 136, 155, 187, 200, 202, 206
  grain-boundary charge, 97–98
  grain-boundary ledge, 97
  grain-boundary migration, 232, 233, 243, 246, 262, 265, 266, 299
  grain-boundary mobility, 234
  grain-boundary process, 100
  grain-boundary sliding, 123, 130, 136–137, 138, 139, 140, 141, 206–207
  high-angle boundary, 94, 243
  low-angle boundary, 94, 243
grain growth, 100, 188, 190, 232, 233, 236, 236–242, 253, 297, 298, 342
  abnormal grain growth, 240
  normal grain growth, 236–237, 239, 240
grain size, 36, 100, 101, 123, 126, 130, 134, 139, 226, 232–254, 271, 273, 274, 286, 295, 317, 318, 320, 322, 338, 340, 341, 342, 354, 357, 358, 362, 385
  grain-size distribution, 101
  grain-size reduction, 265, 267, 295, 301, 359
  grain-size sensitive creep, 130
gravity, 3
  gravity field, 3, 305, 324, 331, 333, 365
  gravity potential, 332
Greenwood–Johnson model, 281–283, 286
Griggs apparatus, 106, 171, 188, 345
growth, 251–245
Grüneisen parameter, 56, 63, 64, 65, 66, 67, 175, 177, 180, 208, 373, 374, 375
  thermodynamic Grüneisen parameter, 57

Handy's model, 220
hardness, 111
hardness test, 111
harmonic oscillation, 64
Harper–Dorn creep, 144, 145, 160–161, 164
hcp, 362
heat flux, 314
Helmholtz free energy, 14, 63
heterogeneity, 363–390
high diffusivity path, 126–127
high pressure, 58
high spin, 61
high temperature, 102–103
high-temperature plasticity, 171–173
Hill average, 216
HIP, 100
Hoff's analogy, 215
homogeneous nucleation, 250
homologous temperature, 178, 277, 280, 358
homologous temperature scaling, 176, 177–178, 193
Hooke's law, 52–53
hot-isostatic-pressing, 100
hotspot, 401

hydrated jog, 192
hydrated kink, 192
hydro-isostasy, 331
hydrostatic equilibrium, 306
hydrostatic stress, 3
hydrous mineral, 318

ICB, 312
ideal gas, 18, 20, 22
ideal solution, 18
ilmenite, 26, 84, 409
impurity, 98
  impurity atom, 149–151, 154
  impurity drag, 234–235
inclusion, 237, 264
  anisotropic inclusion, 219
incompatible element, 197
infrared spectroscopy, 104, 184
inhomogeneous nucleation, 250
inner core, 232, 254, 278, 321, 338, 362, 402, 408, 410–411
  inner core boundary, 312
  inner core rotation, 322, 362
intensive parameter, 30
intensive quantity, 16
intensive variable, 31
interconnected weak layers, 220
interconnectedness, 222
interface, 29
  interface reaction, 135, 136
  interface-reaction-controlled creep, 135
  interfacial boundary, 250
  interfacial energy, 250
internal energy, 13, 15, 29
internal loading, 323
internal load cell, 106
interphase boundary, 225
interstitial atom, 75, 76
intirinsic temperature derivative, 64
intrinsic defect, 76
invariant of stress tensor, 5, 36
inverse pole figure, 257
ionic crystal, 30, 31, 71, 171
ionic radius, 27, 70, 71, 277
ionic solid, 78–82, 132
ionicity, 71
irreversible, 30
  irreversible process, 13, 14, 29–32
island structure, 136
isomechanical group, 275–280
isostasy, 332–333
isothermal elastic constant, 55
IWL, 220

jacket, 101, 102
J-index, 260, 261
jog, 90–91, 151, 152, 154, 165
joint inversion, 386
Jordan–Handy mode, 219–220

Kikuchi pattern, 256
kinetics, 23
  kinetics of chemical equilibrium, 345
kink, 88, 90–91, 146, 206
  geometrical kink, 91, 147, 149, 206
  kink density, 91
Knoop indenter, 111
Kramers–Kronig relation, 41, 201
Kröger–Vink diagram, 80–82
Kröger–Vink notation, 79, 80
Kronecker's delta, 4, 52

Lame's constant, 52
lateral heterogeneity, 51, 363
lattice strain, 107
lattice vibration, 16, 17, 32, 33, 51, 59, 61, 64
lattice-preferred orientation, 12, 36, 85, 139, 141, 246, 255, 255–270, 300, 318, 362, 386, 391, 392, 402, 405–407, 408
law of mass action, 13, 21, 22, 80, 81, 82, 183, 185
layered structure, 391, 402, 403–405, 407
LBF, 220
ledge, 139, 234
Lehmann discontinuity, 318, 358, 386
Levy–von Mises equation, 37
  Levy–von Mises flow law, 113
  Levy–von Mises formulation, 329
Lifshitz–Shikin theory, 140–141
light element, 321, 322
Lindemann's law, 178
linear instability analysis, 292
linear rheology, 329
linear-variable-displacement-transducer, 105
lineation, 11, 257
line-tension, 155
liquid–solid contact, 97
liquidus, 24, 197
lithosphere, 288, 317, 325, 327, 328, 350, 351, 354
  lithosphere–asthenosphere structure, 317, 339, 351
  lithosphere–asthenosphere system, 338
  lithosphere–asthenosphere transition, 351, 354, 355
load cell, 105
load transfer, 226
load-bearing frame, 220
local equilibrium, 29
localization, 288–301
localized deformation, 288, 351
long-term creep, 325, 326
long-term viscosity, 326
Love wave, 397
lower continental crust, 317

lower crust, 254, 408
lower mantle, 130, 254, 306, 317, 320, 325, 360–361, 389–390, 402, 409–410
low-spin, 61
low-temperature plasticity, 161–162, 166, 171
low-velocity zone, 213, 351
  ultra-low velocity layer, 320
  ultra-low velocity region, 213
  ultra-low velocity zone, 385
LPO, 85, 246, 255, 256, 258, 262, 263, 264, 265, 266, 268, 269, 270, 300, 402, 405, 406, 407, 408, 409, 410, 411
Lüders band, 289, 298
LVDT, 105

machine stiffness, 291–292
Madelung constant, 68, 69
magnetic field, 305, 322, 411
mantle, 317
  mantle convection, 301, 316, 323, 335
  mantle viscosity, 336
martensitic transformation, 250
Maxwell model, 42, 43, 45
Maxwell relation, 15, 25, 57, 63
Maxwell time, 42, 202, 354
mechanical equation of state, 38
mechanical microprobe, 111
melt, 408
  melt geometry, 384
  melt pocket, 210, 211
  melt tube, 211
  melt-induced anisotropy, 410
  fraction of melt, 197, 355, 372
melting, 24, 27
  batch melting, 197
  degree of melting, 197, 355, 356
  eutectic melting, 27
  fractional melting, 197, 198, 356
Mg#, 382
micro-crack, 115–116
microstructure, 226
mid-ocean ridge, 352, 366, 367, 370, 382, 384, 388
Miller index, 56
M-index, 261
mineral physics, 338
misorientation, 259
mixing, 361
Moho, 317
Mohr-circle construction, 118
Mohr's circle, 5–6
moment of inertia, 331
M-site vacancy, 129, 183
multi-component aggregate, 341
multi-component system, 5–6, 24
multi-phase material, 214–231

Nabarro model, 159
Nabarro–Herring creep, 130–132, 278
NaCl structure, 86
NaCl-type crystal, 85
Navier–Stokes equation, 327
necking instability, 289, 294
Nernst field, 129
neutron diffraction, 257
nominally anhydrous mineral, 181
non-hydrostatic stress, 28, 29
non-ideal gas, 18
non-linear rheology, 34, 36–38, 328, 337
non-stoichiometry, 27, 28
normal strain, 8
normal stress, 5–6, 29
normalization parameter, 277
nucleation, 250–251
  nucleation and growth, 232, 233, 247, 250

oceanic crust, 317, 319
oceanic lithosphere, 350, 352, 353
oceanic upper mantle, 357, 358, 408
ODF, 258, 259, 260, 261, 269
OH bond, 184
OH dipole, 184
olivine fabric, 409
  A-type fabric, 408, 409
  B-type fabric, 409
  C-type fabric, 409
Onsager reciprocal relation, 31, 32, 125, 128
optical mode, 64
opto-elastic technique, 58
orientation distribution function, 258, 260
orientation of shear zone, 292–293
oriented crystallization, 265
oriented growth, 265
Orowan equation, 145, 156, 158, 159, 284, 285, 329
Ostwald ripening, 236, 238–239, 240
outer core, 312, 320, 361–362
oxide activity, 28, 81, 82, 103
oxygen fugacity, 21, 22, 28, 80, 82, 101, 103
oxygen fugacity buffer, 22

paleo-oceanic crust, 405
paleopiezometer, 108, 244, 248–249
partial melt, 210, 212–213, 214, 408
partial melting, 24, 197, 213, 315, 317, 318, 320, 342, 354–357, 370, 380, 384–385, 387, 390, 408
partial molar thermodynamic potential, 15
partially molten material, 51, 199, 210–213, 227–231
partitioning of an element, 98
Paterson apparatus, 345
Pauling's rule, 70, 71
Peach–Koehler force, 32, 33, 88
Peclet number, 309

Peierls mechanism, 122, 162, 166, 174, 175–176, 192, 340, 345
Peierls potential, 119, 146, 147, 148, 340
Peierls stress, 143, 145, 146–149, 150, 157, 160, 161, 162, 164, 171, 204, 205, 206, 274, 275
percolation, 222–224
percolation threshold, 222, 224, 231
peridotite, 317, 318, 348, 405
permeability, 228
PH wave, 404
phase diagram, 25–28, 268
phase lag, 40, 210
phase transformation, 22–24, 26, 72, 233, 249–253, 271–287, 319, 341, 342, 374, 375, 381, 382
phenomenological coefficient, 30, 31
phenomenological theory, 34
phnon density of state, 59
physical dispersion, 42
pinning, 154, 206
pinning point, 205
pipe diffusion, 159–160
plane strain, 10, 11
planet, 316
plastic anisotropy, 51, 279
plastic deformation, 34–36, 99–113, 114–122, 143–167, 168–198, 214–231, 271–287, 288–302
plastic flow, 3, 6, 30, 51, 75, 99, 114, 119, 188
plastic flow regime, 115, 119, 121, 339
plate tectonics, 122
plume, 350
point defect, 31, 32, 75, 76–82, 125, 126, 182, 202, 361
Poirier model, 283–286
Poisson's equation, 92
Poisson's ratio, 52, 53, 321
polarization, 397
pole figure, 257
polycrystalline aggregate, 162, 163
polycrystalline material, 12, 32, 51
polycrystalline sample, 100
polyhedral model, 70–71
pore pressure, 116
pore-fluid pressure, 102
porosity, 100
Portevin–Le Chatelier effect, 151, 289, 298
post-glacial crustal uplift, 337
post-glacial rebound, 136, 140, 163, 323, 324, 326, 328, 334, 335, 337, 352
power law, 339
  power-law behavior, 208
  power-law creep, 165, 166, 174, 175, 340, 341
  power-law dislocation creep, 171, 175, 176, 278
  power-law rheology, 109
Preliminary Reference Earth Model, 306
PREM, 306, 307, 318, 363, 365
pressure, 3, 102, 189
pressure dependence of activation volume, 175, 180–181
pressure derivative, 61
pressure shadow, 141
pressure solution creep, 130, 135–136, 267
primary recrystallization, 254
principal strain, 9, 10, 11
principal stress, 4–5
principle of minimum entropy production, 32
pure shear, 3, 85
PV wave, 404
P-wave velocity, 52

Q, 45, 46, 47, 200, 201, 321, 324, 326, 362
  Q factor, 41, 324
  Q^{-1}, 200

radial anisotropy, 404
radioactive heating, 312
rate and state dependent friction, 117
Rayleigh number, 309
Rayleigh wave, 397, 399, 400, 401, 408
RDA, 105
recovery, 155, 188
recrystallized grain size, 244, 249
relative sea level, 326, 330
relaxation process, 39
relaxation time, 39, 45, 47
resolved shear stress, 83
Reuss average, 216, 218, 287
reversible, 29
reversible process, 14
$R_{\phi/S}$, 373, 381, 390
rheologically critical melt fraction, 231
rigid body rotation, 3, 7, 8, 85
rotational deformation, 3, 11
rotational deformation geometry, 11
rotational Drickamer apparatus, 105, 106, 274
$R_{\rho/P}$, 373
$R_{\rho/S}$, 373, 378, 379, 380, 381, 382
Rs/p, 368, 373, 377, 379, 380, 381, 382, 384, 390, 405
RSL, 330, 331

S wave, 397
S (P), 397
Sachs average, 216
Sachs model, 218
saddle point, 32, 33
sample preparation, 99–101
sandwich method, 100, 101, 112
S–C mylonite, 11
scaling, 276
scaling law, 268, 270, 276, 277, 278, 286
Schmid factor, 83, 84, 88, 233
Schmid–Boas relation, 263
Schottky defect, 79, 133, 171, 180
Schottky group, 176

Schottky pair, 78–79
ScS, 397
sea-level change, 323
second invariant of deviatoric stress, 6
second invariant of stress, 285
second invariant of the deviatoric stress tensor, 281, 283
second principle of thermodynamics, 14
secondary phase particle, 235
secondary recrystallization, 254
secondary-ion-mass-spectrometer (SIMS), 184
secondary-ion-mass-spectroscopy (SIMS), 104
second-order phase transformation, 23, 73, 74, 271, 286–287
second-order transformation, 23, 272
sectioning effect, 101
segregation, 98
seimic wave propagation, 392–398
seismic anisotropy, 51, 53, 61, 213, 254, 255, 329, 337, 353, 354, 359, 360, 391–411
  amplitude of anisotropy, 401
  azimuthal anisotropy, 393, 395, 397, 398–399, 409
  polarization anisotropy, 393, 399–401, 409
  radial anisotropy, 404
seismic lithosphere, 352
seismic tomography, 61, 363, 365, 370, 387, 391
seismic wave, 305, 324
  P wave, 397, 401, 408
  S wave, 52
  seismic wave attenuation, 34, 199–213, 321, 323, 324, 337, 372, 373
  seismic wave propagation, 51
  seismic wave velocity, 23, 47, 51, 61, 214, 363
  SH wave, 396, 397, 398, 405
  SV wave, 396, 397, 398, 399
seismological observation, 306–309, 312–314, 323–326, 363–390, 391–410
self-consistent approach, 214–231, 263, 264
self-consistent model, 221
self-diffusion, 144
SEM, 102, 164
semi-brittle behavior, 345, 351
semi-brittle regime, 120–122
semiconductor, 149
sense of shear, 267
sensor, 99
servo-control system, 104
servo-controlled actuator, 109
Shannon–Prewitt ionic radius, 61
shape-preferred orientation, 402
  SPO, 402, 408
sharpness of the boundary, 365
shear band, 292
shear localization, 121, 226, 232, 288, 289, 295
shear modulus, 52, 86
shear strain, 3, 8
shear stress, 5–6, 52
shear wave splitting, 399, 400, 401, 409
shear zone, 300
sheared lherzolite, 318
SH-SV polarization anisotropy, 400
simple shear, 3, 10, 11, 37, 264, 292
simple shear deformation, 112–113
Si-site vacancy, 183
site percolation, 223
SKS, 397
SKS wave, 399, 400
slip, 82, 263
  slip direction, 82
  slip plane, 82
  slip system, 82, 83, 87, 100, 148, 162, 258, 269, 360, 410
Snoek peak, 203
soft mode, 74
solar nebula, 316
solar system, 305, 316
solid-medium apparatus, 103
solid skeleton, 228
solid solution, 27, 401
solidus, 24, 178, 197, 354, 356
solubility, 181
solute atmosphere, 298
solvus, 27
Soret effect, 31
S–P mylonite, 299
specific heat, 25
spheroidal mode, 365
splitting function, 364
splitting of peaks, 400
SPO, 402, 408
stability of deformation, 137
stacking fault, 76, 83, 89
stagnant-lid convection, 350
standard linear solid, 44
stationary state, 32
statistical mechanics, 29
statistical physics, 33, 109
steady state
  steady-state creep, 136
  steady-state deformation, 35, 110
  steady-state dislocation creep, 157–161
  steady-state flow, 38
  stereographic projection, 257
Stirling's formula, 16, 77
stochastic process, 76
stoichiometry, 28, 133, 134
strain, 3, 7, 7–12
  dilatational strain, 3
  Eulerian strain, 7
  finite strain ellipsoid, 267, 268
  Lagrangian strain, 7
  strain ellipsoid, 9, 10, 11

strain (cont.)
  strain energy, 29
  strain gradient, 90
  strain hardening, 38
  strain marker, 101
  strain partitioning, 226
  strain tensor, 7–8, 9
  strain-induced grain-boundary migration, 246
strain rate, 35
  constant strain-rate test, 108
stress, 3, 4, 12, 34, 35
  chemical stress, 160
  constant stress test, 109
  deviatoric stress, 3, 6, 29, 31, 104
  equivalent stress, 37
  internal stress, 38, 111, 145, 152, 164, 280, 281, 283
  internal stress–strain, 271
  stress concentration, 114, 203, 229, 299, 345
  stress exponent, 101, 165, 221
  stress invariants, 4–5
  stress partitioning, 226
  stress relaxation function, 40
  stress-dip test, 111, 164
  stress-relaxation test, 110–111
  stress–strain curve, 110
  stress–strain distribution, 214, 215
subboundary, 96
subduction
  subducted slab, 23, 334, 359, 360, 370, 389, 410
  subduction zone, 334, 367, 409
subgrain, 96, 158, 243
  subgrain boundary, 158, 243, 246
  subgrain growth, 248
  subgrain rotation, 243, 246, 248, 265
superplasticity, 109, 129–142, 266, 267, 288–301, 360
  structural superplasticity, 137
  superplastic creep, 266
  superplastic deformation, 264
  superplastic flow, 123
  transformational plasticity, 137, 280–286, 359
surface force, 4
surface reaction, 236
surface tension, 96, 233
surface topography, 328
surface wave, 317, 351, 364, 366, 399, 408
  Love wave, 397
  Rayleigh wave, 397, 399, 400, 401, 408
Suzuki effect, 151
synchrotron-based technique, 108
systematics, 275
Szigetti relation, 177

Taylor
  Taylor average, 216
  Taylor factor, 299
  Taylor model, 218
  Taylor–Bishop–Hill model, 264
tectonic field, 408
TEM, 93, 97, 102, 196, 273
tensor
  fourth-rank tensor, 53
  second-rank tensor, 3, 4, 53
ternary system, 81
terrestrial planet, 314
texture, 255
thermal activation, 33
thermal defect, 76
thermal diffusion, 207
thermal expansion, 23, 25, 56, 61, 63, 66, 374
thermal lithosphere, 352–353
thermal pressure, 56
thermal runaway instability, 294–295, 305–322
thermally activated motion, 35, 76
thermally activated process, 13, 32–33, 123, 125
thermo-chemical environment, 102–104
thermocouple, 103
thermodynamics, 13
  thermodynamic force, 31
  thermodynamic Grüneisen parameter, 57
  thermodynamic potential, 15
thermoelasticity, 207–208
thickness of grain boundary, 97
thin film, 136
thin fluid film, 136
tidal deformation, 324
tidal dissipation, 199
tilt boundary, 94
tomography, 364
topography, 385
  topography on discontinuity, 385–386, 388
torsion apparatus, 99
torsion test, 99, 100, 101, 112–113
transformation kinetics, 190
transformation plasticity, 280–286
transient behavior, 140
transient creep, 38, 46, 143, 146, 156, 326, 329–330, 337
  transient diffusional creep, 203
  transient dislocation creep, 204
transition zone, 254, 271, 306, 312, 317, 319–320, 336, 359–360, 386, 387, 388–389, 401, 405, 409
transmission electron microscope, 93, 97, 164
transpression, 409
transverse isotropy, 400, 404, 407
trench, 409
tri-axial compression, 3, 37, 112
tri-axial compression test, 100, 112
tri-axial testing apparatus, 99
twin boundary, 207–212
twinning, 122, 162, 263, 406
twist boundary, 94

two-phase material, 215, 299
two-phase mixture, 405

ultra-low velocity region, 213, 320, 385
ultra-mylonite, 232
ultrasonic technique, 58
ultrasonic wave, 58, 200
uni-axial compression, 37
unrelaxed model, 281
upper mantle, 130, 254, 306, 317, 350–358, 382, 387–388, 408–409
Urey ratio, 310

*V**, 345
vacancy, 29, 75, 76, 80, 182
variational principle, 216, 217
velocity of elastic waves, 41, 58
Venus, 322, 346
vibrational entropy, 17, 29
Vickers indenter, 111
viscoelasticity, 39, 199, 202
viscosity, 339
  effective viscosity, 36, 37, 342, 354
  viscosity profile, 360
  viscosity tensor, 36
  viscosity-depth profile, 336
viscous motion of melt, 210
Voigt average, 216, 218
  Voigt model, 43, 44
  Voigt notation, 53
volatile, 314, 318
von Mises condition, 85–86
vorticity, 8, 11

Walsh mechanism, 211
waveform inversion, 364
Weertman model, 159
wetting behavior, 230
whole mantle convection, 316
work hardening, 88, 110, 145, 146, 149, 155, 157, 188, 285, 286, 293, 299
work softening, 188, 293

X-ray, 256
X-ray diffraction, 57, 99, 106, 107, 108

yield stress, 33, 116, 148, 161, 351
yielding, 35

Zener model, 43, 44, 45, 47
Zener peak, 203
Zener pinning, 225, 237–238, 296, 358
zirconia sensor, 104